

*LISTERIA MONOCYTOGENES* INFECTION ALTERS TROPHOBLAST EXTRACELLULAR  
VESICLES

By

Jonathan Matthew Kaletka

A DISSERTATION

Submitted to  
Michigan State University  
in partial fulfillment of the requirements  
for the degree of

Microbiology and Molecular Genetics—Doctor of Philosophy

2022

## ABSTRACT

### *LISTERIA MONOCYTOGENES* INFECTION ALTERS TROPHOBLAST EXTRACELLULAR VESICLES

By

Jonathan Matthew Kaletka

*Listeria monocytogenes* (*Lm*) is a bacterial pathogen that utilizes an intracellular lifecycle to spread throughout the body, including the placenta in pregnant individuals. Placental infection and disease can lead to negative fetal outcomes including spontaneous abortion, birth defects, and stillbirths. Extracellular vesicles (EVs) are tiny particles secreted by nearly every cell type in the body and serve as a cellular signaling mechanism. EVs have been implicated in many cellular functions and diseases throughout the body, including those involving the placenta. Placental EVs can have immunomodulatory effects, but during placental disease they can also act in a pro-inflammatory manner, leading to disease progression. EVs can also be proinflammatory during intracellular bacterial infection, where they can communicate the infection and coordinate an immune response. In this dissertation, I investigated how *Lm* infection of trophoblasts alters the EVs produced by the infected cells, and how they can activate an immune response.

Chapter 1 of the dissertation details the current literature on the role that EVs play during bacterial infections and placental development and disease. Chapter 2 focuses on establishing a trophoblast stem cell model (TSC) to study placental infections. TSCs are the source of trophoblasts in the placenta, and cultivation of these cells allow for the continual study of placental disease. Here, I found that TSCs are susceptible to *Lm* infection, although it requires a higher bacterial load and longer time course compared to other cell types. This chapter details ways to model placenta-pathogen interactions *in vitro*, allowing for the study of these interactions in a laboratory setting.

Chapter 3 investigated how *Lm* infection of TSCs altered the cargo of the tEVs produced. Previous studies into EVs from infected cells found components from the bacterial cells loaded into the EVs, including bacterial DNA, RNA, and proteins. We found many more unique proteins in the tEVs from infected cells. The infection tEVs had a substantial increase in the number of peptides identified of ribosomal, histone, and tubulin proteins, among others. Gene ontology (GO) analysis showed that the proteins seen in the tEVs from infected TSCs primarily belonged to RNA-binding pathways. This result piqued our curiosity as to if *Lm* infection also changed the RNA loaded into the tEVs. We performed RNA sequencing to determine the host RNA profiles found in the tEVs. We found different RNA profiles in the tEVs from uninfected and *Lm*-infected cells. GO analysis on the mRNAs overrepresented in the infection tEVs found that they represent genes from vasculogenesis and placental development pathways. Our results in this chapter show that *Lm* infection can alter the production and contents of tEVs from TSCs.

Chapter 4 of this dissertation aimed to determine how tEVs from *Lm*-infected TSCs affect immune cells. We found that macrophages treated with infection tEVs produced TNF- $\alpha$ , a pro-inflammatory cytokine. Surprisingly, when we subsequently infected tEV treated cells with *Lm*, some of the cells became more susceptible to *Lm* infection. Similar results were seen with treatment with macrophage EVs, where infection EVs made the macrophages susceptible to *Lm* infection. The work in this chapter suggests that tEVs from *Lm*-infected TSCs can indeed induce a pro-inflammatory response in macrophages, although this makes the cells more susceptible to infection. Overall, the work presented here explores potential mechanisms as to how the placenta communicates bacterial infections.

This dissertation is dedicated to everyone who helped and supported me throughout my time at Michigan State, without you I would not be where I am today.

## ACKNOWLEDGEMENTS

This section was the most difficult one for me to write in this whole dissertation. Not because I don't have anything to say, but because I don't know how I would even begin to thank every person who impacted my life during my five-year journey to complete this dissertation. I will attempt to fully show my gratification throughout this section, but just know that there is still so much more I could say.

The only place I could start is with my mentor, Dr. Jonathan Hardy. I remember during my first meeting with Jonathan his enthusiasm about science just bubbling over during the entire discussion. His enthusiasm persisted throughout our time together, even when I was discouraged with the results (or lack of results) I was getting. A conversation with him always reassured me that I was doing the right thing and gave me renewed energy to keep attacking the problem to figure out the solution. He supported me through all my endeavors, including me exploring teaching and science communication opportunities, even if it meant taking my time away from the lab. He truly believes that obtaining a Ph.D. is not just about growth as a scientist, but also as a person. Jonathan has always been there when I needed, and I truly could not have asked for a better mentor.

I am also incredibly thankful for my lab mates, particularly my fellow Ph.D. students, Kayla Conner and Justin Lee. I started in the Hardy lab at the same time as Kayla and Justin, and they have been incredible pillars of support. They have offered great feedback on experiments and ideas, as well as words of encouragement when I needed them. I would also like to thank former lab members Angela DeTomaso and Mike Witte, both of whom had great impacts on my life and

the lab during their time in the Hardy lab. My former undergraduate students, Josie Altman and Emily Hawker, both worked diligently on how differentiating trophoblasts, and I greatly appreciate them for their efforts. One final thanks to every other past and former Hardy lab member, who helped create a welcoming and exciting environment for research.

There have also been numerous professors who helped me along the way. My guidance committee, Dr. Peggy Petroff, Dr. Neal Hammer, Dr. Masamitsu Kanada, and Dr. Victor DiRita, has been invaluable in their feedback and support, pushing me to improve my research while also helping me prepare for my future. Additionally, Dr. Chris Waters helped me get started at MSU by taking me in for my first rotation and giving me critical feedback on my preliminary exam proposal. Dr. Cori Fata-Hartley served as my mentor during my teaching practices and helped guide me through a teaching as research project, a different way to conduct research that changed how I viewed the practice.

I would like to thank the Institute for Quantitative Health Science and Engineering (IQ) at MSU for providing the facility and resources for executing this work. We gratefully acknowledge Dr. Melinda Frame and Dr. Alicia Withrow at the Center for Advanced Microscopy at MSU. Additionally, we also gratefully acknowledge Dr. Douglas Whitten at the Research Technology Support Facility Proteomics Core at MSU. We are most grateful for the team at Azenta/Genewiz, including Michael Bullard, Sabbir Siddiqui and Aleksandar Janjic, for their expert consultation and sequencing. Justin Lee performed the RNA sequencing analysis, a process that would not have been completed without his expertise. Finally, I would like to thank the entire MSU Microbiology and Molecular Genetics department, especially Roseann Bills and Katie Conley, otherwise I would not have been organized enough to graduate.

Lastly, but most importantly, I want to thank my family and friends who I have not yet mentioned. Their love and support made all this possible. They have been there at my best and worst moments, cheering me on and reminding me that there is more to life and grad school than just lab work. I am incredibly grateful to be surrounded by the best people possible.

## TABLE OF CONTENTS

<b>LIST OF TABLES .....</b>	<b>xi</b>
<b>LIST OF FIGURES .....</b>	<b>xii</b>
<b>KEY TO ABBREVIATIONS .....</b>	<b>xiv</b>
<b>CHAPTER 1 LITERATURE REVIEW: EXTRACELLULAR VESICLES AND THEIR ROLES IN INFECTION AND PLACENTA HEALTH.....</b>	<b>1</b>
EXTRACELLULAR VESICLES BACKGROUND AND HISTORY .....	2
EV isolation methods.....	3
EXTRACELLULAR VESICLES DURING BACTERIAL INFECTIONS .....	4
Contents of EVs.....	4
Alteration of host components.....	5
Bacterial components.....	6
HOST RESPONSE TO EXTRACELLULAR VESICLES .....	7
Toll-like receptors.....	7
Interferons.....	8
Chemotaxis.....	9
Growth after treatment.....	9
USE OF TREATMENTS AND PREVENTATIVE MEASURES <i>IN VIVO</i> .....	10
Response to EV treatment in animals.....	10
Analysis of EVs isolated from infected animals and humans.....	11
PLACENTAL IMMUNOLOGY.....	12
Placental EVs.....	13
DISSERTATION OVERVIEW .....	14
APPENDIX .....	15
REFERENCES .....	18
<b>CHAPTER 2 MODELING <i>LISTERIA MONOCYTOGENES</i> INFECTIONS.....</b>	<b>25</b>
ABSTRACT .....	26
INTRODUCTION .....	27
MATERIALS AND METHODS.....	28
Bacterial cultures.....	28
Cell culture.....	29
<i>Listeria</i> intracellular growth assay.....	29
Fluorescence microscopy.....	29
RESULTS.....	30
Trophoblast stem cell <i>Listeria</i> infection.....	30
TSC differentiation.....	31
HTR-8/SVneo human trophoblasts.....	32

Neural progenitors. ....	32
DISCUSSION.....	33
APPENDIX .....	37
REFERENCES .....	45

**CHAPTER 3 *LISTERIA MONOCYTOGENES* INFECTION ALETERS  
EXTRACELLULAR VESICLES PRODUCED BY TROPHOBLAST STEM CELLS .....49**

ABSTRACT .....	50
INTRODUCTION.....	51
MATERIALS AND METHODS.....	53
Mice. ....	53
Bacterial cultures. ....	53
Cell culture.....	53
Isolation of extracellular vesicles.....	54
Transmission electron microscopy. ....	54
Nanoparticle tracking analysis. ....	55
Mouse extracellular vesicle isolation.....	55
Proteomics.....	55
Gene Ontology (GO) Enrichment Analysis for proteomics. ....	56
RNA sequencing. ....	56
Lipidomics. ....	57
RESULTS.....	60
Trophoblast stem cell extracellular vesicles quantification. ....	60
Mouse EVs after infection. ....	61
Proteomic analysis on tEVs after infection.....	61
RNA sequencing on S-tEVs.....	62
Lipidomic analysis on S-tEVs. ....	63
DISCUSSION.....	64
APPENDIX .....	68
REFERENCES .....	84

**CHAPTER 4 IMMUNE CELL RESPONSE TO EXTRACELLULAR VESICLES FROM  
INFECTED CELLS.....91**

ABSTRACT .....	92
INTRODUCTION.....	93
MATERIALS AND METHODS.....	95
Bacterial cultures. ....	95
Cell culture.....	95
Isolation of extracellular vesicles.....	95
<i>Listeria</i> intracellular growth assay.....	96
TNF- $\alpha$ quantification. ....	97
Mouse infections.....	97
RESULTS.....	98
tEV-mediated stimulation of macrophages.....	98
<i>Listeria</i> infection after tEV treatment.....	98

Effect of <i>Lm</i> mutants on tEV capabilities.....	99
Macrophage EVs.....	100
Treatment of mice with tEVs.....	100
DISCUSSION.....	101
APPENDIX.....	104
REFERENCES.....	116
<b>CHAPTER 5 CONCLUSIONS AND FUTURE DIRECTIONS .....</b>	<b>120</b>
Chaper 2: Modeling <i>Listeria monocytogenes</i> infections.....	121
Chapter 3: <i>Listeria monocytogenes</i> infection alters extracellular vesicles produced by trophoblast stem cells.....	124
Chapter 4: Immune cell response to extracellular vesicles from infected cells.....	126
Final Takeaways.....	128
REFERENCES.....	129

## LIST OF TABLES

Table 3.1.	EVs isolated from mouse blood during <i>Lm</i> infection	78
Table 3.2.	Proteins that were found in higher abundance in infection EVs	79
Table 3.3.	Proteins found in higher abundance in uninfected EVs	81
Table 3.4.	Panther Gene Ontology analysis of proteins found in infection EVs	82

## LIST OF FIGURES

Figure 1.1.	Extracellular vesicles in bacterial infections.	16
Figure 1.2.	Placental extracellular vesicles.	17
Figure 2.1.	<i>Lm</i> replicate and polymerize actin in TSCs.	38
Figure 2.2.	TSCs infected with bioluminescent <i>Lm</i> .	39
Figure 2.3.	Pictures of differentiated TSCs.	40
Figure 2.4.	IVIS <i>Lm</i> infection of differentiated trophoblasts.	41
Figure 2.5.	Microscopy of <i>Lm</i> -infected HTR-8/SVneo cells.	42
Figure 2.6.	NE-4C neural progenitors infected with bioluminescent <i>Lm</i> .	43
Figure 2.7.	Microscopy of <i>Lm</i> -infected C17.2 neural progenitor cells.	44
Figure 3.1.	Extracellular vesicle isolation protocol.	69
Figure 3.2.	Extracellular vesicles from <i>Lm</i> -infected TSCs.	70
Figure 3.3.	TSCs infected with <i>Lm</i> produce tEVs.	71
Figure 3.4.	<i>Lm</i> infection changes L-tEV concentrations.	72
Figure 3.5.	<i>Lm</i> infection did not change tEV size.	73
Figure 3.6.	Protein interaction networks of proteins found in S-tEVs from <i>Lm</i> -infected TSCs.	74
Figure 3.7.	<i>Lm</i> -infected TSCs produce S-tEVs with altered RNA profiles.	75

Figure 3.8.	Gene Ontology analysis of differing RNAs found in S-tEVs from uninfected and <i>Lm</i> -infected TSCs.	76
Figure 3.9.	Lipidomic analysis on tEVs.	77
Figure 4.1.	tEVs from <i>Lm</i> -infected TSCs induce the production of TNF- $\alpha$ .	105
Figure 4.2.	tEVs from <i>Lm</i> -infected TSCs alter macrophage susceptibility to infection.	106
Figure 4.3.	tEVs slightly affect TSC susceptibility to <i>Lm</i> infection.	107
Figure 4.4.	<i>Lm</i> mutants of initial infection alter tEV effect on recipient cells.	108
Figure 4.5.	Macrophage S-EVs alter RAW 264.7 cells susceptibility to <i>Lm</i> .	109
Figure 4.6.	Macrophage S-EVs alter J774 cells susceptibility to <i>Lm</i> .	110
Figure 4.7.	BMDM S-tEVs alter BMDMs susceptibility to <i>Lm</i> .	111
Figure 4.8.	tEVs do not change mouse resistance to <i>Lm</i> .	112
Figure 4.9.	tEVs do not change mouse resistance to <i>Lm</i> in different experimental setup.	114

## KEY TO ABBREVIATIONS

EVs	Extracellular vesicles
MVEs	Multivesicular endosomes
LPS	Lipopolysaccharide
MHCII	Major histocompatibility complex class II
S-EVs	Small EVs
mRNA	Messenger RNA
miRNA	MicroRNA
iEVs	Infection EVs
BMDMs	Bone marrow-derived macrophages
DCs	Dendritic cells
LSM	Laser scanning microscopy
<i>Mtb</i>	<i>Mycobacterium tuberculosis</i>
ATP	Adenosine triphosphate
HSP70	Heat shock protein 70
<i>Lm</i>	<i>Listeria monocytogenes</i>
TLRs	Toll-like receptors

PRRs	Pattern recognition receptors
PAMPs	Pathogen-associated molecular patterns
DAMPs	Danger-associated molecular patterns
IFNs	Interferons
BMDCs	Bone marrow-derived dendritic cells
CFP	Culture filtrate protein
IV	Intravenous
DT	Diphtheria toxin
tEVs	Trophoblast EVs
uNK	Uterine natural killer
TSC	Trophoblast stem cell
LLO	Listeriolysin O
Xen32	<i>Lm</i> 10403S bioluminescent strain 2C
GFP	Green fluorescence protein
BHI	Brain heart infusion medium
FBS	Fetal bovine serum
FGF-4	Fibroblast growth factor 4
MOI	Multiplicity of infection

HPI	Hours post infection
DAPI	4',6-diamidino-2-phenylindole
PBS	Phosphate buffered saline
IVIS	In Vivo Imaging System
WT	Wild type
SynTs	Syncytiotrophoblasts
TGCs	Trophoblast giant cells
RA	Retinoic acid
HIF	Hypoxia-induced factor
BM	Base media
CHIR	CHIR99021
CNS	Central nervous system
E11	Gestation day 11
L-tEVs	Large tEVs
S-tEVs	Small tEVs
MS	Mass spectrometry
LC-MS/MS	Liquid chromatography with tandem MS
PANTHER	Protein analysis through evolutionary relationships

PE	Paired end
HCS	HiSeq Control Software (HCS)
HCD	Higher-energy collisional dissociation
LIMSA	Lipid Mass Spectrum Analysis
TEM	Transmission electron microscopy
GO	Gene ontology
CDC	Cholesterol-dependent cytotoxin
FDR	False discovery rate
ELISA	Enzyme-linked immunosorbent assay
HK	Heat-killed
RNAseq	RNA sequencing

## CHAPTER 1

# LITERATURE REVIEW: EXTRACELLULAR VESICLES AND THEIR ROLES IN INFECTION AND PLACENTAL HEALTH

## EXTRACELLULAR VESICLES BACKGROUND AND HISTORY

A recently discovered mechanism that could play a role in mediating cellular immunity is intercellular communication mediated by extracellular vesicles (EVs). EVs are small, membrane-enclosed vesicles that are excreted by nearly every cell type in the human body and across all domains of life (1). Two of the major types of EVs in eukaryotes have been historically designated as exosomes and microvesicles, which are differentiated based on how they are formed. Exosomes are smaller (50-150 nm) and form by the inward folding of the plasma membrane. Multiple vesicles form in multivesicular endosomes (MVEs), which translocate to the cell membrane, leading to membrane fusion and the release of the exosomes to the extracellular environment. Microvesicles, which have a wider range in size (100-1000 nm), are formed by the outward budding of the plasma membrane directly into the extracellular space (2). While these two EV types are a major focus of study, there are other variations. Apoptotic bodies are large EVs, ranging from 500-2,000 nm in size. They are formed during the disassembly of a cell into subcellular compartments during apoptosis, a type of programmed cell death (3). Exomeres are tiny (<50 nm) protein aggregates that lack membranes, although they still have the ability to signal and alter recipient cells (4). Another recently discovered nanoparticle that was proposed to be an EV type are macrolets. Macrolets are quite large, 10-30  $\mu\text{m}$  in size, and are formed when macrophages are treated with the immunostimulatory bacterial component lipopolysaccharide (LPS). While they lack nuclei, these macrolets can contain and even kill *Escherichia coli* (5). EV preparations have often been referred to as microvesicles and exosomes, but as there are other types of EVs and each of these entities are formed by distinct processes, the current consensus among experts in the field is to refer to them by their size (such as large or small EVs) unless specific formation mechanism is addressed (6).

EVs were first identified 1981 when electron microscopy identified what appeared to be vesicles inside of vesicles, which is where the term “exosomes” originated (7). Further work around this time characterized EVs from reticulocytes transporting transferrin receptors out of cells (8, 9). These initial findings led to the original belief that EVs were simply a mechanism for cellular waste removal. It was not until 1996, though, when the interest in EVs really started. Raposo *et al.* discovered that EVs transport major histocompatibility complex class II (MHCII) proteins and activate recipient cells (10). This launched interest in EVs as a potential mechanism in cell signaling in different aspects of human health, in particular the immune response.

#### *EV isolation methods.*

As EVs are much smaller than eukaryotic cells or even bacteria, their isolation is complex and has been the subject of controversy. Currently, differential ultracentrifugation is still regarded as the most used method for isolating small EVs (S-EVs), which are often referred to as exosomes. Initially, low speed centrifugation removes cells and larger cell debris, followed by spinning the samples at high speeds, usually at 100,000 x g at a minimum, which pools the tiny vesicles separate from the cells. Recent literature suggests that different isolation methods can affect EV profiles. Precipitation, density gradients, and filtration have all been used to isolate EVs, although each of these methods have their own benefits and drawbacks (11). The issues with ultracentrifugation are that the method is time consuming, it requires expensive equipment and large amounts of initial starting material, and it can co-isolate non-EV protein aggregates. Precipitation has also been commonly used for EV isolation through commercially available kits, such as ExoQuick. This process is quicker and requires less starting material, but also isolates lipoproteins and may not yield enough EVs for downstream analysis (12, 13). The use of ultrafiltration is also faster than ultracentrifugation, but the high pressure required for this technique may damage EVs (13).

Density gradients can separate EVs into different subtypes based on their molecular weights, but these EVs may not be suitable for functional analysis (14). Currently, ultracentrifugation is still considered the “gold standard” for EV isolation, although the optimal method may vary depending on the starting material and the intended purpose of the EVs (6). It is important to consider that any results involving EVs may be affected by how they were isolated.

## EXTRACELLULAR VESICLES DURING BACTERIAL INFECTIONS

### *Contents of EVs.*

Interest in EVs stems from the fact that they can carry a wide variety of nucleic acids, proteins, and lipids to other cells. Interestingly, this cargo is often different than what is found in the cell that it came from, and the molecules transported can induce changes in recipient cells. One of the original studies that sparked this interest was by Valadi *et al.*, who discovered that EVs transport messenger RNA (mRNA) and microRNA (miRNA). Most interestingly, though, the mRNAs were functional in the recipient cells. In this study, mouse cells produced rabbit proteins when treated with EVs from rabbit cells (15). A similar study found that the mRNA and miRNA loaded into the EVs have a different profile compared to the cells of origin, suggesting that these RNAs are preferentially loaded into the EVs. They also found that cancer patients carried oncogenic miRNAs, giving rise to the possibility that EVs could be used for disease diagnostics (16). Additionally, DNA can be transported in EVs, which can be incorporated into the recipient cells, piquing the interest for biomedical applications (17). These results led researchers to wonder how bacterial infections may change EVs produced by the host cells and what we can learn about infections from studying these EVs. In this section, I will show that not only does infection change

the host contents of EVs produced, but that bacterial components being transported by EVs are a conserved and well documented mechanism (Fig. 1.1).

*Alteration of host components.*

The first reported investigation into infection EVs (iEVs) was from the Russell group out of Washington University around the turn of the century. Previous work with EVs associated with other diseases found components of the MHCII being transported in EVs (10). As MHCII is utilized by phagocytes to present foreign antigens, they believed that MHCII proteins are also be found in iEVs. Bone marrow derived macrophages (BMDMs) infected with *Mycobacterium bovis* produced iEVs carrying increased amounts of the  $\beta$ -subunit of MHC II compared to EVs from uninfected BMDMs (18). Dendritic cells (DCs) treated with LPS, a component of Gram-negative bacteria, also produced EVs that had MHCII proteins (19). MHCII molecules were also detected in iEVs from *Mycobacterium tuberculosis* (*Mtb*) infected BMDMs by western blot, and this result was especially true for large iEVs (20). These results indicate that iEVs could be used in antigen presentation and serve as a potential mechanism for immune activation.

In addition to MHCII components, other host proteins have been observed to differentially loaded into iEVs. In LPS treated DCs, laser scanning microscopy (LSM) revealed the EVs contained an increased amount of CD40, CD83, and TNF- $\alpha$ , all of which are involved in immune cell activation (19). Heat shock protein 70 (HSP70), which is a chaperone that can interact with toll-like receptors (TLRs) and induce NF- $\kappa$ B activation, are found on iEVs from RAW 264.7 macrophage-like cells infected with *Mycobacterium avium* or *Mycobacterium smegmatis*. Further, a proteomic analysis of iEVs from *M. avium* infected THP-1 monocytes revealed an increase in cytoplasm proteins compared to EVs from uninfected cells (21). Additionally, *Mtb* infection leads to different mRNAs

and miRNAs being loaded into iEVs, and the transcripts delivered by the iEVs are active and can be translated in the recipient cells (22). Altogether, the literature shows that bacterial infections can alter the host cargo being transported in EVs, including proteins involved in antigen presentation and immune cell activation.

#### *Bacterial components.*

Nucleic acids have been of major focus for the EV community, with DNA, mRNA, and miRNA all being found in EVs and active in the recipient cells (23). Interestingly, iEVs can transport bacterial nucleic acids in addition to the host's own DNA and RNA. Cells infected with *Listeria monocytogenes* (*Lm*) produce iEVs that house DNA originating from the bacteria (24). This is dependent on the cGAS-STING pathway in the infected cell, which senses DNA in the cytosol and has been found to be a defense mechanism against intracellular *Lm* (25). There appears to be no preference for the DNA that is loaded, as sequencing the DNA revealed that it evenly mapped to the *Lm* genome (24). Similarly, *Mtb* RNA is found in iEVs, and this is dependent on the RIG-1/MAVS system, which detects cytosolic RNA (22, 26). While the cGAS-STING and the RIG-1/MAVS systems typically are implicated for viral defense, it appears that they can also help host immunity against bacterial pathogens; their roles in iEV response will be discussed later in this chapter (27–29). In addition to nucleic acids, other bacterial components are transported in iEVs. During *M. avium* infection, glycopeptidolipids are found on the surface of the bacteria are trafficked in MVEs and subsequently loaded into exosomes (30). Mass spectrometry analysis performed on iEVs from *Mtb* infected cells found many *Mycobacterium* proteins in the iEVs. Interestingly, most of these proteins are secreted outside of *Mtb*, suggesting that the presence of these proteins in the cytosol is a critical step for loading them into the iEVs (31, 32). In *Salmonella enterica* serovar Typhimurium infection, LPS is transported in iEVs, as well outer membrane

proteins (33, 34). Additionally, cells infected with *Bacillus anthracis* secrete iEVs that contain active lethal factor toxin (35). These findings show that a variety of bacterial components can be transported in EVs from infected cells and suggest one likely primary mechanism for iEV-elicited immune responses.

## HOST RESPONSE TO EXTRACELLULAR VESICLES

So far, this chapter has discussed how bacterial infections alter the EVs produced by the host cells. Here, I will delve into how these iEVs affect other cells, typically in a pro-inflammatory manner, and how this cellular communication mechanism could serve as a defense to infection.

### *Toll-like receptors.*

TLRs are a class of pattern recognition receptor (PRRs) that are a part of the innate immune system. Different TLRs recognize different pathogen-associated molecular patterns (PAMPs) or danger-associated molecular patterns (DAMPs), such as LPS, lipopeptides, and nucleic acids. When a TLR binds to a PAMP or DAMP, they recruit the adapter protein MyD88, which uses the transcription factor NF- $\kappa$ B to induce the production of immunostimulatory cytokines (36). These pathogen sensing mechanisms were some of the first implicated in the response to iEVs. The Schorey group in 2007 found that iEVs from *M. avium* infected J774 macrophage-like cells induced the production of RANTES and TNF- $\alpha$ , two cytokines produced in response to TLR activation. This response is dependent on MyD88, further suggesting that this phenotype is due to TLR binding PAMPs (30). A similar report, also from the Schorey group in 2007, found that RANTES and TNF- $\alpha$  are produced in response to iEVs derived *M. bovis* BCG infected cells. This response was greatly decreased or completely abolished when treating macrophages lacking functional MyD88, TLR2, or TLR4, and similar results were seen with *Salmonella* infections (37).

RAW 264.7 cells, BMDMs, and DCs also produced TNF $\alpha$  in response to treatment with iEVs from *Salmonella* infected cells. A cytokine array panel found that these iEVs also increased the amount of other TLR-associated cytokines. Using BMDMs from TLR2 or TLR4 knockout mice confirmed that this production of cytokines was dependent on the presence of those TLRs in the recipient cells (33). In confirmation, human embryonic kidney cells that were transfected to express TLR2 and TLR6 produced IL-8 in response to iEVs from *Mtb* treated neutrophils. Interestingly, this result was not seen in cells that expressed TLR4 or TLR5. Macrophages treated with these iEVs also produced IL-6 and TNF $\alpha$ , but not other cytokines such as IL-1 $\beta$ , which is produced in response to inflammasome activation, further supporting that the TLRs are responsible for this response (38).

#### *Interferons.*

Interferons (IFNs) are key aspects of the response to pathogens, and are required for certain activation of immune cells to an antimicrobial state (39). Flow cytometric analysis on splenocytes treated with iEVs from BCG infected macrophages found that CD4 $^{+}$  and CD8 $^{+}$  T cells produced IFN $\gamma$ , an activator of macrophages. This response was increased when CD3 T cells were cultured with bone marrow-derived dendritic cells (BMDCs), suggesting that antigen presentation plays a role in this response (40). Type I interferons, such as IFN- $\alpha$  and IFN- $\beta$ , have typically been associated with helping to defend against viral infections, but they also play a role in bacterial infections (27). Work with *Lm* infections found that iEVs induced IFN- $\beta$  production in macrophages. This was dependent on the cGAS-STING system, which senses cytosolic DNA, in both the infected and recipient cells. As previously discussed in this chapter, *Lm* infections lead to *Lm* DNA being loaded into iEVs, and this bacterial DNA is likely the cause of this response. In fact, cells loaded with double-stranded DNA also triggered IFN- $\beta$  response, confirming that this

response is due to the presence of bacterial DNA in the iEVs (24). Likewise, during *Mtb* infection, iEVs once again induce Type 1 IFNs. This time, the response was dependent on MAVS, an adapter protein to RIG-1, which responds to foreign RNA (26).

#### *Chemotaxis.*

This section thus far has focused on the pro-inflammatory aspect of the iEVs, but that is not the only way that vesicles may aid in defense. Recruitment of immune cells to sites of infection is also critical to stop invasion, and iEVs may also play a part in this immune cell migration and chemotaxis. A cytokine array to measure the response to iEVs during *Mtb* infection found an increase in chemokines in addition to cytokines previously mentioned in this chapter. To determine if these chemokines induced chemotaxis, BMDMs treated with EVs were plated on the bottom of a transwell setup. They found an increase in the chemotaxis of the top layer of cells when the bottom cells were treated with iEVs. This was also seen when the top cells were primary splenocytes, and the cells migrating were primarily neutrophils and T cells (41). Additionally, SVEC-40 endothelial cells treated with *Mtb* iEVs expressed more of the chemokines VCAM1 and CCL2 and allowed for increased migration of BMDMs (42). These responses suggest that iEVs can recruit immune cells to an infection site, although further work needs to be done to fully understand this response.

#### *Growth after treatment.*

Activation of immune cells often results in increased resistance to bacterial infections, even intracellular pathogens who have evolved to grow inside these cells (43). This activation is mimicked by researchers by adding either cytokines such as IFN $\gamma$  or stimulatory components such as LPS. Because of this phenomenon, researchers wondered if activation by iEVs could also have

this protective effect. Macrophages treated with iEVs from *Mtb* infected neutrophils were more resistant to *Mtb* infection, having close to a 10-fold decrease in growth at 24- and 48-hours post infection (38). Similar results were seen with macrophages treated with iEVs from *Mtb* infected macrophages, although this required co-stimulation with IFN $\gamma$ , but there was a difference compared to stimulation with EVs from uninfected cells (26). Despite these promising findings, there remains considerable work to confirm the ability of iEVs to confer non-specific resistance to bacterial infections.

#### USE OF TREATMENTS AND PREVENTATIVE MEASURES *IN VIVO*

The findings so far have all been performed *in vitro*, but several *in vivo* studies regarding EVs have been conducted to determine if iEV treatment generates an immune response *in vivo* like the results seen *in vitro*.

##### *Response to EV treatment in animals.*

Promisingly, treatment of BALB/c and C57BL/6 mice treated intranasally with iEVs from *Mycobacterium* treated cells stimulated the production of TNF- $\alpha$  and IL-12 in lung lysates, like when macrophages were treated with these iEVs. iEV treatment also led to an increase in neutrophil infiltration in the lungs, further suggesting iEVs can have chemotactic properties (37). Further experiments also found that the iEVs increased the expression of IFN $\gamma$  in the spleen, lung, and mediastinal lymph nodes. This treatment also led to an increase in memory CD4 $^{+}$  and CD8 $^{+}$  T cells. Importantly, this response was independent of adding an adjuvant, suggesting that iEVs are sufficient in activating a preemptive defense against infection by themselves (26, 40). Similar immune responses were observed when treating mice with EVs from culture filtrate proteins (CFP)

from *Mtb*, suggesting that preparing iEVs may not actually require an active infection, but just exposure to *Mtb* proteins (31, 44).

Further, iEVs have been found to elicit antibody responses. Intravenous (IV) injection of BALB/c mice with iEVs from BMDCs exposed to diphtheria toxin (DT) resulted in the production of IgM and especially IgG antibodies against DT. Interestingly, these were larger antibody titers than when mice were treated with a combination of DT and LPS (45). Similarly, iEVs from *Salmonella* infected macrophages induced the production of antibodies to *Salmonella* outer membrane proteins, which were found in the iEVs (34). These responses do seem to have a potential effect on defense against these pathogens. When used in combination with the BCG vaccine, a booster with iEVs helped protect mice against a subsequent *Mtb* infection, suggesting potential synergy between these treatments (32, 44). Additionally, iEV treatment helped treatment of moxifloxacin lower the amount of *Mtb* recovered, further suggesting that iEVs could be used in combination with other treatments to protect and treat bacterial infections, although much work remains to be done (26).

#### *Analysis of EVs isolated from infected animals and humans.*

In addition to EVs being explored as treatment for diseases, they also have been predicted to serve as a diagnostic tool. When characterizing EVs produced by animals infected with bacteria, the Schorey group found that the number of EVs isolated from *Mtb* infected mice increased with the level of infection (41). Interestingly, when characterizing the EVs from *Mtb* patients, researchers were able to identify *Mtb* RNA, similar to what they saw during *in vitro* infections (22). Additionally, when probing the urine EVs of *Mtb* patients, they were able to detect the *Mycobacterium* components lipoarabinomannan and CFP-10 by Immuno-PCR, which uses nucleic

acid amplification to increase the sensitivity of enzyme-linked immunosorbent assays. They did have false positives and these EVs could have potentially been produced directly by the bacteria, but this pilot study suggests that EVs could be a way to detect infections in the future (46). To further characterize the role of EVs during *in vivo* infections, researchers used a mouse line lacking Rab27a, a protein involved in EV formation, and found that there was a dampened cytokine response compared to the response of wild-type mice (47). In a similar experiment, mice were treated with an exosome inhibitor and infected with *Lm*, and the CFUs recovered from the spleen were increased compared to the untreated mice (28). EVs from *Lm* infected cells have been found to induce the production of Type I IFNs, and previous works have found that Type I IFN activation actually aids *Lm* infections, giving rise to the possibility that EVs are a way for *Lm* to manipulate the immune system to help the infection, although there is still much to learn about this interaction as whole body systems are quite complex and simple inhibition of proteins may have effects independent of EV depletion (48).

## PLACENTAL IMMUNOLOGY

The placenta is a remarkable organ in which the immune system plays a precarious role, balancing protective responses and potentially deleterious inflammation. The maternal decidua is an immune privileged environment that permits the development of the semi-allogenic placental tissues and fetus. The remodeling of the surrounding environment occurs with the induction of spiral arteries, new blood vessels that increase the access of blood for the placenta. After implantation, where the developing embryo adheres to the lining of the uterus, the invasion of specialized leukocytes and trophoblasts from the placenta aid in further development of this vasculature (49). In humans, roughly 40% of the cells in the decidua are immune cells, and the most notable of these are uterine natural killer (uNK) cells (50). uNK cells aid in the formation and expansion of the spiral arteries

and invasion of the trophoblasts, key steps in placental development (51). There are also macrophages in the decidua, although they mostly exist in an immunoregulatory and anti-inflammatory state. This response is controlled by trophoblasts as they secrete regulatory cytokines (52). The ability of the placenta to regulate the maternal immune response is required for a successful pregnancy, as the fetus and the placenta carry antigens from the other parent, which would normally be targeted by the immune system. Failure to alter this response leads to miscarriages and diseases like preeclampsia (53). Some pathogens exploit this immunosuppressed site, invading and replicating inside the placenta. Placental pathogens include viruses, parasites, and bacteria (54, 55). That said, the placental barrier is not one that is easily crossed. Even pathogens that can invade the placenta do so at a low rate (56). The placenta has a physical barrier with the syncytium of trophoblasts, a fused form of many cells and lacking cell junctions for pathogens to exploit (57, 58). Additionally, trophoblast cells are typically more resistant to infection than other cell types, such as macrophages or endothelial cells (58, 59). The placenta can stimulate a response to infection, although often inflammation of the placenta leads to detrimental outcomes for the fetus.

#### *Placental EVs.*

EVs play a critical role in placental development and immune regulation during pregnancy (Fig. 1.2). The number of EVs per volume of blood in a healthy mother greatly increases during pregnancy, and the majority of these EVs originate from fetal trophoblasts (60). Trophoblast EVs (tEVs) have been found to carry immunoregulatory molecules, presumably suppressing the immune response to allow for the successful development of the fetus (61, 62). However, tEVs also play a detrimental role during placental disease, such as preeclampsia (63, 64). In fact, treatment of mice with tEVs from an injured placenta induced symptoms that are characteristic of

preeclampsia, such as increased blood pressure, suggesting that tEVs are involved with the progression of the disease (65).

## DISSERTATION OVERVIEW

Extracellular vesicles represent an exciting new field of research with many possibilities. This dissertation will explore how bacterial infections alter the EVs produced by the placenta, and how they can affect an immune response. Little is known about this interaction, as prenatal infections are difficult to model, especially considering the extra hurdle of EV isolation. Here, I established a trophoblast stem cell model to study *Lm* placental infections (Chapter 2). We see levels of infection like what is expected in whole placentas. With this infection system, we can isolate EVs and compare their contents of those from infected cells to those from uninfected ones (Chapter 3). Lastly, we then determined how these infection EVs activate immune cells, giving insight into how placentas can defend against infections (Chapter 4).

## APPENDIX

**Figure 1.1. Extracellular vesicles in bacterial infections.** Intracellular bacterial infections alter EVs produced by host cells. EVs then carry bacterial components or have altered host cargo compared to those from uninfected cells. These EVs can activate immune cells into a pro-inflammatory state, suggesting that EVs are a potential host defense mechanism. Made with BioRender.

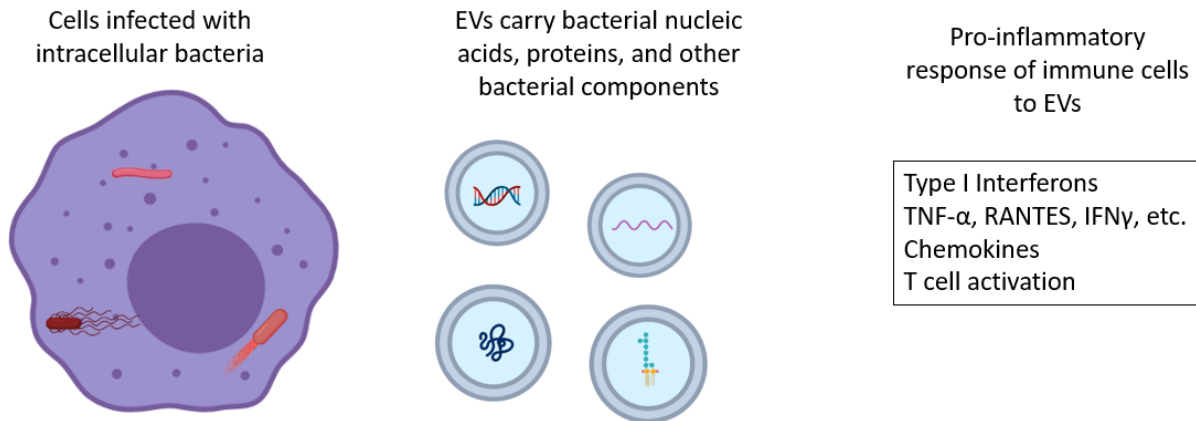
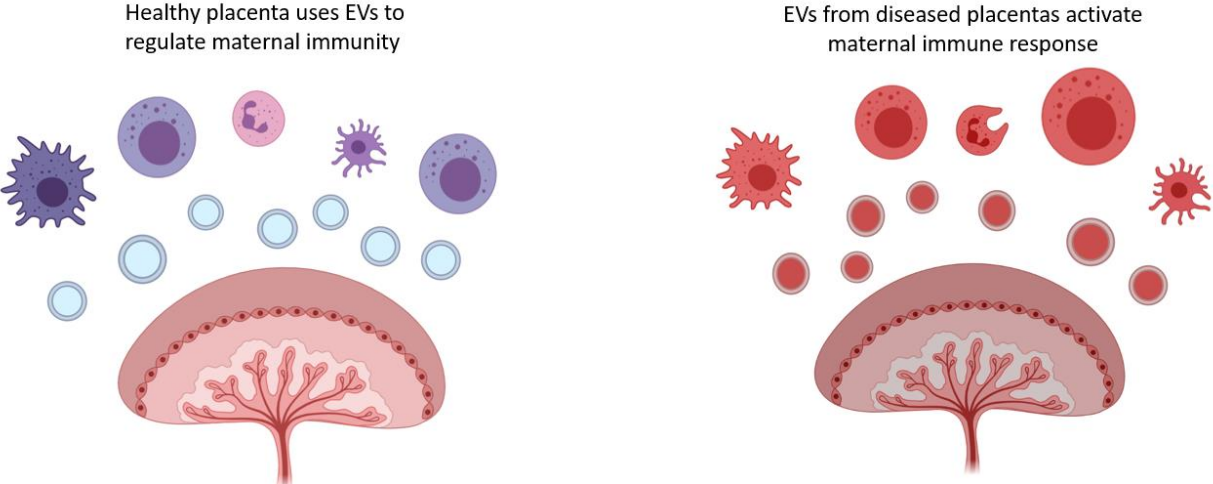


**Figure 1.2. Placental extracellular vesicles.** EVs produced by placental cells help create an altered immune environment that allows the fetus and placenta to grow and develop. During disease, EVs also aid in the inflammatory response that harms the placenta. Made in Biorender.



## REFERENCES

## REFERENCES

1. Ñahui Palomino RA, Vanpouille C, Costantini PE, Margolis L. 2021. Microbiota-host communications: Bacterial extracellular vesicles as a common language. *PLoS Pathog* 17:e1009508.
2. Raposo G, Stoorvogel W. 2013. Extracellular vesicles: exosomes, microvesicles, and friends. *J Cell Biol* 200:373–383.
3. Battistelli M, Falcieri E. 2020. Apoptotic bodies: particular extracellular vesicles involved in intercellular communication. *Biology (Basel)* 9.
4. Yuan K-M, Zhang P-H, Qi S-S, Zhu Q-Z, Li P. 2018. Emerging role for exosomes in the progress of stem cell research. *Am J Med Sci* 356:481–486.
5. Ding W, Rivera OC, Kelleher SL, Soybel DI. 2020. Macrolets: Outsized Extracellular Vesicles Released from Lipopolysaccharide-Stimulated Macrophages that Trap and Kill *Escherichia coli*. *iScience* 23:101135.
6. Théry C, Witwer KW, Aikawa E, Alcaraz MJ, Anderson JD, Andriantsitohaina R, Antoniou A, Arab T, Archer F, Atkin-Smith GK, Ayre DC, Bach J-M, Bachurski D, Baharvand H, Balaj L, Baldacchino S, Bauer NN, Baxter AA, Bebawy M, Beckham C, et al. 2018. Minimal information for studies of extracellular vesicles 2018 (MISEV2018): a position statement of the International Society for Extracellular Vesicles and update of the MISEV2014 guidelines. *J Extracell Vesicles* 7:1535750.
7. Trams EG, Lauter CJ, Salem N, Heine U. 1981. Exfoliation of membrane ecto-enzymes in the form of micro-vesicles. *Biochim Biophys Acta* 645:63–70.
8. Harding C, Heuser J, Stahl P. 1984. Endocytosis and intracellular processing of transferrin and colloidal gold-transferrin in rat reticulocytes: demonstration of a pathway for receptor shedding. *Eur J Cell Biol* 35:256–263.
9. Johnstone RM. 1992. Maturation of reticulocytes: formation of exosomes as a mechanism for shedding membrane proteins. *Biochem Cell Biol* 70:179–190.
10. Raposo G, Nijman HW, Stoorvogel W, Liejendekker R, Harding CV, Melief CJ, Geuze HJ. 1996. B lymphocytes secrete antigen-presenting vesicles. *J Exp Med* 183:1161–1172.
11. Coughlan C, Bruce KD, Burgy O, Boyd TD, Michel CR, Garcia-Perez JE, Adame V, Anton P, Bettcher BM, Chial HJ, Koenigshoff M, Hsieh EWY, Graner M, Potter H. 2020. Exosome isolation by ultracentrifugation and precipitation and techniques for downstream analyses. *Curr Protoc Cell Biol* 88:e110.

12. Serrano-Pertierra E, Oliveira-Rodríguez M, Rivas M, Oliva P, Villafani J, Navarro A, Blanco-López MC, Cernuda-Morollón E. 2019. Characterization of Plasma-Derived Extracellular Vesicles Isolated by Different Methods: A Comparison Study. *Bioengineering (Basel)* 6.
13. Lobb RJ, Becker M, Wen SW, Wong CSF, Wiegmans AP, Leimgruber A, Möller A. 2015. Optimized exosome isolation protocol for cell culture supernatant and human plasma. *J Extracell Vesicles* 4:27031.
14. Tauro BJ, Greening DW, Mathias RA, Ji H, Mathivanan S, Scott AM, Simpson RJ. 2012. Comparison of ultracentrifugation, density gradient separation, and immunoaffinity capture methods for isolating human colon cancer cell line LIM1863-derived exosomes. *Methods* 56:293–304.
15. Valadi H, Ekström K, Bossios A, Sjöstrand M, Lee JJ, Lötvall JO. 2007. Exosome-mediated transfer of mRNAs and microRNAs is a novel mechanism of genetic exchange between cells. *Nat Cell Biol* 9:654–659.
16. Skog J, Würdinger T, van Rijn S, Meijer DH, Gainche L, Sena-Esteves M, Curry WT, Carter BS, Krichevsky AM, Breakefield XO. 2008. Glioblastoma microvesicles transport RNA and proteins that promote tumour growth and provide diagnostic biomarkers. *Nat Cell Biol* 10:1470–1476.
17. Kanada M, Bachmann MH, Hardy JW, Frimannson DO, Bronsart L, Wang A, Sylvester MD, Schmidt TL, Kaspar RL, Butte MJ, Matin AC, Contag CH. 2015. Differential fates of biomolecules delivered to target cells via extracellular vesicles. *Proc Natl Acad Sci USA* 112:E1433-42.
18. Beatty WL, Ullrich HJ, Russell DG. 2001. Mycobacterial surface moieties are released from infected macrophages by a constitutive exocytic event. *Eur J Cell Biol* 80:31–40.
19. Obregon C, Rothen-Rutishauser B, Gerber P, Gehr P, Nicod LP. 2009. Active uptake of dendritic cell-derived exovesicles by epithelial cells induces the release of inflammatory mediators through a TNF-alpha-mediated pathway. *Am J Pathol* 175:696–705.
20. Ramachandra L, Qu Y, Wang Y, Lewis CJ, Cobb BA, Takatsu K, Boom WH, Dubyak GR, Harding CV. 2010. Mycobacterium tuberculosis synergizes with ATP to induce release of microvesicles and exosomes containing major histocompatibility complex class II molecules capable of antigen presentation. *Infect Immun* 78:5116–5125.
21. Wang J, Chen C, Xie P, Pan Y, Tan Y, Tang L. 2014. Proteomic analysis and immune properties of exosomes released by macrophages infected with Mycobacterium avium. *Microbes Infect* 16:283–291.
22. Singh PP, Li L, Schorey JS. 2015. Exosomal RNA from Mycobacterium tuberculosis-Infected Cells Is Functional in Recipient Macrophages. *Traffic* 16:555–571.

23. Momen-Heravi F, Getting SJ, Moschos SA. 2018. Extracellular vesicles and their nucleic acids for biomarker discovery. *Pharmacol Ther* 192:170–187.
24. Nandakumar R, Tschismarov R, Meissner F, Prabakaran T, Krissanaprasit A, Farahani E, Zhang B-C, Assil S, Martin A, Bertrams W, Holm CK, Ablasser A, Klause T, Thomsen MK, Schmeck B, Howard KA, Henry T, Gothelf KV, Decker T, Paludan SR. 2019. Intracellular bacteria engage a STING-TBK1-MVB12b pathway to enable paracrine cGAS-STING signalling. *Nat Microbiol* 4:701–713.
25. Hansen K, Prabakaran T, Laustsen A, Jørgensen SE, Rahbæk SH, Jensen SB, Nielsen R, Leber JH, Decker T, Horan KA, Jakobsen MR, Paludan SR. 2014. *Listeria monocytogenes* induces IFN $\beta$  expression through an IFI16-, cGAS- and STING-dependent pathway. *EMBO J* 33:1654–1666.
26. Cheng Y, Schorey JS. 2019. Extracellular vesicles deliver *Mycobacterium* RNA to promote host immunity and bacterial killing. *EMBO Rep* 20.
27. Ma Z, Damania B. 2016. The cGAS-STING Defense Pathway and Its Counteraction by Viruses. *Cell Host Microbe* 19:150–158.
28. Nandakumar R, Windross SJ, Paludan SR. 2019. Intercellular communication in the innate immune system through the cGAS-STING pathway. *Meth Enzymol* 625:1–11.
29. Reikine S, Nguyen JB, Modis Y. 2014. Pattern Recognition and Signaling Mechanisms of RIG-I and MDA5. *Front Immunol* 5:342.
30. Bhatnagar S, Schorey JS. 2007. Exosomes released from infected macrophages contain *Mycobacterium avium* glycopeptidolipids and are proinflammatory. *J Biol Chem* 282:25779–25789.
31. Giri PK, Kruh NA, Dobos KM, Schorey JS. 2010. Proteomic analysis identifies highly antigenic proteins in exosomes from *M. tuberculosis*-infected and culture filtrate protein-treated macrophages. *Proteomics* 10:3190–3202.
32. García-Martínez M, Vázquez-Flores L, Álvarez-Jiménez VD, Castañeda-Casimiro J, Ibáñez-Hernández M, Sánchez-Torres LE, Barrios-Payán J, Mata-Espinosa D, Estrada-Parra S, Chacón-Salinas R, Serafín-López J, Wong-Baeza I, Hernández-Pando R, Estrada-García I. 2019. Extracellular vesicles released by J774A.1 macrophages reduce the bacterial load in macrophages and in an experimental mouse model of tuberculosis. *Int J Nanomedicine* 14:6707–6719.
33. Hui WW, Hercik K, Belsare S, Alugubelly N, Clapp B, Rinaldi C, Edelmann MJ. 2018. *Salmonella enterica* Serovar Typhimurium Alters the Extracellular Proteome of Macrophages and Leads to the Production of Proinflammatory Exosomes. *Infect Immun* 86.

34. Hui WW, Emerson LE, Clapp B, Sheppe AE, Sharma J, del Castillo J, Ou M, Maegawa GHB, Hoffman C, Larkin, III J, Pascual DW, Edelman MJ. 2021. Antigen encapsulating host extracellular vesicles derived from Salmonella-infected cells stimulate pathogen-specific Th1-type responses in vivo . *PLoS Pathog* 17:1–27.
35. Abrami L, Brandi L, Moayeri M, Brown MJ, Krantz BA, Leppla SH, van der Goot FG. 2013. Hijacking multivesicular bodies enables long-term and exosome-mediated long-distance action of anthrax toxin. *Cell Rep* 5:986–996.
36. Kawai T, Akira S. 2010. The role of pattern-recognition receptors in innate immunity: update on Toll-like receptors. *Nat Immunol* 11:373–384.
37. Bhatnagar S, Shinagawa K, Castellino FJ, Schorey JS. 2007. Exosomes released from macrophages infected with intracellular pathogens stimulate a proinflammatory response in vitro and in vivo. *Blood* 110:3234–3244.
38. Alvarez-Jiménez VD, Leyva-Paredes K, García-Martínez M, Vázquez-Flores L, García-Paredes VG, Campillo-Navarro M, Romo-Cruz I, Rosales-García VH, Castañeda-Casimiro J, González-Pozos S, Hernández JM, Wong-Baeza C, García-Pérez BE, Ortiz-Navarrete V, Estrada-Parra S, Serafín-López J, Wong-Baeza I, Chacón-Salinas R, Estrada-García I. 2018. Extracellular Vesicles Released from Mycobacterium tuberculosis-Infected Neutrophils Promote Macrophage Autophagy and Decrease Intracellular Mycobacterial Survival. *Front Immunol* 9:272.
39. Lee AJ, Ashkar AA. 2018. The dual nature of type I and type II interferons. *Front Immunol* 9:2061.
40. Giri PK, Schorey JS. 2008. Exosomes derived from M. Bovis BCG infected macrophages activate antigen-specific CD4+ and CD8+ T cells in vitro and in vivo. *PLoS ONE* 3:e2461.
41. Singh PP, Smith VL, Karakousis PC, Schorey JS. 2012. Exosomes isolated from mycobacteria-infected mice or cultured macrophages can recruit and activate immune cells in vitro and in vivo. *J Immunol* 189:777–785.
42. Li L, Cheng Y, Emrich S, Schorey J. 2018. Activation of endothelial cells by extracellular vesicles derived from Mycobacterium tuberculosis infected macrophages or mice. *PLoS ONE* 13:e0198337.
43. Portnoy DA, Schreiber RD, Connelly P, Tilney LG. 1989. Gamma interferon limits access of Listeria monocytogenes to the macrophage cytoplasm. *J Exp Med* 170:2141–2146.
44. Cheng Y, Schorey JS. 2013. Exosomes carrying mycobacterial antigens can protect mice against Mycobacterium tuberculosis infection. *Eur J Immunol* 43:3279–3290.

45. Colino J, Snapper CM. 2006. Exosomes from bone marrow dendritic cells pulsed with diphtheria toxoid preferentially induce type 1 antigen-specific IgG responses in naive recipients in the absence of free antigen. *J Immunol* 177:3757–3762.
46. Dahiya B, Khan A, Mor P, Kamra E, Singh N, Gupta KB, Sheoran A, Sreenivas V, Mehta PK. 2019. Detection of Mycobacterium tuberculosis lipoarabinomannan and CFP-10 (Rv3874) from urinary extracellular vesicles of tuberculosis patients by immuno-PCR. *Pathog Dis* 77.
47. Smith VL, Cheng Y, Bryant BR, Schorey JS. 2017. Exosomes function in antigen presentation during an in vivo Mycobacterium tuberculosis infection. *Sci Rep* 7:43578.
48. Osborne SE, Sit B, Shaker A, Currie E, Tan JMJ, van Rijn J, Higgins DE, Brumell JH. 2017. Type I interferon promotes cell-to-cell spread of Listeria monocytogenes. *Cell Microbiol* 19.
49. Pijnenborg R, Vercruyssen L, Hanssens M. 2006. The uterine spiral arteries in human pregnancy: facts and controversies. *Placenta* 27:939–958.
50. Manaster I, Mandelboim O. 2010. The unique properties of uterine NK cells. *Am J Reprod Immunol* 63:434–444.
51. Hanna J, Goldman-Wohl D, Hamani Y, Avraham I, Greenfield C, Natanson-Yaron S, Prus D, Cohen-Daniel L, Arnon TI, Manaster I, Gazit R, Yutkin V, Benharroch D, Porgador A, Keshet E, Yagel S, Mandelboim O. 2006. Decidual NK cells regulate key developmental processes at the human fetal-maternal interface. *Nat Med* 12:1065–1074.
52. Svensson-Arvelund J, Mehta RB, Lindau R, Mirrasekhian E, Rodriguez-Martinez H, Berg G, Lash GE, Jenmalm MC, Ernerudh J. 2015. The human fetal placenta promotes tolerance against the semiallogeneic fetus by inducing regulatory T cells and homeostatic M2 macrophages. *J Immunol* 194:1534–1544.
53. Ander SE, Diamond MS, Coyne CB. 2019. Immune responses at the maternal-fetal interface. *Sci Immunol* 4.
54. Arora N, Sadovsky Y, Dermody TS, Coyne CB. 2017. Microbial Vertical Transmission during Human Pregnancy. *Cell Host Microbe* 21:561–567.
55. Megli C, Morosky S, Rajasundaram D, Coyne CB. 2021. Inflammasome signaling in human placental trophoblasts regulates immune defense against Listeria monocytogenes infection. *J Exp Med* 218.
56. Bakardjiev AI, Theriot JA, Portnoy DA. 2006. Listeria monocytogenes traffics from maternal organs to the placenta and back. *PLoS Pathog* 2:e66.

57. Robbins JR, Skrzypczynska KM, Zeldovich VB, Kapidzic M, Bakardjiev AI. 2010. Placental syncytiotrophoblast constitutes a major barrier to vertical transmission of *Listeria monocytogenes*. *PLoS Pathog* 6:e1000732.
58. Zeldovich VB, Clausen CH, Bradford E, Fletcher DA, Maltepe E, Robbins JR, Bakardjiev AI. 2013. Placental syncytium forms a biophysical barrier against pathogen invasion. *PLoS Pathog* 9:e1003821.
59. Robbins JR, Zeldovich VB, Poukchanski A, Boothroyd JC, Bakardjiev AI. 2012. Tissue barriers of the human placenta to infection with *Toxoplasma gondii*. *Infect Immun* 80:418–428.
60. Mitchell MD, Peiris HN, Kobayashi M, Koh YQ, Duncombe G, Illanes SE, Rice GE, Salomon C. 2015. Placental exosomes in normal and complicated pregnancy. *Am J Obstet Gynecol* 213:S173-81.
61. Sabapatha A, Gercel-Taylor C, Taylor DD. 2006. Specific isolation of placenta-derived exosomes from the circulation of pregnant women and their immunoregulatory consequences. *Am J Reprod Immunol* 56:345–355.
62. Stenqvist A-C, Nagaeva O, Baranov V, Mincheva-Nilsson L. 2013. Exosomes secreted by human placenta carry functional Fas ligand and TRAIL molecules and convey apoptosis in activated immune cells, suggesting exosome-mediated immune privilege of the fetus. *J Immunol* 191:5515–5523.
63. Han C, Wang C, Chen Y, Wang J, Xu X, Hilton T, Cai W, Zhao Z, Wu Y, Li K, Houck K, Liu L, Sood AK, Wu X, Xue F, Li M, Dong J-F, Zhang J. 2019. Placenta-derived extracellular vesicles induce preeclampsia in mouse models. *Haematologica* <https://doi.org/10.3324/haematol.2019.226209>.
64. Gill M, Motta-Mejia C, Kandzija N, Cooke W, Zhang W, Cerdeira AS, Bastie C, Redman C, Vatish M. 2019. Placental Syncytiotrophoblast-Derived Extracellular Vesicles Carry Active NEP (Neprilysin) and Are Increased in Preeclampsia. *Hypertension* 73:1112–1119.
65. Han C, Han L, Huang P, Chen Y, Wang Y, Xue F. 2019. Syncytiotrophoblast-Derived Extracellular Vesicles in Pathophysiology of Preeclampsia. *Front Physiol* 10:1236.

## CHAPTER 2

### MODELING *LISTERIA MONOCYTOGENES* INFECTIONS

## ABSTRACT

In an ideal world, we would be able to study infections in model systems that perfectly represent every aspect of the infection. Unfortunately, this is not feasible, as any animal model is expensive and has its drawbacks. For example, cellular interactions can be difficult to study in animals because of the complexity of tissues and the inability to easily obtain kinetic data. Therefore, we must sometimes use *in vitro* models to study host-pathogen interactions in molecular detail. Here, we established a trophoblast stem cell (TSC) model to study placental infections by *Listeria monocytogenes* (*Lm*). Trophoblasts are one of the primary cell types of the placenta and come into direct contact with the parental bloodstream. As such, *Lm* needs to invade these cells to establish an infection in the placenta. TSCs offer an opportunity to study this invasion in the lab, as much is still unknown about this aspect of the infection since placentas are complex tissues that are difficult to model *in vitro*. TSCs represent a useful model, as they differentiate to form a large part of the placenta, but importantly, they are replicative with the use of growth factors, allowing for continued experiments. Here, I report that TSCs can be infected *Lm*, where we see bacterial replication and cytosolic invasion, although these events occur at later timepoints compared to other cell types, such as macrophages. Differentiated trophoblasts were even more resistant to infection, with barely any *Lm* growth seen days after infection. In addition to placental infections, *Lm* also crosses the blood-brain barrier, leading to poor outcomes to the infected. I also modeled this infection using neural progenitor cells, observing high levels of *Lm* replication at even low number of bacteria to cells. This chapter focuses on studying these interactions, establishing models to study *Lm* infections in systems that have not previously been fully investigated.

## INTRODUCTION

The placenta is a remarkable organ in which the immune system plays a precarious role, balancing protective responses and potentially deleterious inflammation. The placenta and the surrounding tissue are an altered immune environment that permits the development of the semi-allogenic placental tissues and fetus; some pathogens exploit this immunosuppressed site, invading and replicating inside the placenta. Placental pathogens include viruses, parasites, and bacteria (1). One such organism is the Gram-positive bacterium *Listeria monocytogenes* (*Lm*) (2). This facultative intracellular parasite is the causative agent of listeriosis, an illness that affects approximately 1600 people annually in the United States, resulting in around 300 deaths (3). Listeriosis typically afflicts the immunocompromised, with pregnant people being especially at risk (4). Prenatal listeriosis can lead to spontaneous abortions, stillbirths, and birth defects, while pregnant mothers may show only mild symptoms (5). *Lm* is initially ingested with contaminated food such as deli meats, soft cheeses, and other dairy products. It escapes from the gastrointestinal tract and into the bloodstream, where it disseminates throughout the body and invades the liver, spleen, and the placenta (6). This pathogen has a well-characterized intracellular lifecycle which allows it to spread throughout host tissues, within monocytes and other cells. *Lm* enters the cell either by phagocytosis or by means of internalins, virulence factors that bind host surface proteins and induce uptake (7). Once in the cell, *Lm* is first contained in a phagosomal vacuole, which it lyses by means of the cholesterol-dependent cytolysin listeriolysin O (LLO), encoded by the *hly* gene, gaining access to the cytosol (8). LLO is active in the low pH environment of the vacuole, and acts by binding to membrane-bound cholesterol and creating a pore in the membrane, leading to the lysis of the whole vacuole (9). Once in the cytoplasm, *Lm* scavenges the host for nutrients and replicates. Eventually, the bacterium uses the protein ActA to hijack and polymerize host actin to

create actin rockets, which facilitate intracellular motility and entry into neighboring cells, where it restarts this process (10, 11). Importantly, the ability of *Lm* to replicate intracellularly allows it to undergo cell-to-cell spread in trophoblasts, breaching placental barrier while minimizing exposure to the extracellular environment (6).

Modeling placental function *in vitro* is a challenge. Replicating trophoblast cell lines are convenient, but their genetic alterations conferring proliferation may compromise their response to infection (12). Primary human or mouse cells or explants are a superior representation of *in vivo* trophoblasts, but they are expensive and laborious to isolate and cannot be maintained in culture, requiring repeated isolation (13). TSCs offer an alternative between the two extremes. They are isolated from mouse blastocysts and are naturally replicating with the addition of growth factors, facilitating repeated controlled experiments while also maintaining many biological properties (14, 15). In this chapter, I describe cellular models to study *Lm* infections in laboratory settings, allowing for the study of placental infections and beyond.

## MATERIALS AND METHODS

### *Bacterial cultures.*

*Listeria monocytogenes* 10403S bioluminescent strain 2C (Xen32) was used throughout the study (16). This strain has a *lux-kan* insertion in the *flaA* locus and has a four-fold increase in intravenous 50% lethal dose compared to wild type 10403S. Constitutively green fluorescent protein (GFP)-expressing *Lm* (10403S wild-type strain transformed with pMB2044) was kindly provided by Dr. Daniel A. Portnoy (University of California, Berkeley, CA). All strains were grown in brain heart infusion medium (BHI) to mid-logarithmic phase for infection.

### *Cell culture.*

TSCs were originally isolated from C57BL/6 mice and were graciously donated by Dr. Julie Baker (Stanford University, Palo Alto, CA) (14). They were grown in RPMI 1640 medium with GlutaMAX, 20% fetal bovine serum (FBS), and 1  $\mu$ M sodium pyruvate, as well as 35  $\mu$ g/mL fibroblast growth factor 4 (FGF-4), 10 ng/mL activin, and 1  $\mu$ g/mL heparin to maintain TSC replication (15). HTR-8/SVneo cells were acquired from ATCC and were grown in RPMI medium with GlutaMAX and 5% FBS. C17.2 and NE-4C neural progenitor cells were obtained from ATCC and grown in RPMI medium with GlutaMAX, 10% FBS, and 1  $\mu$ M sodium pyruvate.

### *Listeria intracellular growth assay.*

Cells were plated into a 24 well plate at  $5 \times 10^4$  cells/well. After sufficient time to allow the cells to replicate and reach confluence, they were washed three times with PBS. Medium with *Lm* was added at the given multiplicity of infection (MOI) for colony forming units of *Lm* per cell. After 1 h, the wells were washed 3 times with phosphate buffered saline (PBS) and medium with 5  $\mu$ g/mL gentamicin was added. Bioluminescence images were taken at the given timepoints using an *In Vivo* Imaging System (IVIS) Lumina System (Perkin Elmer, Inc.), with 5 min of exposure and large binning, starting upon infection. The signal was quantified using Living Image software (Perkin Elmer). Images were again taken at the given time points.

### *Fluorescence microscopy.*

Flame-sterilized glass coverslips were placed into a 6-well dish.  $10^5$  cells were seeded into each well. The trophoblasts were infected 24 h later with mid-log GFP expressing *Lm* at an MOI of 100 or 1000 as previously reported for trophoblasts (17). For C17.2 neural progenitor cells, MOIs of 100, 10, and 1 were used. After one hour, the cells were washed three times with PBS and the

media were replaced with medium containing 5 µg/mL gentamicin. At the listed periods post-infection, the cells were fixed with 4% paraformaldehyde and solubilized with 0.1% Triton X-100. The coverslips were treated with Rhodamine phalloidin (Invitrogen) for 30 min. The coverslips were then mounted to slides with 4',6-diamidino-2-phenylindole (DAPI) Fluoromount-G (SouthernBiotech). The slides were imaged with Olympus Filter FV1000 confocal microscope and images were taken at 60x magnification.

## RESULTS

### *Trophoblast stem cell Listeria infection.*

Trophoblast stem cells (TSCs) from C57BL/6 mice were used to model placental infections. TSCs were infected with either *Lm* at a multiplicity of infection (MOI) of 100, and fluorescence microscopy was used to visualize the infection at 24 h post-infection (HPI), confirming that *Lm* infects these cells, as well as replicate and polymerize actin in this time frame (Fig. 2.1). To determine what *Lm* virulence factors are involved with the TSC invasion, we infected these cells with bioluminescent strains of either wild type (WT),  $\Delta hly$  (used for vacuolar escape),  $\Delta actA$  (polymerizes host actin), or  $\Delta inlA/inlB$  *Lm* (used to invade into cells). We saw that *Lm* lacking InlA and InlB, internalins that are primary responsible for allowing *Lm* to gain access into non-phagocytic cells, did not have growth differences compared to the WT infection. We did see a decrease in growth when infecting with *Lm* lacking LLO ( $\Delta hly$ ) or ActA. Importantly, these infections required an MOI of 100, a higher number of bacteria compared to typical macrophage infections. These results show that TSCs are readily infected with *Lm*, albeit less efficiently than J774 macrophages or other professional phagocytes (18).

### *TSC differentiation.*

In the mouse placenta, TSCs differentiate into different trophoblast types, such as syncytiotrophoblasts (SynTs) and trophoblast giant cells (TGCs), a to serve various functions. Previous studies found that removal of the growth factors FGF-4 and activin, which are used to continue the proliferation of TSCs, pushes the cells toward the TGC phenotype. Additionally, addition of retinoic acid (RA), the active derivative of vitamin A, has been found to further push cells towards TGC differentiation (19). Similarly, the activation of either the Wnt pathway or the inhibition of the hypoxia-induced factor (HIF) response pushes TSCs to SynTs (20, 21). Here, we tested if differentiation of TSCs altered their susceptibility to *Lm* infection.

We treated TSCs with either GFs, base media (BM) alone, 5  $\mu$ M RA, 3  $\mu$ M CHIR99021 (CHIR), or 10  $\mu$ g/mL U0126. The cells that received RA, CHIR, or U0126 did not receive any growth factors. CHIR is an activator of the Wnt pathway, a cascade that is involved in many functions throughout the body and is required for proper placental development (20). U0126 is a MAP2K1/2 inhibitor, which is a part of the HIF response (22). Both treatments were predicted to lead to SynTs, where BM and RA treatments were expected to produce TGCs.

After 96 hours, we imaged the cells with a light microscope to see if there were any visible differences. Our images show that removal of GFs and the treatment of RA did indeed change the cellular morphology of TSCs (Fig. 2.3 B,C). Instead of clusters of tightly packed cells that we see with GFs, these cells have large areas of cytoplasm and branching reaches of the cellular membrane. These morphologies are in line with what has been reported with TGCs, suggesting that we have successfully differentiated the TSCs. Additionally, there appeared to be less cellular growth as compared to the GFs conditions, further suggesting that the treated cells were

differentiated away from their previously replicative state. We also saw that treatment with CHIR and U0126 changed the morphology of the TSCs (Fig. 2.3 D,E). These cells were larger and the barriers between the cells were not as distinct. This is agreement with the phenotypes of SynTs, which fuse together to form a multinucleated syncytium.

Finally, we infected the differentiated trophoblasts with bioluminescent *Lm* to determine if there was any difference in susceptibility. We found that the differentiated trophoblasts were more resistant to *Lm* than TSCs grown with GFs. This was true whether the TSCs were treated with BM alone, RA, or CHIR (Fig. 2.4).

#### *HTR-8/SVneo human trophoblasts.*

While TSCs have been used as our primary model throughout most of the work, they are not the only model available to study trophoblast infections. For example, HTR-8/SVneo cells are derived from human trophoblasts and are continuously replicating due to the presence of the simian virus 40 large T antigen gene, a helicase that leads to the expression of host genes involved in replication (23, 24). Importantly, these cells are derived from human extravillous trophoblasts, a type of trophoblasts that mice do not have. Like our observations of TSCs, we found replicating *Lm* at 24 HPI and bacteria polymerizing actin, signaling that *Lm* can go through its normal intracellular life cycle in these cells (Fig. 2.5). Again, it required a high MOI, further suggesting that trophoblasts are more resistant to *Lm* infection compared to some other cell types.

#### *Neural progenitors.*

So far, I have primarily focused on placental infections, but that is not the only area of concern when it comes to *Lm*. *Lm* also crosses the blood-brain barrier and establishes an infection in the brain. We used neural progenitor cells, NE-4C and C17.2 cells, to model this infection. We infected

NE-4C cells with various MOIs of *Lm* to determine how susceptible these cells are to infection (Fig. 2.6). We saw growth of *Lm* with as low of an MOI of 10:1, although growth was not observed until 24 HPI. We also imaged the infection of C17.2 cells using confocal microscopy. Once again, we see replicating *Lm* and polymerized actin at 24 HPI, telling us that these cells can support the invasion and growth of *Lm*. Interestingly, these observations were seen at an MOI of just 1, meaning that an equal number of bacterial cells were added to the neural progenitors (Fig. 2.7). This contrasts with our observations of trophoblasts, suggesting that neural progenitor cells are more susceptible to infection.

## DISCUSSION

Creating models to study specific aspects of biology has been critical for the advancement of research. The ability to safely and accurately study infections in a laboratory setting allows for development of treatments and preventative measures with better understanding of the host-pathogen interactions.

Animal models have exhibited conflicting results with *Lm* infections. Mice are typically the model of choice for most infections because of the relatively low cost, well characterized genetic background, and established protocols. Unfortunately, mice are not ideal to use as a model for *Lm* infection. Researchers originally were not able to see *Lm* infection in mice when they administered the bacteria orally, the route of transmission in humans. This is because the mouse version of the protein E-cadherin, which *Lm* binds with InlA to induce uptake, differs from the human homolog by a single amino acid, making the host cells resistant to *Lm* invasion (7). Subsequent genetic manipulation of either the mouse E-cadherin or *Lm* InlA allows for the binding of these factors, and thus epithelial cell invasion. That said, it still requires large amounts of an oral gavage to

observe the symptoms common during human infections. These problems are even more pronounced when studying placental infections. From a strictly anatomical perspective, guinea pigs offer the best non-primate animal model to study this infection. Their E-cadherin binds with InlA, and their placenta structure is quite like that of humans. Unfortunately, guinea pigs are substantially more expensive and require larger and specialized housing facilities, thus limit researchers' opportunities to use these animals. Our lab does have an established mouse model of infection, where we see growth of *Lm* in the placenta using IVIS imaging (25). That said, it is important to consider the limitations of this model, such as mice having different placental structure than humans. Humans have only a single layer of SynTs, where mice have two. Likewise, humans have extravillous trophoblasts that invade into the surrounding decidua while mice have a labyrinth bathed in maternal blood. That said, mice and human placentas share similarities at the cellular level, with both containing TSCs and SynTs. Focusing on using these cells to model placental infections allows us to study this complex system in a controlled laboratory setting (26).

Here, we found that TSCs isolated from C57BL/6 could be infected with *Lm* (Figs. 1.1+1.2). *Lm* lacking *inlA* and *inlB* do not have any growth defects in the TSCs compared to the WT (Fig. 1.1). This suggests that *Lm* enters the cells independently of these two proteins. Trophoblasts are phagocytic, providing one potential mechanism of cellular entry (27). Additionally, InlP has been found to bind to afadin in trophoblasts and contributes to placental infection (28–30). We did see decreased growth with the *Lm* strains lacking LLO or ActA. The lack of growth with the  $\Delta hly$  strain was expected, as it encodes the protein LLO, which *Lm* utilizes to escape the vacuole and into the cytosol, where it replicates. Typically,  $\Delta hly$  *Lm* are severely deficient in infectivity, often several logs lower in growth than WT strains (8). In contrast,  $\Delta actA$  mutants typically do not have decreased growth in cellular models similar to the ones deployed here, as the ActA protein is

responsible for actin polymerization and cell-to-cell spread, an event that typically occurs after replication (11). That we saw similar growth for the two models is surprising and could be a feature of the TSCs biology or a product of the IVIS imaging. Further work is required to fully understand these findings.

As previously stated, there are different types of trophoblasts throughout the placenta that serve diverse functions. In both humans and mice, SynTs fuse together to form a syncytium, a multinucleated conglomerate of cells. These cells are in direct contact with the parental bloodstream, and the syncytium acts as an additional barrier against pathogens (31). While humans do not have TGCs (instead the placentas contain cytotrophoblasts and extravillous trophoblasts), studying TGCs may still give us insight into *Lm* infections. In the placenta, these different trophoblast types differentiated from TSCs similar to our *in vitro* model. Here, we differentiated TSCs to resemble these different trophoblasts. We withheld the GFs required for the TSCs to continually proliferate, as well as adding retinoic acid, which pushed TSCs to TGC phenotypes. Treatment with U0126 or CHIR helped for a visible syncytium, especially U0126 (Fig. 2.3). Interestingly, when these cells were infected with *Lm*, the differentiated cells did not permit any *Lm* growth, unlike TSCs themselves. This is fascinating, as the differentiated cells are more likely to encounter *Lm*, particularly the SynTs. A previous study suggests that the formation of a syncytium helps defend against invasion by acting as a mechanical barrier to pathogens, and this could be a mechanism as to why the placenta is infected at a relatively low rate as SynTs are the trophoblasts that interact with the maternal bloodstream (32). The cells differentiated to a TGC cell type were also resistant to infection, potentially because there are less cell-to-cell junctions so there are less opportunities for *Lm* to attach and invade. In summary, we can differentiate the TSCs to phenotypes that resemble different trophoblast types. This differentiation also made the cells

resistant to *Lm* infection, potentially modeling the placental barrier that is a big challenge for pathogens to cross.

TSCs are not the only cells used to model the placenta *in vitro*. There are numerous trophoblast cell lines that have genetic alterations that allow them to continually replicate, providing a relatively cheap and easy way to study infections. HTR-8/SVneo cells are transfected with the gene encoding simian virus 40 large T antigen (33). This gene alters the host cell cycle, allowing for continual replication. Importantly, these cells are derivatives of human extravillous trophoblasts, which are not found in mice and thus we are not able to model them using TSCs. Additionally, as far as we are aware, no studies have shown if they are susceptible to *Lm* infection. Indeed, like TSCs, we see *Lm* in the cytosol and polymerizing actin at 24 HPI (Fig. 1.5). That said, this infection occurred using a MOI of 1000:1, suggesting that while these cells can get infected, they are still relatively resistant to *Lm* invasion.

In addition to invading the placenta, *Lm* also can infect the brain and the central nervous system (CNS) (34). Like the placenta, this invasion is rare, it does lead to dangerous outcomes for the patient. Modeling this infection in a laboratory setting can help lead to further understanding of this infection. We used neural progenitor cell lines to create a model to study the blood-brain barrier invasion. Like TSCs in the placenta, neural progenitors act as the source cells for the glial and neuronal cells in the CNS (35). In C17.2 and NE-4C neural progenitors, we see cytosolic *Lm* polymerizing actin at 24 HPI, suggesting that these cells are permissive to *Lm* infection. In fact, this image was taken at an MOI of 1, so an equal number of bacteria were added to cells. This further suggests that these cells are not only permissive for growth but are readily infected by *Lm*. The establishment of these neural progenitor cells as a model to study *Lm* brain invasion could be a key step in further understanding the mechanisms of this infection.

## APPENDIX

**Figure 2.1. *Lm* replicate and polymerize actin in TSCs.** Trophoblast stem cells (TSCs) from C57BL/6 mice were infected with GFP-expressing *Lm* at a multiplicity of infection (MOI) of 100:1. At 24 hours post infection, the cells were fixed and stained with DAPI (Blue) and Rhodamine phalloidin (Red) which bind to DNA and polymerized actin, respectively. The cells were later imaged with an Olympus FluoView scanning confocal light microscope. The white arrows point to host actin polymerized by cytosolic *Lm*. The scale bar is 20  $\mu$ m.

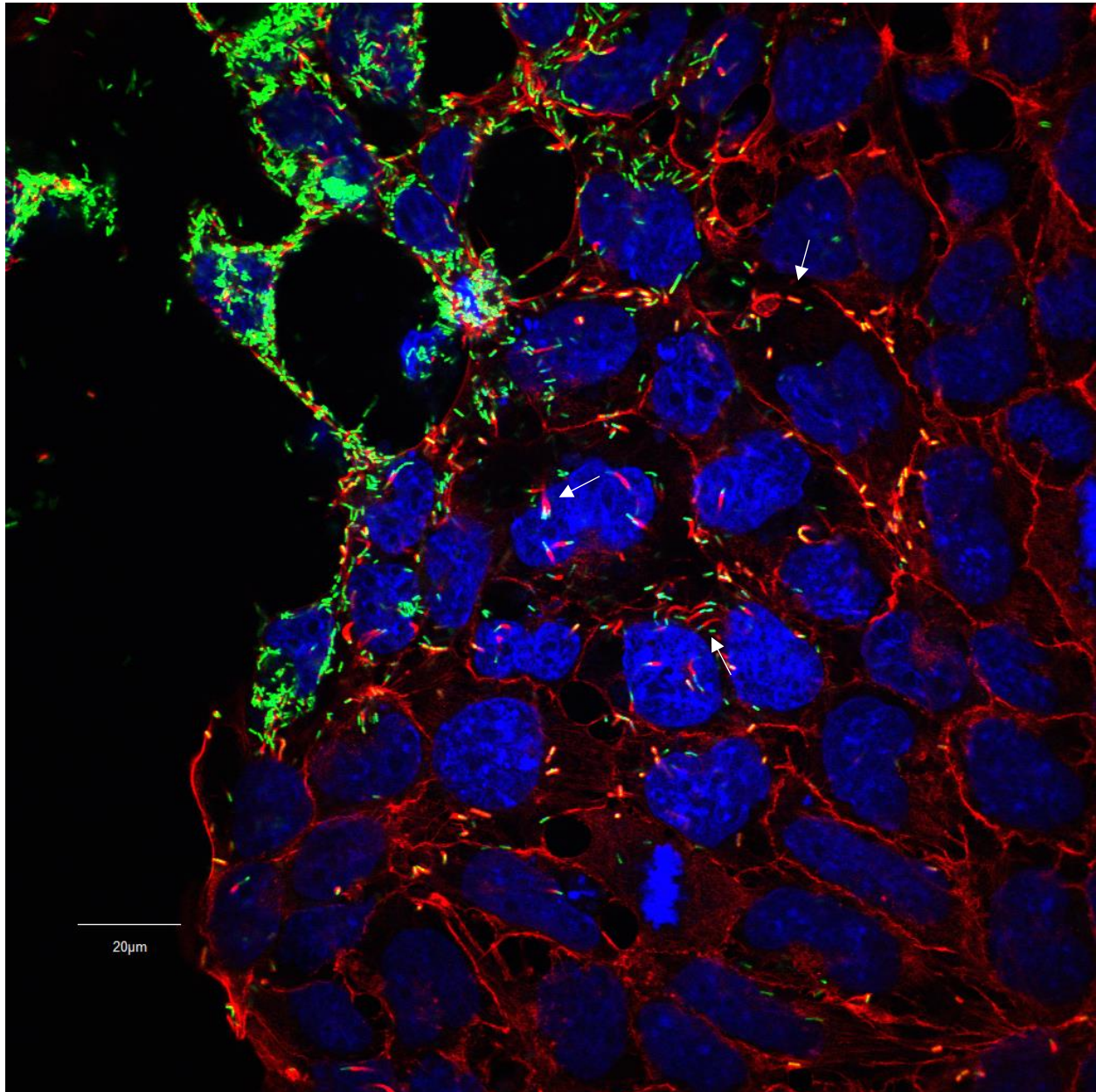


**Figure 2.2. TSCs infected with bioluminescent *Lm*.**  $5 \times 10^5$  TSCs were infected at MOI=100 with the indicated strains of mid-log bioluminescent *Lm*. The cells were imaged using the PerkinElmer in vivo imaging system (IVIS). Six replicates were used for each group.

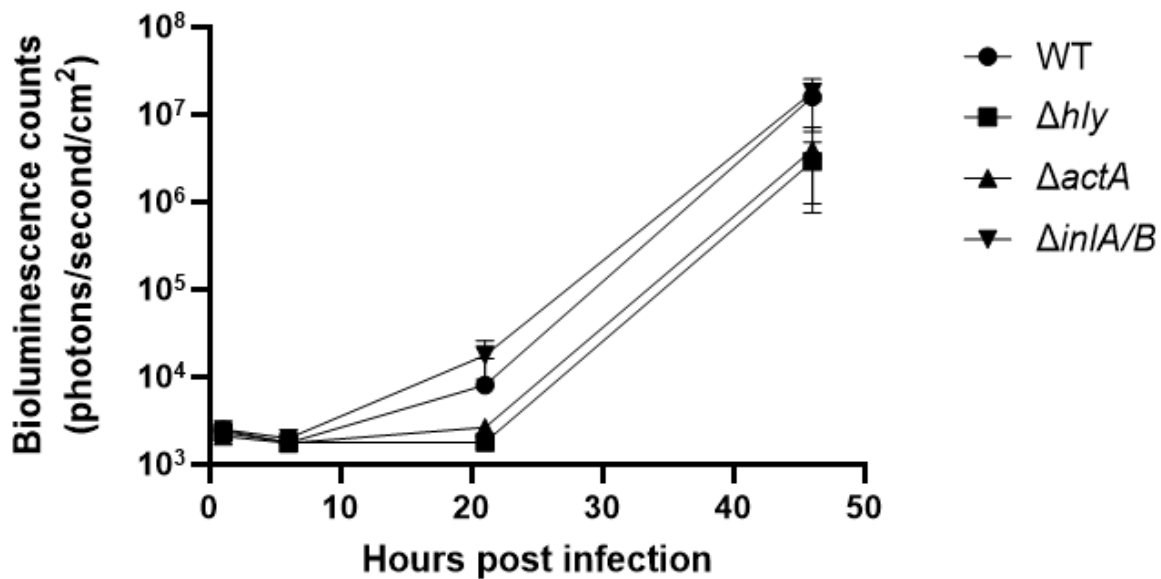


**Figure 2.3. Pictures of differentiated TSCs.** TSCs were treated with either GFs (A), BM (B), RA (C), CHIR (D), or U0126 (E). Four days after treatment, the cells were imaged at 40x magnification.

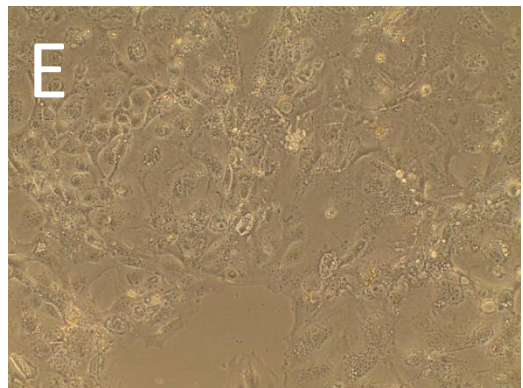
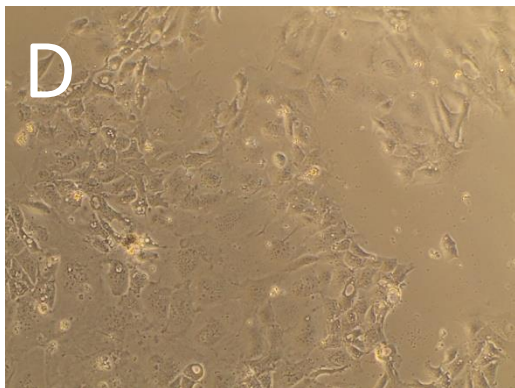
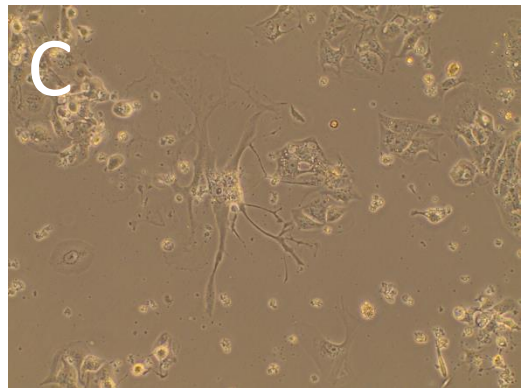
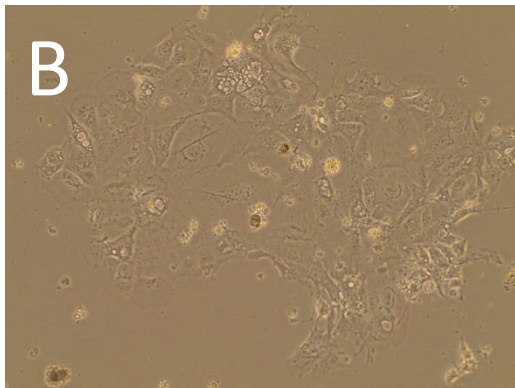
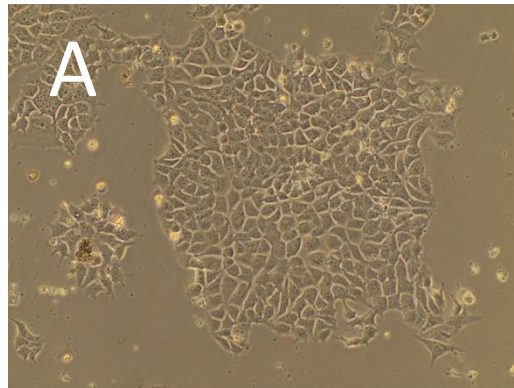


**Figure 2.4. IVIS *Lm* infection of differentiated trophoblasts.**  $5 \times 10^5$  TSCs were treated with the indicated treatments for 96 hours. They were then infected at MOI=100 with mid-log bioluminescent *Lm*. The cells were imaged using the PerkinElmer IVIS.

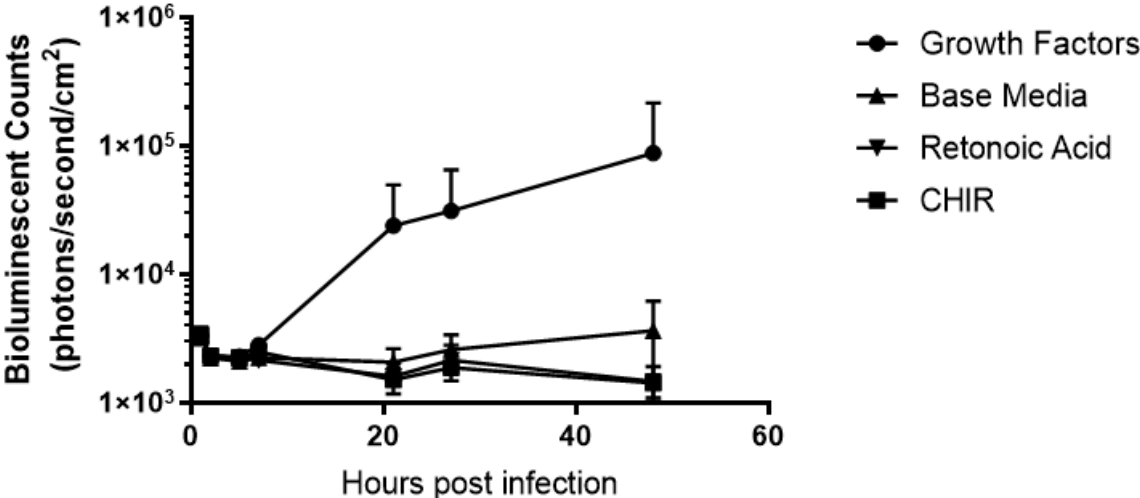


**Figure 2.5. Microscopy of *Lm*-infected HTR-8/SVneo cells.** HTR-8/SVneo trophoblast cells were infected with GFP-expressing *Lm* at a MOI of 1000:1. At 24 hours post infection, the cells were fixed and stained with DAPI (Blue) and Rhodamine phalloidin (Red) which bind to DNA and polymerized actin, respectively. The cells were later imaged with an Olympus FluoView scanning confocal light microscope. The white arrows point to host actin polymerized by cytosolic *Lm*. The scale bar is 10  $\mu$ m.

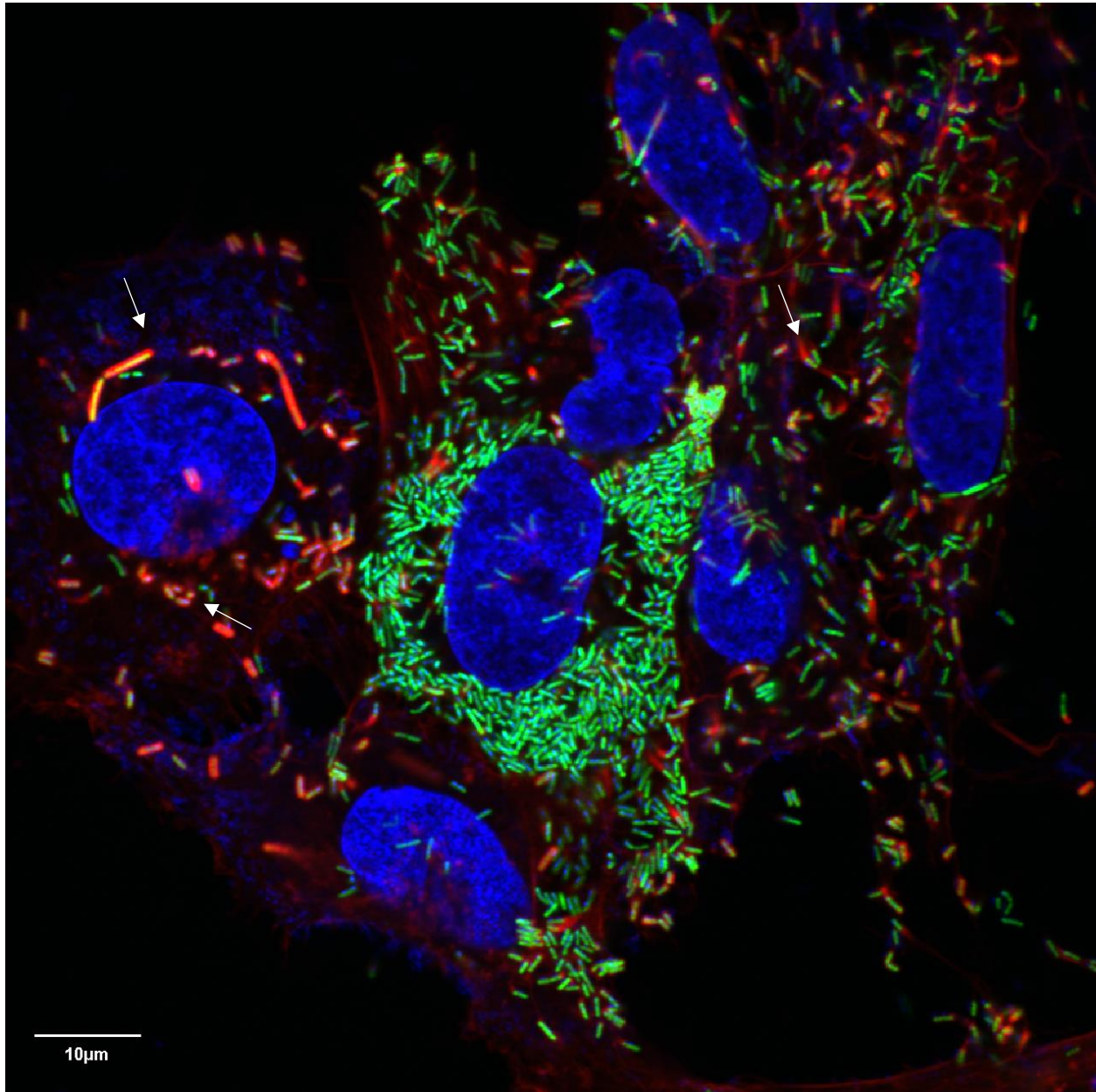


**Figure 2.6. NE-4C neural progenitors infected with bioluminescent *Lm*.**  $5 \times 10^5$  NE-4C cells were infected at MOIs of 10, 100, and 1,000 of mid-log bioluminescent *Lm*. The cells were imaged using the PerkinElmer IVIS.

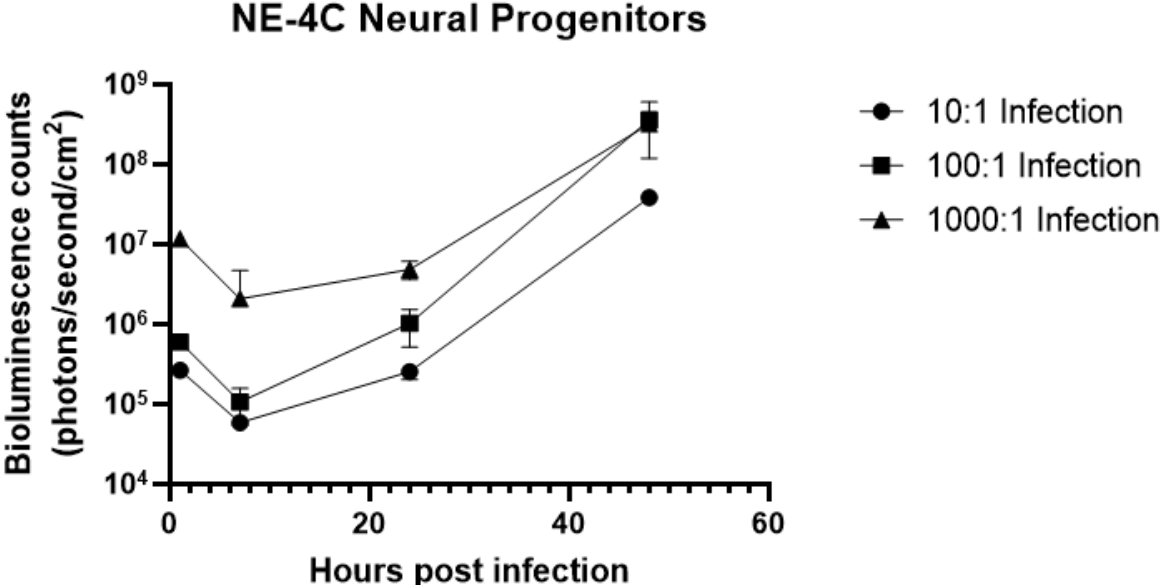
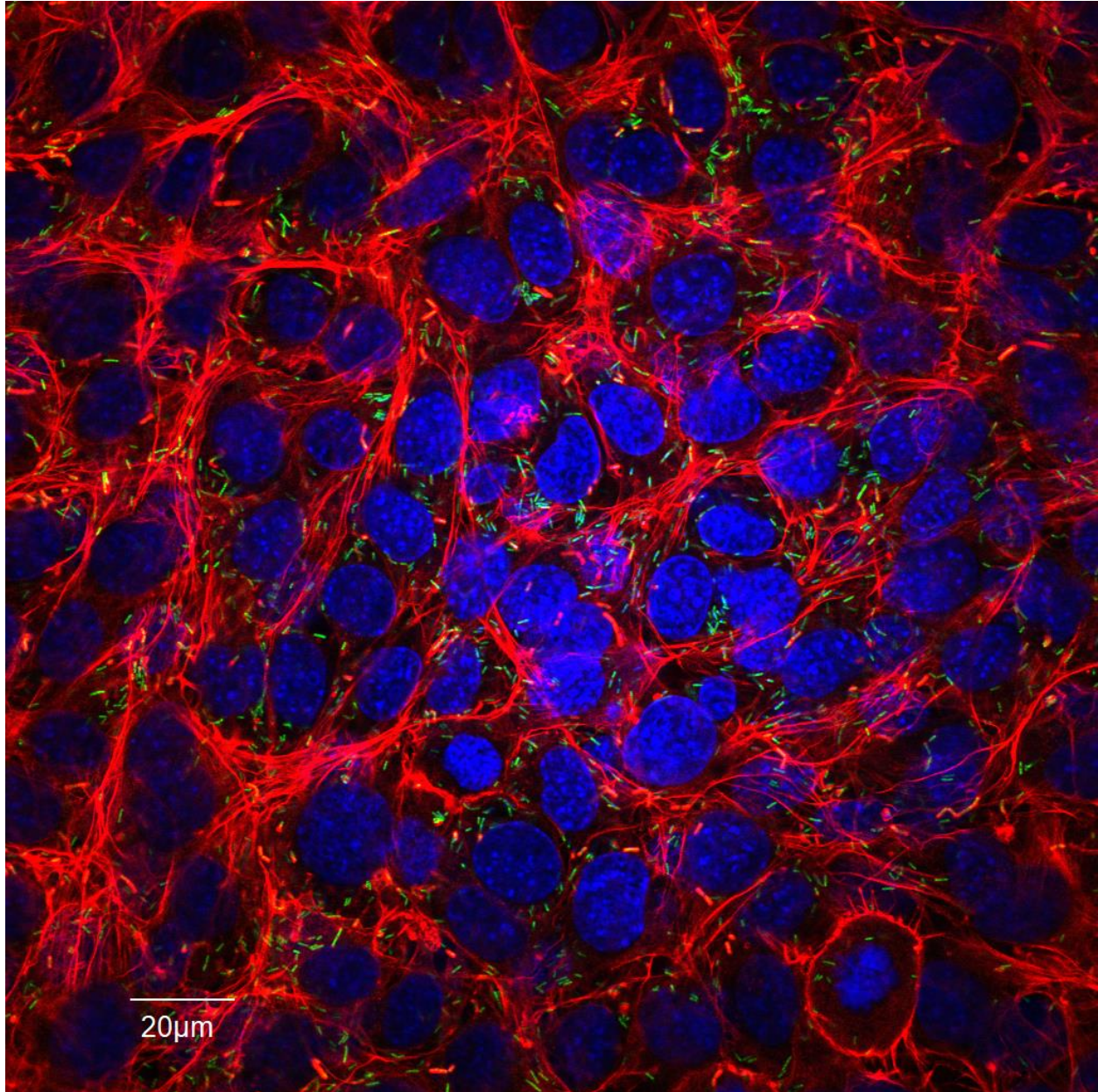


**Figure 2.7. Microscopy of *Lm*-infected C17.2 neural progenitor cells.** C17.2 were infected with GFP-expressing *Lm* at a MOI of 1:1. At 24 hours post infection, the cells were fixed and stained with DAPI (Blue) and Rhodamine phalloidin (Red) which bind to DNA and polymerized actin, respectively. The cells were later imaged with an Olympus FluoView scanning confocal light microscope. The scale bar is 20  $\mu\text{m}$ .



## REFERENCES

## REFERENCES

1. Arora N, Sadovsky Y, Dermody TS, Coyne CB. 2017. Microbial Vertical Transmission during Human Pregnancy. *Cell Host Microbe* 21:561–567.
2. Vázquez-Boland JA, Kuhn M, Berche P, Chakraborty T, Domínguez-Bernal G, Goebel W, González-Zorn B, Wehland J, Kreft J. 2001. *Listeria* pathogenesis and molecular virulence determinants. *Clin Microbiol Rev* 14:584–640.
3. Scallan E, Hoekstra RM, Angulo FJ, Tauxe RV, Widdowson MA, Roy SL, Jones JL, Griffin PM. 2011. Foodborne illness acquired in the United States—major pathogens. *Emerging Infect Dis* 17:7–15.
4. Pohl AM, Pouillot R, Bazaco MC, Wolpert BJ, Healy JM, Bruce BB, Laughlin ME, Hunter JC, Dunn JR, Hurd S, Rowlands JV, Saupe A, Vugia DJ, Van Doren JM. 2019. Differences Among Incidence Rates of Invasive Listeriosis in the U.S. FoodNet Population by Age, Sex, Race/Ethnicity, and Pregnancy Status, 2008-2016. *Foodborne Pathog Dis* 16:290–297.
5. Vázquez-Boland JA, Kryptou E, Scortti M. 2017. *Listeria* Placental Infection. *MBio* 8.
6. Bakardjiev AI, Theriot JA, Portnoy DA. 2006. *Listeria monocytogenes* traffics from maternal organs to the placenta and back. *PLoS Pathog* 2:e66.
7. Lecuit M, Vandormael-Pournin S, Lefort J, Huerre M, Gounon P, Dupuy C, Babinet C, Cossart P. 2001. A transgenic model for listeriosis: role of internalin in crossing the intestinal barrier. *Science* 292:1722–1725.
8. Camilli A, Paynton CR, Portnoy DA. 1989. Intracellular methicillin selection of *Listeria monocytogenes* mutants unable to replicate in a macrophage cell line. *Proc Natl Acad Sci USA* 86:5522–5526.
9. Nguyen BN, Peterson BN, Portnoy DA. 2019. Listeriolysin O: A phagosome-specific cytolysin revisited. *Cell Microbiol* 21:e12988.
10. Tilney LG, Portnoy DA. 1989. Actin filaments and the growth, movement, and spread of the intracellular bacterial parasite, *Listeria monocytogenes*. *J Cell Biol* 109:1597–1608.
11. Portnoy DA, Auerbuch V, Glomski IJ. 2002. The cell biology of *Listeria monocytogenes* infection: the intersection of bacterial pathogenesis and cell-mediated immunity. *J Cell Biol* 158:409–414.
12. Rothbauer M, Patel N, Gondola H, Siwetz M, Huppertz B, Ertl P. 2017. A comparative study of five physiological key parameters between four different human trophoblast-derived cell lines. *Sci Rep* 7:5892.

13. Morrish DW, Whitley GSTJ, Cartwright JE, Graham CH, Caniggia I. 2002. In vitro models to study trophoblast function and dysfunction— A workshop report. *Placenta* 23:S114–S118.
14. Tanaka S, Kunath T, Hadjantonakis AK, Nagy A, Rossant J. 1998. Promotion of trophoblast stem cell proliferation by FGF4. *Science* 282:2072–2075.
15. Erlebacher A, Price KA, Glimcher LH. 2004. Maintenance of mouse trophoblast stem cell proliferation by TGF-beta/activin. *Dev Biol* 275:158–169.
16. Hardy J, Francis KP, DeBoer M, Chu P, Gibbs K, Contag CH. 2004. Extracellular replication of *Listeria monocytogenes* in the murine gall bladder. *Science* 303:851–853.
17. Rocha CE, Mol JPS, Garcia LNN, Costa LF, Santos RL, Paixão TA. 2017. Comparative experimental infection of *Listeria monocytogenes* and *Listeria ivanovii* in bovine trophoblasts. *PLoS ONE* 12:e0176911.
18. Portnoy DA, Jacks PS, Hinrichs DJ. 1988. Role of hemolysin for the intracellular growth of *Listeria monocytogenes*. *J Exp Med* 167:1459–1471.
19. Yan J, Tanaka S, Oda M, Makino T, Ohgane J, Shiota K. 2001. Retinoic acid promotes differentiation of trophoblast stem cells to a giant cell fate. *Dev Biol* 235:422–432.
20. Zhu D, Gong X, Miao L, Fang J, Zhang J. 2017. Efficient Induction of Syncytiotrophoblast Layer II Cells from Trophoblast Stem Cells by Canonical Wnt Signaling Activation. *Stem Cell Reports* 9:2034–2049.
21. Lee JH, Choi C-W, Lee T, Kim SI, Lee J-C, Shin J-H. 2013. Transcription factor  $\sigma B$  plays an important role in the production of extracellular membrane-derived vesicles in *Listeria monocytogenes*. *PLoS ONE* 8:e73196.
22. Choi HJ, Sanders TA, Tormos KV, Ameri K, Tsai JD, Park AM, Gonzalez J, Rajah AM, Liu X, Quinonez DM, Rinaudo PF, Maltepe E. 2013. ECM-dependent HIF induction directs trophoblast stem cell fate via LIMK1-mediated cytoskeletal rearrangement. *PLoS ONE* 8:e56949.
23. Graham CH, Hawley TS, Hawley RG, MacDougall JR, Kerbel RS, Khoo N, Lala PK. 1993. Establishment and Characterization of First Trimester Human Trophoblast Cells with Extended Lifespan. *Exp Cell Res* 206:204–211.
24. Gomez-Lorenzo MG, Valle M, Frank J, Gruss C, Sorzano COS, Chen XS, Donate LE, Carazo JM. 2003. Large T antigen on the simian virus 40 origin of replication: a 3D snapshot prior to DNA replication. *EMBO J* 22:6205–6213.

25. Hardy J, Kirkendoll B, Zhao H, Pisani L, Luong R, Switzer A, McConnell MV, Contag CH. 2012. Infection of pregnant mice with *Listeria monocytogenes* induces fetal bradycardia. *Pediatr Res* 71:539–545.
26. Lowe DE, Robbins JR, Bakardjiev AI. 2018. Animal and Human Tissue Models of Vertical *Listeria monocytogenes* Transmission and Implications for Other Pregnancy-Associated Infections. *Infect Immun* 86.
27. Amarante-Paffaro A, Queiroz GS, Corrêa ST, Spira B, Bevilacqua E. 2004. Phagocytosis as a potential mechanism for microbial defense of mouse placental trophoblast cells. *Reproduction* 128:207–218.
28. Harter E, Lassnig C, Wagner EM, Zaiser A, Wagner M, Rychli K. 2019. The Novel Internalins InlP1 and InlP4 and the Internalin-Like Protein InlP3 Enhance the Pathogenicity of *Listeria monocytogenes*. *Front Microbiol* 10:1644.
29. Faralla C, Rizzuto GA, Lowe DE, Kim B, Cooke C, Shiow LR, Bakardjiev AI. 2016. InlP, a New Virulence Factor with Strong Placental Tropism. *Infect Immun* 84:3584–3596.
30. Faralla C, Bastounis EE, Ortega FE, Light SH, Rizzuto G, Gao L, Marciano DK, Nocadello S, Anderson WF, Robbins JR, Theriot JA, Bakardjiev AI. 2018. *Listeria monocytogenes* InlP interacts with afadin and facilitates basement membrane crossing. *PLoS Pathog* 14:e1007094.
31. Robbins JR, Skrzypczynska KM, Zeldovich VB, Kapidzic M, Bakardjiev AI. 2010. Placental syncytiotrophoblast constitutes a major barrier to vertical transmission of *Listeria monocytogenes*. *PLoS Pathog* 6:e1000732.
32. Zeldovich VB, Clausen CH, Bradford E, Fletcher DA, Maltepe E, Robbins JR, Bakardjiev AI. 2013. Placental syncytium forms a biophysical barrier against pathogen invasion. *PLoS Pathog* 9:e1003821.
33. Weber M, Knoefler I, Schleussner E, Markert UR, Fitzgerald JS. 2013. HTR8/SVneo cells display trophoblast progenitor cell-like characteristics indicative of self-renewal, repopulation activity, and expression of “stemness-” associated transcription factors. *Biomed Res Int* 2013:243649.
34. Drevets DA, Dillon MJ, Schawang JS, Van Rooijen N, Ehrchen J, Sunderkötter C, Leenen PJM. 2004. The Ly-6Chigh monocyte subpopulation transports *Listeria monocytogenes* into the brain during systemic infection of mice. *J Immunol* 172:4418–4424.
35. Martínez-Cerdeño V, Noctor SC. 2018. Neural progenitor cell terminology. *Front Neuroanat* 12:104.

## CHAPTER 3

### *LISTERIA MONOCYTOGENES* INFECTION ALTERS EXTRACELLULAR VESICLES PRODUCED BY TROPHOBLAST STEM CELLS

## ABSTRACT

Extracellular vesicles (EVs) are a cellular communication mechanism that has gained substantial attention in recent years. This interest stems from EVs having different cargo when they originate from diseased or cancerous cells as compared to EVs from healthy cells. It is believed that these altered EVs can serve as a way for the disease to persist or spread, or to alert the immune system to the threat. Studies into host EVs produced during bacterial infection have found that infection changes the host nucleic acids and proteins loaded into EVs. Importantly, though, cellular compounds of bacterial origin have also been found in the EVs from infected cells. In this chapter, I will explore how infection with *Listeria monocytogenes* (*Lm*) changes the EVs of trophoblast stem cells, and the implications for placental infections. Interestingly, we found many RNA binding proteins in higher abundance in EVs from *Lm* infected cells. RNA sequencing found that these EVs carry vastly different RNA profiles compared to EVs from uninfected cells, and that the major pathways represented in the RNA relate to vascular and morphological development, major steps required for the successful growth of the placenta. These findings may lead to new understandings of the role of EVs not only during bacterial infections, but also placental development.

## INTRODUCTION

A recently discovered mechanism that could play a role in mediating cellular immunity is intercellular communication mediated by extracellular vesicles (EVs). EVs are small (50-1000 nm) membrane-enclosed vesicles that are excreted by nearly every type of cell in the human body and across all domains of life (1). Two of the major types of eukaryotic EVs have been historically designated as exosomes and microvesicles, which are differentiated based on how they are formed. Exosomes are smaller (50-150 nm) and are formed by the inward folding of the plasma membrane. Multiple vesicles are gathered and transported in multivesicular endosomes (MVEs), which fuse to the cell membrane and release the exosomes to the extracellular environment. Microvesicles, which have a wider range in size (100-1000 nm), are formed by the outward budding of the plasma membrane directly into the extracellular space (2).

EVs play a critical role in placental development and immune regulation during pregnancy. The number of EVs per volume of blood in a healthy mother greatly increases during pregnancy, and the majority of these EVs originate from fetal trophoblasts (3). Trophoblast EVs (tEVs) have been found to carry immunoregulatory molecules, presumably suppressing the immune response to allow for the successful development of the fetus (4). However, tEVs have also been shown to play a detrimental role during placental disease, such as preeclampsia (5, 6).

The role that EV-mediated communication plays during intracellular bacterial infections has only recently been explored with a select number of pathogens, and the role of tEVs during prenatal infection is unknown. Previous studies of *Mycobacterium*-infected macrophages showed that host EVs carry bacterial components such as RNA, proteins, and glycopeptidolipids (7–9). Other studies of *Salmonella enterica* serovar Typhimurium infections found similar results, in which

EVs from infected macrophages carried *Salmonella* proteins and induced the production of pro-inflammatory cytokines through TLR2 and TLR4 dependent mechanisms (10). Additionally, mice treated with EVs from *S. enterica* infected cells generated antibodies against proteins found on the EVs, specifically *Salmonella* outer membrane proteins (11). EVs from *Lm*-infected macrophages carry bacterial DNA, and that this response is dependent on the DNA sensing cGAS-STING system (12). These findings show that EVs play a potential role in immune responses to intracellular bacterial infection. The purpose of the work presented here is to begin to decipher the role of tEVs produced in response to *Lm* placental infection.

We used an *Lm*-infected TSC system to model placental infections and tEV production and contents. Using an untargeted proteomics approach, we found that tEVs from infected and uninfected TSCs had distinct protein profiles, with the infected tEVs containing more unique protein signatures than tEVs from uninfected TSCs. Ribosomal and other RNA binding proteins were increased in the tEVs by infection. However, in contrast to previous studies using macrophages, no bacterial proteins were found. RNA sequencing on the EVs revealed many mRNAs that were overrepresented in the tEVs from infected cells, including genes involved in vasculogenesis and morphogenesis, processes involved in placental development. These data suggest that *Lm* infection substantially alters the contents being carried in EVs.

## MATERIAL AND METHODS

### *Mice.*

All animal experiments were performed under IACUC-approved animal protocol 201800030 in accordance with BSL-2 guidelines established by Michigan State University Campus Animal Resources. Michigan State is an AAALAC International accredited institution. Timed gestation day 11 (E11) pregnant CD-1 mice were delivered on that day from Charles River Laboratories. They were housed in the Clinical Center Animal Wing at Michigan State University.

### *Bacterial cultures.*

*Listeria monocytogenes* 10403S bioluminescent strain 2C (Xen32) was used throughout the study (13). This strain has a *lux-kan* insertion in the *flaA* locus and has a four-fold increase in intravenous 50% lethal dose compared to wild type 10403S. It was grown in brain heart infusion medium (BHI) broth to mid-logarithmic phase for infection.

### *Cell culture.*

TSCs were originally isolated from C57BL/6 mice and were graciously donated by Dr. Julie Baker (Stanford University, Palo Alto, CA) (14). They were grown in RPMI 1640 medium with GlutaMAX, 20% fetal bovine serum (FBS), and 1  $\mu$ M sodium pyruvate, as well as 35  $\mu$ g/mL fibroblast growth factor 4 (FGF-4), 10 ng/mL activin, and 1  $\mu$ g/mL heparin to maintain TSC replication (15). RAW 264.7 and J774 cells were obtained from ATCC and were grown in RPMI medium with GlutaMAX, 10% FBS, and 1  $\mu$ M sodium pyruvate.

### *Isolation of extracellular vesicles.*

A 150 cm<sup>2</sup> flask containing 10<sup>7</sup> TSCs was infected with *Lm* at a MOI of 100 or treated with an equivalent volume of BHI. After 1 hour, the cells were washed three times with PBS and medium depleted of EVs by centrifugation and containing 5 µg/mL gentamicin was added to ensure that there were no extracellular bacteria (16). At 24 hours of infection, the conditioned medium from the infected and uninfected TSCs was collected and centrifuged at 4000 x g for 20 minutes in 50 mL conical tubes. The supernatants were transferred to fresh conical tubes and centrifuged again at 4000 x g for 30 minutes. The supernatants were then filtered with a 0.22 µm filter using the Steriflip system. To collect large vesicles (L-tEVs), the filter was washed once with phosphate buffered saline (PBS), then 1 mL of PBS was repeatedly added to the top of the filter, which resuspended the tEVs from the filter. This preparation was then stored at -80° C. To collect the small tEVs (S-tEVs), the flow through from the filter was ultracentrifuged at 100,000 x g for 2 hours. The supernatant was carefully removed leaving 0.5 mL left at the bottom of the tube, then 25 mL of PBS was added, and the preparation was ultracentrifuged again at 100,000 x g for 2 hours. The supernatant was carefully removed, and the pellet was resuspended in an additional 1 mL PBS. The preparation was stored at -80° C.

### *Transmission electron microscopy.*

10<sup>8</sup> tEVs were fixed in 2% paraformaldehyde for 5 min. 5 µL of the sample solution was placed on carbon-coated EM grids and tEVs were immobilized for 1 min. The grids were washed by transferring to five 100 µL drops of distilled water and letting it dry for 2 min on each drop. The samples were stained with 1% uranyl acetate. Excess uranyl acetate was removed gently with filter

paper and the grids were air dried. The grids were imaged with a JEOL 100CXII transmission electron microscope operating at 100 kV. Images were captured on a Gatan Orius Digital Camera.

#### *Nanoparticle tracking analysis.*

tEV preparations were diluted 1:100 in PBS and were injected into a Zetaview machine (Particle Metrix). The Zetaview was set to a sensitivity of 89, a shutter speed of 300, and a frame rate of 30 frames per second. Cutoffs of 10 nm minimum and 1200 nm maximum were used.

#### *Mouse extracellular vesicle isolation.*

On E14.5, mice were infected via tail vein injection with  $2 \times 10^5$  CFU of *Lm* Xen32 in 200  $\mu$ L PBS prepared as described above (see Bacterial Culture). Uninfected control mice were not injected. On E18.5, four days post infection, mice were imaged using the PerkinElmer In Vivo Imaging System (IVIS) to confirm placental infection.

500  $\mu$ L of blood was extracted from uninfected or *Lm*-infected mice through the tail vein. Blood coagulated by incubation at room temperature for 30 minutes, then the blood was spun at 2,000 x g for 10 minutes at 4C. EVs were isolated by using ExoQuick Exosome Precipitation Solution (System Biosciences) and resuspended in 500  $\mu$ L of PBS.

#### *Proteomics.*

The protein profile of the purified tEVs was determined using untargeted mass spectrometry performed at the MSU Genomics Core Facility. Briefly, three independent EVs preparations, each of  $10^9$  S-tEVs from uninfected and infected TSCs were lysed and the proteins were precipitated using acetone and digested with trypsin. Nanospray liquid chromatography with tandem mass spectrometry (LC-MS/MS) was used to determine the peptide profile. The peptide data was

analyzed using the Scaffold proteome software, which mapped the identified peptides back to the mouse and *Lm* references (genome used as referencr) to determine the originating proteins.

*Gene Ontology (GO) Enrichment Analysis for proteomics.*

GO analysis was performed using the Gene Ontology Resource (<http://geneontology.org/>) and Protein Analysis Through Evolutionary Relationships (PANTHER) program to identify the biological processes of the proteins seen in the + *Listeria* S-tEVs (17). Additionally, protein interaction networks were generated using STRING program (18). Proteins that had twice the number of peptides identified in the + *Listeria* EV samples vs the – *Listeria* EV samples were used for the analysis.

*RNA sequencing.*

RNA extraction, RNA library preparations, sequencing reactions, and initial bioinformatics analysis were conducted at GENEWIZ, LLC. (South Plainfield, NJ, USA). Three independent EV preparations each of  $10^9$  S-tEVs from uninfected and infected TSCs were used. Total RNA was extracted following the Trizol Reagent User Guide (Thermo Fisher Scientific). RNA was quantified using Qubit Fluorometer (Life Technologies, Carlsbad, CA, USA) and RNA integrity was checked with TapeStation (Agilent Technologies, Palo Alto, CA, USA). SMART-Seq v4 Ultra Low Input Kit for Sequencing was used for full-length cDNA synthesis and amplification (Clontech, Mountain View, CA), and Illumina Nextera XT library was used for sequencing library preparation. Briefly, cDNA was fragmented, and adapter was added using transposase, followed by limited-cycle PCR to enrich and add index to the cDNA fragments. The final library was assessed with Agilent TapeStation. The sequencing libraries were multiplexed and clustered on one lane of a flowcell. After clustering, the flowcell was loaded on the Illumina HiSeq instrument

according to manufacturer's instructions. The samples were sequenced using a 2x150 Paired End (PE) configuration. Image analysis and base calling were conducted by the HiSeq Control Software (HCS). Raw sequence data (.bcl files) generated from Illumina HiSeq was converted into fastq files and de-multiplexed using Illumina's bcl2fastq 2.17 software. One mis-match was allowed for index sequence identification.

The raw PE reads sequencing data were uploaded to the Galaxy web platform, and we used the public server at [usegalaxy.org](http://usegalaxy.org) to process the RNA-seq data (19). Briefly, PE reads were processed to trim sequencing adapter and low-quality bases using Trimmomatic (20). The clean PE RNA-seq reads were mapped to the mouse reference genome (*Mus Musculus*) using HISAT2 (21). Gene expression of mapped reads were then measured with featureCounts (22).

Differential gene expression analysis was performed using DESeq2 v1.32.0 in R version 4.1.1 (23). Genes with a minimum 5 reads in at least 4 samples were filtered out, resulting in a total of 23,836 genes. Differentially expressed genes with  $p\text{-adj} < 0.05$  were used to perform gene ontology analysis using the g:Profiler system (<https://biit.cs.ut.ee/gprofiler/gost>) (24). Biological processes with  $p\text{-adj} < 0.05$  were considered significant. Volcano plot was generated using EnhancedVolcano package in R using fold change  $> 1$  and  $p\text{-value} < 10^{-5}$  parameters (25).

### *Lipidomics.*

One technical replicate of S-tEVs from either uninfected, WT *Lm*-infected, or  $\Delta hly$  *Lm*-infected TSCs were used for analysis. Samples were thawed on ice and spiked with an internal standard and calibration mixture consisting of di-myristoyl phospholipids (PG, PE, PS, PA), PC (46:0), SM (30:1) and TG (14:1) to give a final sample concentration of 5  $\mu\text{M}$  of each standard. To each sample, 300  $\mu\text{L}$  of  $-20^{\circ}\text{C}$  chilled methanol containing 1 mM butylated hydroxytoluene (an

antioxidant) was added, one mL of MTBE was added to each sample, and samples were vortexed for 60 minutes at room temperature. 150  $\mu$ L of water were added, and the samples were vortexed for an additional 15 minutes and then centrifuged for 15 minutes. The supernatants were collected to new test tubes and precipitated proteins were re-extracted as above. Pooled extracts were dried overnight in a speedvac and resuspended in 100  $\mu$ L of isopropanol containing 0.01% BHT.

Immediately prior to analysis, aliquots of each lipid extract were diluted in isopropanol:methanol (2:1, v:v) containing 20 mM ammonium formate.

Full scan MS spectra at 100,000 resolution (defined at  $m/z$  400) were collected on a Thermo Scientific LTQ-Orbitrap Velos mass spectrometer in both positive and negative ionization modes. Scans were collected from  $m/z$  200 to  $m/z$  1200. For each analysis, 10  $\mu$ L of sample was directly introduced by flow injection (no LC column) at 10  $\mu$ L/min using an electrospray ionization source equipped with a heated ESI needle. A Shimadzu Prominence HPLC served as the sample delivery unit. The sample and injection solvent were 2:1 (v: v) isopropanol: methanol containing 20 mM ammonium formate. The spray voltage was 4.5 kV, ion transfer tube temperature was 275  $^{\circ}$ C, the S-lens value was 50 percent, and the ion trap fill time was 100 ms. The autosampler was set to 15 degrees C. After two minutes of MS signal averaging, the LC tubing, autosampler, and ESI source were flushed with 1 mL of isopropanol, prior to injection of the next sample. Samples were analyzed in random order, interspersed by solvent blank injections. Following MS data acquisition, offline mass recalibration was performed with the "Recalibrate Offline" tool in Thermo Xcalibur software according to the vendor's instructions, using the theoretical computed masses for the internal calibration standards and several common endogenous mammalian lipid species. MS/MS confirmation and structural analysis of lipid species identified by database searching were performed using higher-energy collisional dissociation (HCD) MS/MS at 60,000 resolution and a

normalized collision energy of 25 for positive ion mode, and 60 for negative ion mode. MS/MS scans were triggered by inclusion lists generated separately for positive and negative ionization modes.

Lipids were identified using the Lipid Mass Spectrum Analysis (LIMSA) v.1.0 software linear fit algorithm, in conjunction with an in-house database of hypothetical lipid compounds, for automated peak finding and correction of  $^{13}\text{C}$  isotope effects. Peak areas of found peaks were quantified by normalization against an internal standard of a similar lipid class. The top ~300 most abundant peaks in both positive and negative ionization mode were then selected for MS/MS inclusion lists and imported into Xcalibur software for structural analysis on a pooled sample as described above. For this untargeted analysis, no attempt was made to correct for differences in lipid species ionization due to the length or degree of unsaturation of the esterified fatty acids. Therefore, lipid abundance values are inherently estimates rather than true absolute values.

Prior to the analysis, the mass spectrometer inlet capillary was removed and cleaned by sonication, and the ESI tubing and spray needle were cleaned by extensive flushing with isopropanol. During the analysis, several injection solvent blanks and extraction blanks were interspersed between the randomized study samples to monitor for background ions and any potential sample carryover throughout the run. The offline external mass recalibration routine described above was used to eliminate in-run drift in mass calibration and improve the consistency of mass accuracy over the measured  $m/z$  range.

Each lipid species is identified at minimum as a sum composition of lipid headgroup and fatty acyl total carbons: total double bonds, based on accurate mass measurement and isotopic distribution. Where possible, individual lipid species isomers were further delineated by MS/MS and are listed

in the column adjacent to the lipid species ID. As many lipid molecular species exist as mixtures of SN1 and SN2 positional isomers, the fatty acyl substituents are designated using the convention (fatty acid\_fatty acid) in which the underscore indicates a fatty acid may be located at either SN1 or SN2 position of the glycerol backbone.

Under the extraction conditions used, some lipid species are partially or completely lost during phase separation and therefore are often not reliably quantified with this method. These include free sphingosine and its analogues and derivatives, as well as gangliosides and other highly polar lipid species.

## RESULTS

### *Trophoblast stem cell extracellular vesicle quantification.*

Trophoblast stem cells (TSCs) from C57BL/6 mice were used to model placental infections. TSCs were infected with *Lm* at a MOI of 100. At 24 HPI, the medium from uninfected and *Lm*-infected TSCs was collected and large tEVs (L-tEVs) were isolated by collecting the vesicles from the top of the 0.22  $\mu\text{m}$  filter, while small tEVs (S-tEVs) were purified by ultracentrifugation at 100,000 x g (Fig. 3.1). EV preparations have often been referred to as microvesicles and exosomes, but as these entities are formed by distinct processes and are not just differentiated based on their size, we will refer to our separated samples as L-tEVs and S-tEVs throughout this report (26). Transmission electron microscopy (TEM) on the tEV preparations show the distinctive round shape in both vesicle preparations (Fig. 3.2 A,B). The TEM images show S-tEVs and L-tEVs that appear to be similar size to each other despite the different isolation methods. A possible explanation for this is that the L-tEV preparations display a greater size range than the S-tEVs. To determine if infection alters tEV production, we performed nanoparticle tracking analysis on them

using a Zetaview instrument (Fig. 3.3). We found that infection decreased the number of L-tEVs produced by TSCs but did not affect the number of S-tEVs (Fig. 3.4). In addition, infection did not alter the size of either L-tEVs or S-tEVs (Fig. 3.5). Thus, *Lm* differentially affected tEV production, decreasing the number of L-tEVs isolated.

#### *Mouse EVs after infection.*

Previous studies found that EV levels in bloodstream of a pregnant person can increase dramatically during disease (5). Our lab has an established pregnant mouse infection model using CD1 mice (27). Isolated blood from one uninfected and two *Lm*-infected mice were used for EV analysis. Due to the small volume of blood, the ExoQuick kit was used to isolate the EVs (28). We found that the two *Lm* infected mice lower blood EV levels compared to the one uninfected mouse (Table 3.1). A decrease in plasma EV levels was also seen with pregnant mice treated with LPS, a stimulant of the immune response (29). Further replication of this study and of using other infectious agents will give additional insight into the effect infection has on tEV production.

#### *Proteomic analysis on tEVs after infection.*

EVs carry a wide range of signaling molecules to deliver to recipient cells (30). We performed proteomic analysis to determine if *Lm* infection alters the protein profile of S-tEVs. Using shotgun tandem mass spectrometry, we found that there were many more unique proteins identified in S-tEVs from infected TSCs (331 proteins) compared to S-tEVs from uninfected cells (13 proteins). Additionally, in proteins that were shared between the two tEV groups (187 proteins), there were often more peptides identified in the infection condition, indicating higher amounts of that protein being transported in the tEVs from infected TSCs. Ribosomal proteins, histones, and tubulin proteins are some of the categories where there were increased amounts in the infected tEVs. The

full list of proteins that had at least a two-fold increase in peptide signature in the tEVs from the infected TSCs are listed in (Table 3.2). Meanwhile, only 4 proteins saw a two-fold increase in peptide signatures in the S-tEVs from uninfected TSCs (Table 3.3).

Gene ontology (GO) enrichment was performed to determine biological functions that were represented by the proteins that were increased in S-tEVs from *Lm*-infected TSCs. The main processes that were seen were related to ribosomes and translation, which was expected given the many ribosomal and other RNA-binding proteins in these samples (Table 3.4). A protein interaction map was created using the proteins that had at least a 2-fold increase in peptides in the S-tEVs from infected cells (Fig. 3.6). We found that these proteins have high levels of interaction with each other, and we can see clusters of ribosomal, cytoskeleton, and histone proteins. There were not enough proteins that were relatively increased in the tEVs from uninfected TSCs to perform GO analysis. Altogether, our results show that *Lm* infection does lead to different proteins loaded in tEVs, with more unique proteins seen in tEVs from infected cells. In contrast to other reports of EVs isolated from infected cells, no *Lm* proteins were detected in tEVs from any sample.

#### *RNA sequencing on S-tEVs.*

Our finding that S-tEVs from infected TSCs have increased amounts of RNA-binding proteins led us to believe that these EVs could also carry different RNAs. We performed RNA sequencing on S-tEVs from uninfected and *Lm*-infected TSCs. We identified 22,836 genes in the mRNAs from the S-tEVs, with 68 genes being overrepresented in the S-tEVs from infected cells and 116 genes underrepresented in the S-tEV mRNAs from those cells (Fig. 3.7). These differentially represented genes were used for GO analysis (Fig. 3.8). Interestingly, two of the pathways upregulated in the genes of *Lm*-infected S-tEVs involved vascular development and morphogenesis, and functions

involved in placenta implantation and development. The pathways downregulated in the S-tEVs from infected TSCs involved metabolic processes. Overall, we found that *Lm* infection of TSCs altered the host mRNAs found in the S-tEVs.

#### *Lipidomic analysis on S-tEVs.*

EVs are membrane-bound particles and thus consist of lipids. Interestingly, EVs, specifically exosomes, have a different lipid composition compared to the cells of origin, with EVs having higher relative abundances of glycerophosphocholine, sphingomyelin, and diradylglycerol, among others (31). This suggests that the formation of EVs is not just budding the plasma membrane and processing it to vesicles, but that there is a dedicated process that selective creates vesicles with certain lipid species. One such mechanism is by sphingomyelinases, a category of proteins that are involved with EV formation. The overrepresentation of sphingomyelins and ceramides in EVs could be a result of this pathway (32). Here, we compared the lipid composition of tEVs from uninfected TSCs to tEVs from WT and  $\Delta hly$  *Lm*-infected cells. The  $\Delta hly$  *Lm* infection was used as LLO is a cholesterol-dependent cytotoxin (CDC) and may directly interact with lipids being loaded into the tEVs.

Overall, infection did not greatly change the relative abundance of most lipid species (Fig. 3.9). That said, ceramides, sphingomyelin, sterols, and sphingolipids all appear to have been identified in greater amounts in the infection condition tEVs compared to those from uninfected cells. Inversely, phosphatidylcholine, phosphatidyl ethanolamine, phosphatidyl glycerol, and monoacylglycerol all had higher amounts in the uninfected tEVs. In addition to sphingomyelins, ceramides are also involved in the sphingomyelinase-dependent EV formation pathway (32). Previous work found that *Lm* infection increases the level of cellular ceramides in macrophages,

and that this lipid turnover was performed by *Lm* phospholipases (33). Interestingly, ceramides can activate and regulate various immune pathways, so the increase in tEV ceramides could be responsible for the pro-inflammatory effects that are detailed in Chapter 4 of this dissertation (34). While we do see differences in relative lipid amounts with infection, the differences were not that striking and only a single replicate of each tEV type was used for this analysis. Further replication will be required to confirm the effect on tEV lipid composition during infection.

## DISCUSSION

EVs are the subject of exciting new research that offers the potential for novel approaches for diagnosis and treatment of many diseases. A primary function of EVs appears to be the stimulation of cell signaling pathways in recipient cells, including immune cells, activating them in some instances and dampening responses in others. This delicate balance can be altered during disease and infection. For example, certain cancers secrete EVs that suppress immune cell activity, allowing the malignancy to proliferate (35). Conversely, cells infected with intracellular pathogens secrete pro-inflammatory EVs that help to control infection, although EVs from infected cells may sometimes have the opposite effect (36).

During normal, healthy pregnancy, the number of EVs in the maternal bloodstream greatly increases (3). These EVs, produced by fetal trophoblasts of the placenta, have been shown to modulate immune responses but also can cause inflammation, leading to diseases such as the life-threatening preeclampsia. However, the function of placental EVs in prenatal bacterial infection remains unknown. Considering their large number and the above-mentioned effects on immune cells, placental EVs may play an important role in either ameliorating or exacerbating prenatal

infection. We sought to study the effect of *Lm* infection on EV production and function by trophoblasts.

There were several interesting proteins detected in the tEVs. We were particularly interested to see an enrichment of ribosomal proteins in tEVs derived from infected cells. Other groups have also found ribosomal proteins when performing proteomic analysis of EVs (37–39). These studies usually focus on the RNA-binding aspects of these proteins as RNA has been heavily associated with EVs (2). However, the appearance of ribosomal proteins in EVs could be independent of RNA. A potential explanation is that translation levels are increased during cell stress (such as an infection), which could lead to higher ribosome numbers, and eventually more ribosomal proteins in EVs. Another RNA-binding protein identified in our infection tEVs is PEG10. PEG10 is a Gag-like protein that is required for trophoblast differentiation and placental development (40). This protein can also selectively bind and load mRNA into exosomes, and these EVs alter the gene expression of the recipient cell (41). The ability of EV-associated PEG10 to alter gene expression could be an explanation for the altered behavior of cells treated with tEVs from *Lm*-infected cells that will be discussed in Chapter 4. Surprisingly, these EVs lacked any *Lm* proteins in our analysis, contrasting previous EV studies during infection (8, 11, 42, 43). Most previous reports used macrophages as the initially infected cells, and the lack of *Lm* proteins may reflect reduced bactericidal mechanisms of trophoblasts compared to macrophages. This difference in protein processing and EV protein content could have important implications for the function of tEVs during pregnancy.

In addition to altered proteins found in the tEVs, we also saw a change in mRNAs during infection. One notable type of mRNAs observed in the S-tEVs from infected cells correspond to histone protein products. We also found histone proteins themselves in the tEVs from *Lm*-infected

TSCs. Interestingly, histones have been identified in EVs in response to treatment with the gram-negative bacterial component LPS (37, 44). Additionally, histones are seen in the bloodstreams of animal models of sepsis and patients with sepsis (45–47). These results in tandem with our findings suggest that packaging of histones, and potentially host RNA along with them, may be a mechanism to communicate infections.

Some of the other genes that we saw overrepresented in the mRNAs from the infected S-tEVs involved vasculature development and morphogenesis. Vasculogenesis of fetal and maternal vessels are required steps for placenta implantation and development (48). Previous works with tEVs found that they recruit vascular smooth muscle cells and promote invasion of extravillous trophoblasts, key steps that are essential for remodeling the decidua surrounding the placenta (49, 50). EVs have also been found to play a direct role in implantation of the embryo (51), and inflammation is a key part of implantation (52). Additionally, morphogenesis of the placenta is required for the proper development of the organ (53, 54). One intriguing gene that had increased mRNA in the tEVs from infected is syncytin-A, which is responsible for the cellular fusion necessary for the development of the multinucleated syncytiotrophoblasts (55, 56). It is possible that *Lm* invasion of the placenta activates the release of tEVs required to carry out these processes, with the mRNAs housed in the vesicles acting on the recipient cells. Otherwise, the RNA profiles of the tEVs could represent the mRNAs being transcribed in the TSCs during infection, although the mRNAs we identified in the tEVs differ than those seen in human trophoblasts infected with *Lm* (57). Additionally, EVs have been previously found to have enriched levels of mRNA that differ significantly from the mRNA levels in the cell of origin, and EV mRNAs can be translated in recipient cells (58, 59). More work is required to determine the exact function of tEV RNAs during infections.

Overall, we found that *Lm* infection greatly changes the contents of EVs produced by TSCs. We found different host proteins and mRNAs, as well as potentially lipids, in the tEVs from infected cells. Follow-up work may reveal that other host components, such as DNA and microRNA, may also be altered in the infection EVs. The following chapter will focus on how these altered vesicles differentially affect any recipient cells, and what that might mean for placental infection immunity.

## APPENDIX

**Figure 3.1. Extracellular vesicle isolation protocol.** tEVs from uninfected and *Lm* infected TSCs were isolated using a combination of filtration and ultracentrifugation. Made with BioRender.

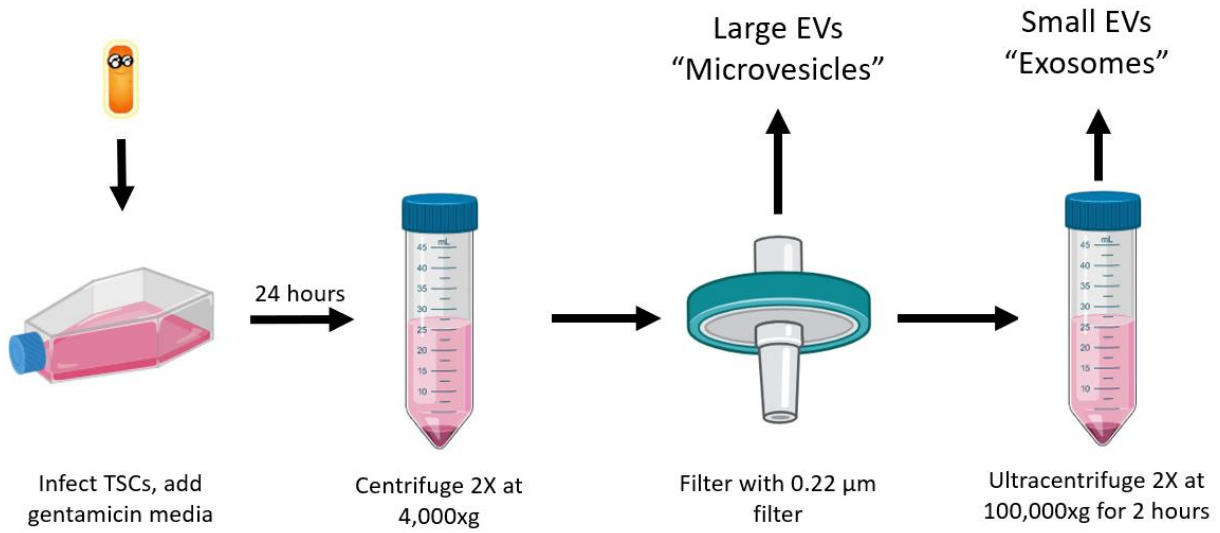


**Figure 3.2. Extracellular vesicles from *Lm*-infected TSCs.** Transmission electron microscopy images of L-tEVs (A) and S-tEVs (B) from *Lm*-infected TSCs.

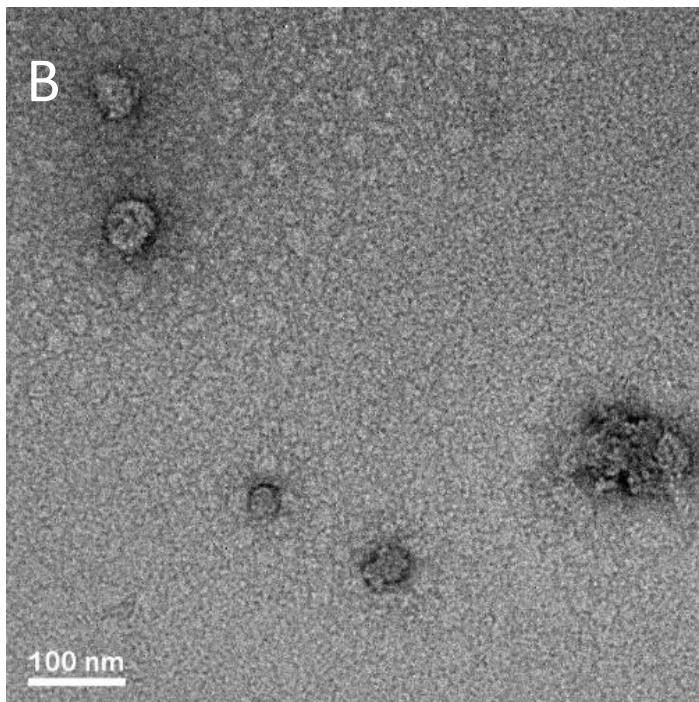
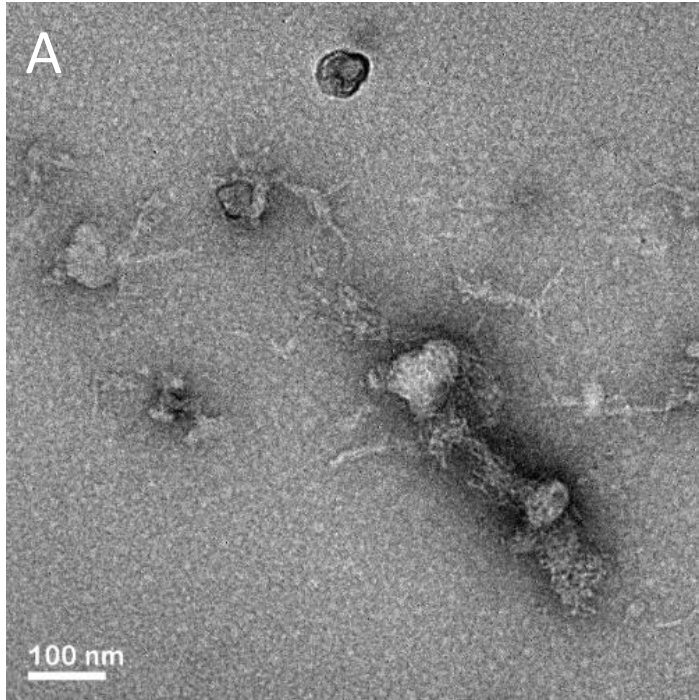


**Figure 3.3: TSCs infected with *Lm* produce tEVs.** Example nanoparticle tracking analysis histograms giving the size distribution of tEVs. (A, B) Density plots for L-tEVs from uninfected (A) and *Lm*-infected (B) TSCs. Density plots for S-tEVs from uninfected (C) and *Lm*-infected (D) TSCs.

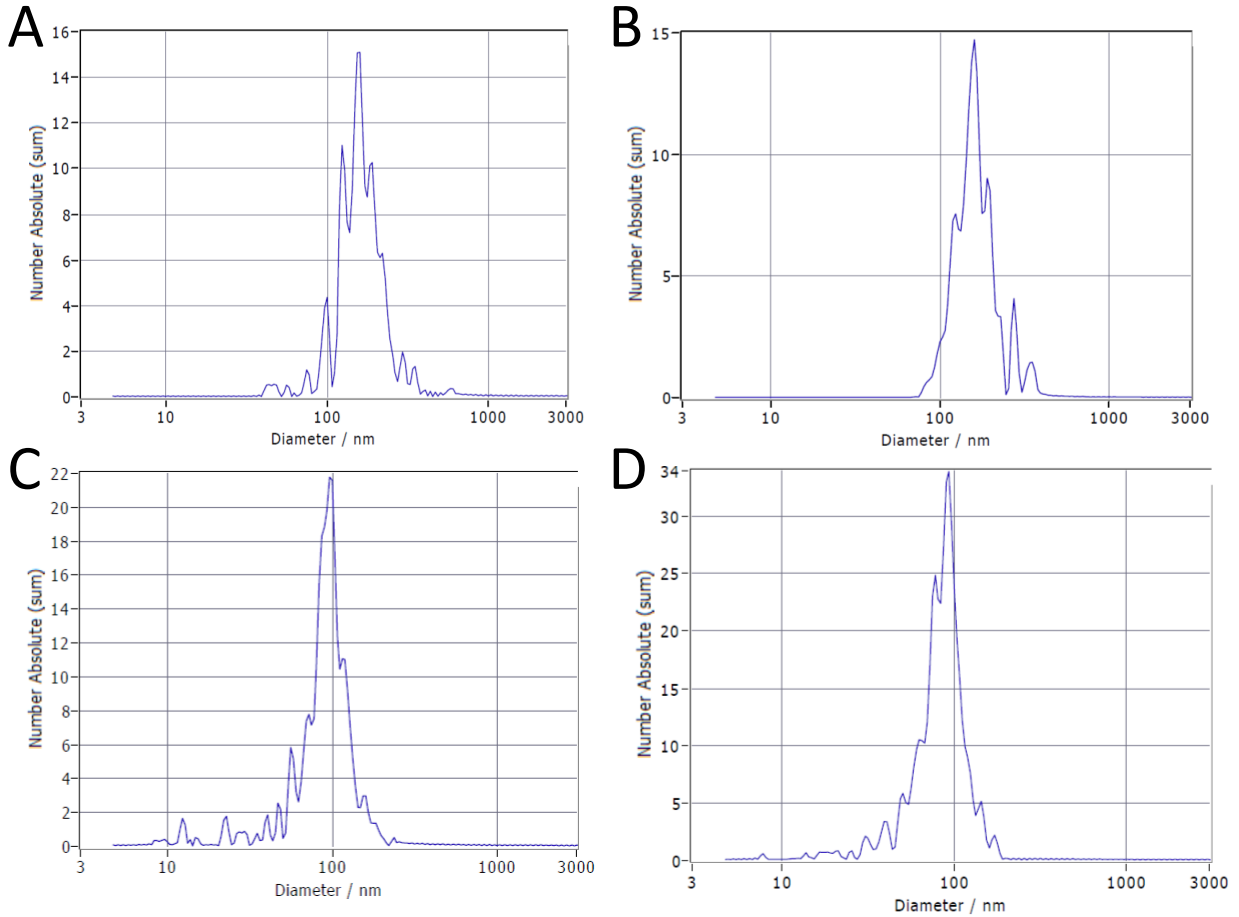


**Figure 3.4. *Lm* infection changes L-tEV Concentrations.** TSC derived EVs were analyzed by nanoparticle tracking analysis that gives the concentration of the nanoparticles. The concentration of the L-tEVs (A) and S-tEVs (B) with and without infection are given. Error bars represent the standard deviation. Sample means were compared using Student's T-test, \*  $P < 0.05$ .

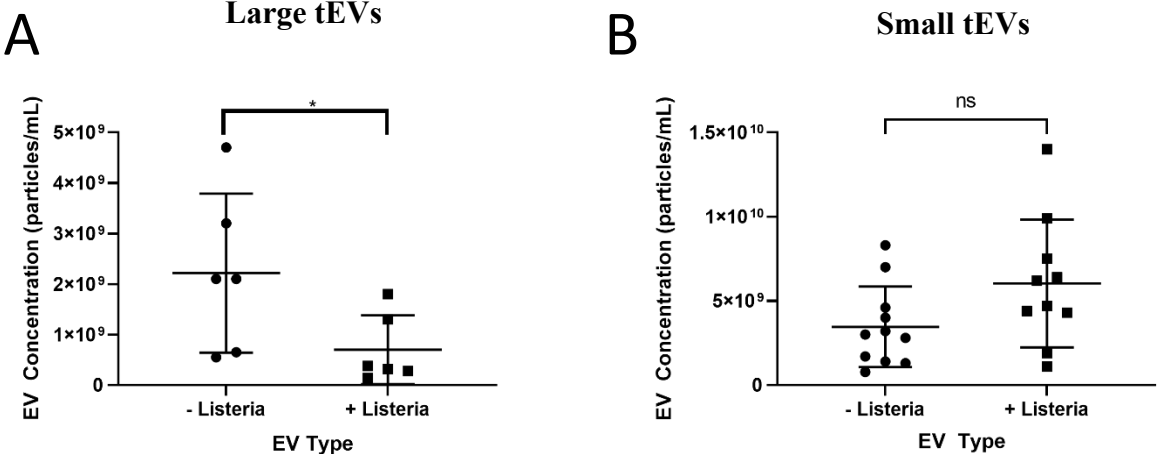


**Figure 3.5: *Lm* infection did not change tEV size.** TSC derived EVs were analyzed by nanoparticle tracking analysis that gives the size distribution of the nanoparticles. The mean size of the L-tEVs (A) and S-tEVs (B) with and without infection are given, with each dot representing the average size of one EV isolation preparation. Error bars represent the standard deviation. Sample means were compared using Student's T-test, \*  $P < 0.05$ .

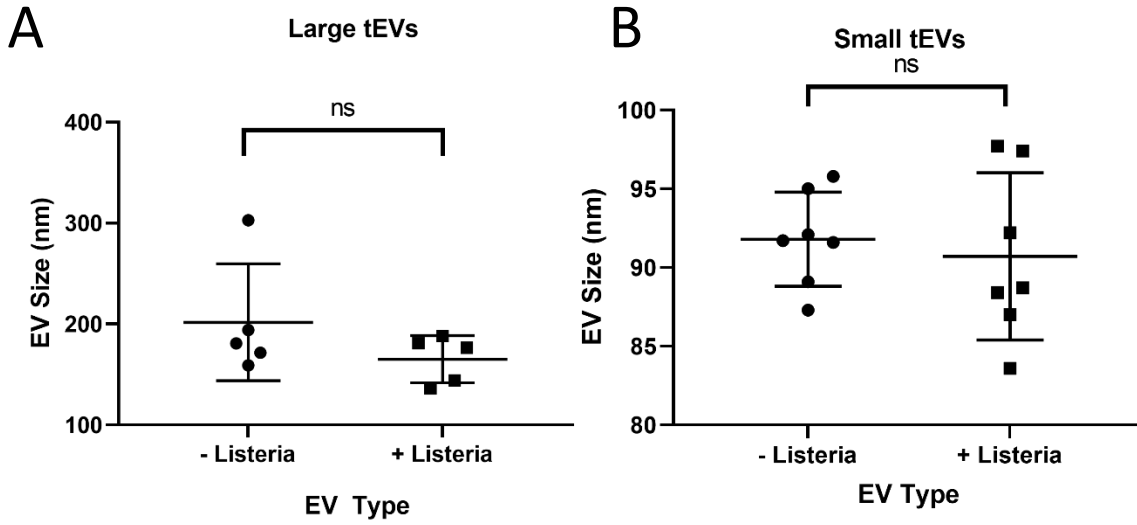


**Figure 3.6. Protein interaction networks of proteins found in S-tEVs from *Lm*-infected TSCs.** The proteins of the S-tEVs from uninfected and *Lm*-infected TSCs were determined by mass spectrometry. Protein interaction networks of the proteins identified in the S-tEVs from *Lm*-infected TSCs were generated using STRING program (18). The proteins involved in translation, microtubule cytoskeleton organization, and nucleosome core pathways are highlighted in blue, green, and red, respectively. Proteins that had twice the number of peptides identified in the *Lm*-infected tEV samples versus the uninfected tEV samples were used for the analysis. The thickness of the line represents the confidence of the interaction between the proteins.

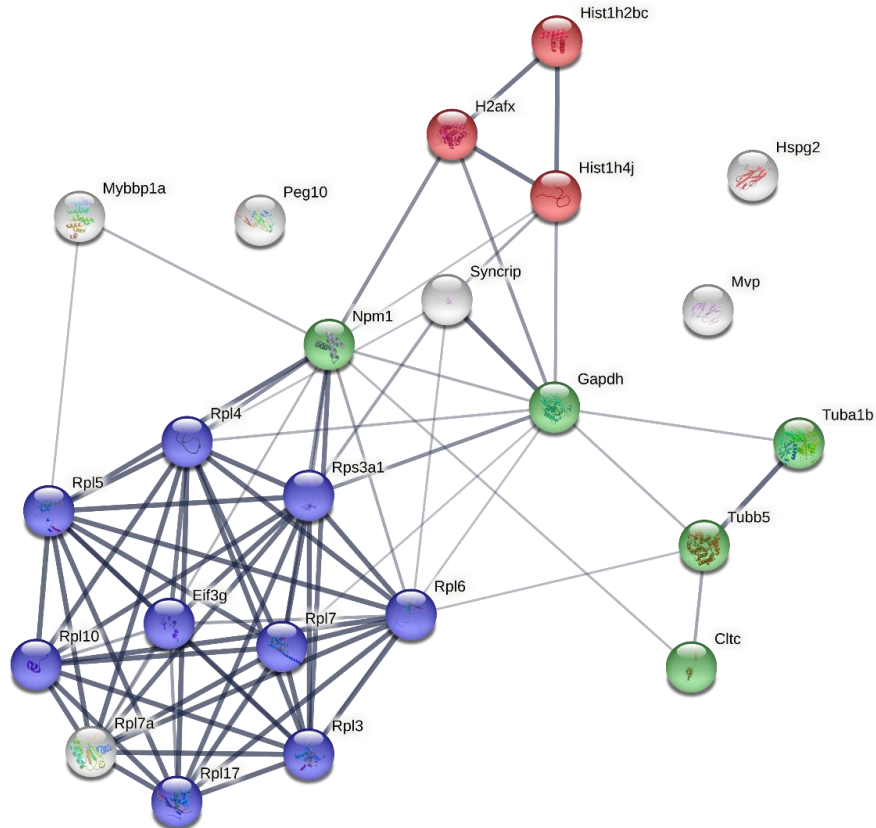


**Figure 3.7. *Lm*-infected TSCs produce S-tEVs with altered RNA profiles.** Volcano plot of differentially expressed genes in S-tEVs from *Lm*-infected and uninfected TSCs. Red dots represent statistical significance ( $p\text{-val} < 10^{-5}$ ) and  $\log_2(\text{fold change})$  greater or less than 1. Total variables represent the number of genes that were used to generate a volcano plot.

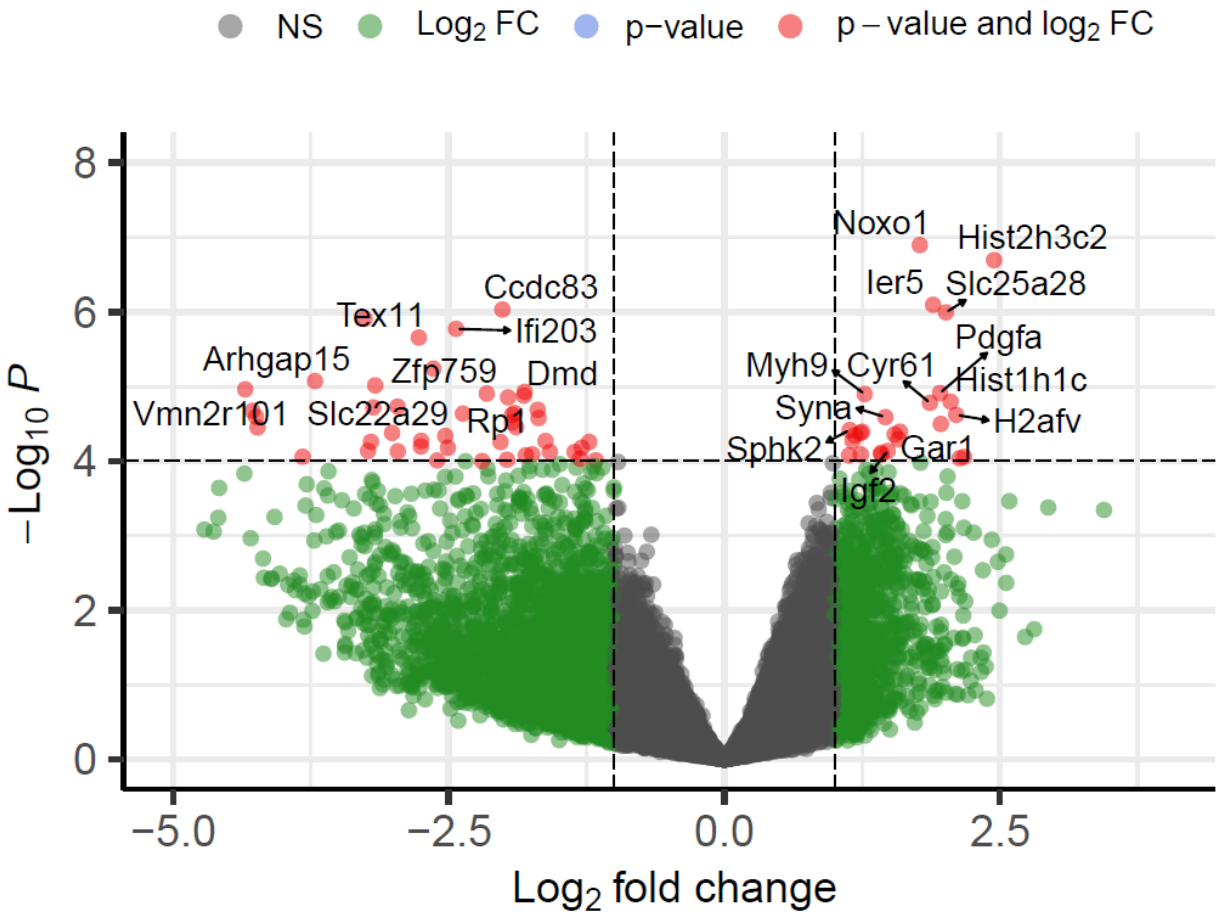


**Figure 3.8. Gene Ontology analysis of differing RNAs found in S-tEVs from uninfected and *Lm*-infected TSCs.** Gene ontology analysis of differentially expressed genes ( $p\text{-adj} < 0.05$ ) were used to investigate biological process pathways of downregulated and upregulated in *Lm*-infected cells using gProfileR (24).

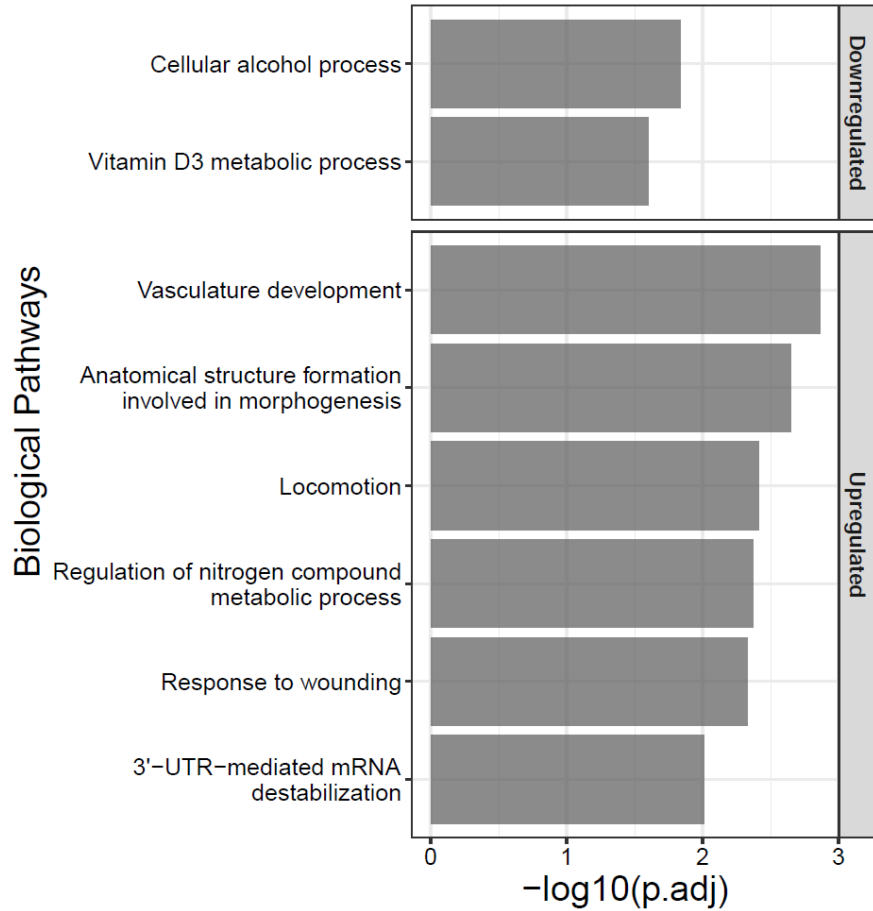
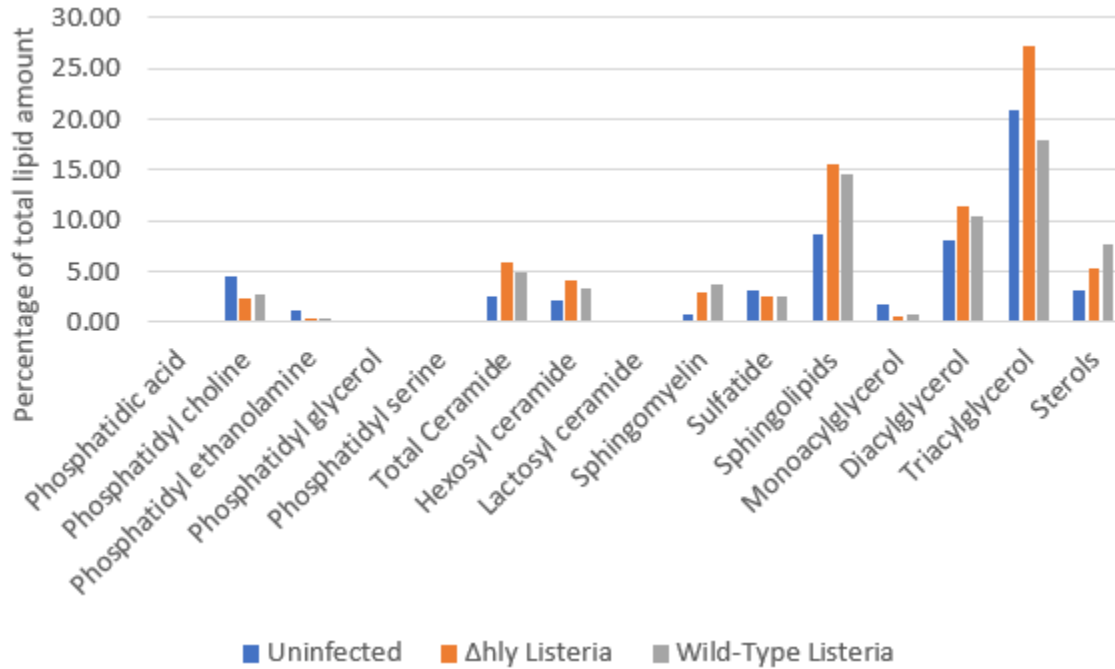


**Figure 3.9. Lipidomic analysis on tEVs.** A single replicate of S-tEVs from either uninfected TSCs, WT *Lm*-infected TSCs, or  $\Delta hly$  *Lm*-infected TSCs were analyzed by mass spectrometry to determine their lipid profiles. The relative percentage of each lipid species for each EV condition is reported.



<b>Table 3.1. EVs isolated from mouse blood during <i>Lm</i> infection</b>	
Mouse Condition	Blood EV Concentration (particles/mL)
Uninfected	$9.7 \times 10^{11}$
<i>Lm</i> -infection	$2.1 \times 10^{11}$
<i>Lm</i> -infection	$2.6 \times 10^{11}$

<b>Table 3.2. Proteins that were found in higher abundance in infection EVs</b>			
<b>Protein Name</b>	<b>- <i>Listeria</i></b>	<b>+ <i>Listeria</i></b>	<b>+ <i>Listeria</i>/- <i>Listeria</i></b>
PEG10	0	6.33	Infinite <sup>a</sup>
60S ribosomal protein L10	0	6.67	Infinite
60S ribosomal protein L3	0.33	11.33	34
60S ribosomal protein L5	0.33	9	27
Myb-binding protein 1A	0.33	7.67	23
40S ribosomal protein S3a	0.33	5	15
Nucleophosmin	1	11	11
Clathrin heavy chain 1	2.33	25.33	10.86
60S ribosomal protein L4	2	19.33	9.67
Tubulin beta-5 chain	2.33	22.33	9.57
60S ribosomal protein L6	1	8.67	8.67
60S ribosomal protein L7a	1	8	8
60S ribosomal protein L17	1.33	10.33	7.75
Major vault protein	1	6.67	6.67
Heterogenous nuclear Ribonucleoprotein	1.33	7.67	5.75
Basement membrane-specific heparan sulfate proteoglycan	3.33	18.67	5.6
40S ribosomal protein 1A	2	8.67	4.33
Histone H2AX	5.67	22.33	3.94
60S ribosomal protein L7	1.67	5.67	3.4
Tubulin alpha-1B	6	14.67	2.44
GAPDH	6	13.33	2.22
Histone H2B	11.67	23.33	2
Histone H4	6.67	13.33	2

**Table 3.2 (cont'd)**

List of proteins that had twice the number of peptides identified in the S-tEVs from the infected TSCs vs. the S-tEVs from uninfected cells. Peptide counts were done in Scaffold Software. Included proteins that had at least 10 peptide signatures in either EV condition.

<b>Table 3.3. Proteins found in higher abundance in uninfected EVs</b>			
<b>Protein Name</b>	<b>- <i>Listeria</i></b>	<b>+ <i>Listeria</i></b>	<b>+ <i>Listeria</i>/- <i>Listeria</i></b>
Keratin type 1 cytoskeleton (A6BLY7)	11	3	0.27
Trypsin	66.67	23.33	0.35
Lactotransferrin	9.33	4	0.43
Keratin type 1 cytoskeleton (E9Q0F0)	14.33	7	0.49
List of proteins that had twice the number of peptides identified in the S-tEVs from the uninfected TSCs vs. the S-tEVs from infected cells. Peptide counts were done in Scaffold Software. Included proteins that had at least 10 peptide signatures in either EV condition.			

<b>Table 3.4. Panther Gene Ontology analysis of proteins found in infection EVs</b>			
<b>GO biological process</b>	<b>fold Enrichment</b>	<b>raw P-value</b>	<b>FDR<sup>a</sup></b>
ribosomal large subunit assembly	> 100	2.44E-08	3.84E-05
maturation of LSU-Rrna	> 100	4.11E-08	5.40E-05
maturation of LSU-rRNA from tricistronic rRNA transcript	> 100	1.58E-04	4.89E-02
ribosomal large subunit biogenesis	> 100	8.98E-15	1.41E-10
ribosome assembly	62.69	5.88E-07	4.63E-04
cytoplasmic translation	41.57	5.67E-05	2.23E-02
nucleosome assembly	36.77	8.06E-05	2.76E-02
ribosome biogenesis	30.19	8.31E-12	6.54E-08
translation	26.64	2.46E-11	1.29E-07
peptide biosynthetic process	25.01	4.25E-11	1.67E-07
rRNA processing	23.2	2.26E-06	1.55E-03
ribonucleoprotein complex assembly	23.04	2.71E-05	1.22E-02
rRNA metabolic process	22.13	2.83E-06	1.78E-03
ribonucleoprotein complex subunit organization	22.1	3.18E-05	1.35E-02
ribonucleoprotein complex biogenesis	21.56	1.54E-10	4.84E-07
amide biosynthetic process	19.42	3.80E-10	9.97E-07
non-membrane-bounded organelle assembly	19.06	5.80E-07	4.81E-04
peptide metabolic process	17.7	8.45E-10	1.90E-06
negative regulation of transferase activity	14.94	1.41E-04	4.54E-02
ncRNA processing	13.62	2.85E-05	1.25E-02
regulation of translation	12.85	3.75E-05	1.55E-02
posttranscriptional regulation of gene expression	12.08	7.77E-06	4.22E-03
cellular amide metabolic process	11.93	2.49E-08	3.56E-05

<b>Table 3.4 (cont'd)</b>			
ncRNA metabolic process	11.14	7.31E-05	2.62E-02
regulation of cellular amide metabolic process	11.12	7.39E-05	2.59E-02
cellular protein-containing complex assembly	11.1	3.12E-07	2.73E-04
<sup>a</sup> the false discovery rate (FDR).			

## REFERENCES

## REFERENCES

1. Ñahui Palomino RA, Vanpouille C, Costantini PE, Margolis L. 2021. Microbiota-host communications: Bacterial extracellular vesicles as a common language. *PLoS Pathog* 17:e1009508.
2. Raposo G, Stoorvogel W. 2013. Extracellular vesicles: exosomes, microvesicles, and friends. *J Cell Biol* 200:373–383.
3. Mitchell MD, Peiris HN, Kobayashi M, Koh YQ, Duncombe G, Illanes SE, Rice GE, Salomon C. 2015. Placental exosomes in normal and complicated pregnancy. *Am J Obstet Gynecol* 213:S173-81.
4. Sabapatha A, Gercel-Taylor C, Taylor DD. 2006. Specific isolation of placenta-derived exosomes from the circulation of pregnant women and their immunoregulatory consequences. *Am J Reprod Immunol* 56:345–355.
5. Han C, Wang C, Chen Y, Wang J, Xu X, Hilton T, Cai W, Zhao Z, Wu Y, Li K, Houck K, Liu L, Sood AK, Wu X, Xue F, Li M, Dong J-F, Zhang J. 2019. Placenta-derived extracellular vesicles induce preeclampsia in mouse models. *Haematologica* <https://doi.org/10.3324/haematol.2019.226209>.
6. Gill M, Motta-Mejia C, Kandzija N, Cooke W, Zhang W, Cerdeira AS, Bastie C, Redman C, Vatish M. 2019. Placental Syncytiotrophoblast-Derived Extracellular Vesicles Carry Active NEP (Neprilysin) and Are Increased in Preeclampsia. *Hypertension* 73:1112–1119.
7. Bhatnagar S, Shinagawa K, Castellino FJ, Schorey JS. 2007. Exosomes released from macrophages infected with intracellular pathogens stimulate a proinflammatory response in vitro and in vivo. *Blood* 110:3234–3244.
8. Giri PK, Kruh NA, Dobos KM, Schorey JS. 2010. Proteomic analysis identifies highly antigenic proteins in exosomes from *M. tuberculosis*-infected and culture filtrate protein-treated macrophages. *Proteomics* 10:3190–3202.
9. Cheng Y, Schorey JS. 2019. Extracellular vesicles deliver *Mycobacterium* RNA to promote host immunity and bacterial killing. *EMBO Rep* 20.
10. Hui WW, Hercik K, Belsare S, Alugubelly N, Clapp B, Rinaldi C, Edelmann MJ. 2018. *Salmonella enterica* Serovar Typhimurium Alters the Extracellular Proteome of Macrophages and Leads to the Production of Proinflammatory Exosomes. *Infect Immun* 86.
11. Hui WW, Emerson LE, Clapp B, Sheppe AE, Sharma J, del Castillo J, Ou M, Maegawa GHB, Hoffman C, Larkin, III J, Pascual DW, Edelmann MJ. 2021. Antigen encapsulating

- host extracellular vesicles derived from Salmonella-infected cells stimulate pathogen-specific Th1-type responses in vivo . *PLoS Pathog* 17:1–27.
12. Nandakumar R, Tschismarov R, Meissner F, Prabakaran T, Krissanaprasit A, Farahani E, Zhang B-C, Assil S, Martin A, Bertrams W, Holm CK, Ablasser A, Klause T, Thomsen MK, Schmeck B, Howard KA, Henry T, Gothelf KV, Decker T, Paludan SR. 2019. Intracellular bacteria engage a STING-TBK1-MVB12b pathway to enable paracrine cGAS-STING signalling. *Nat Microbiol* 4:701–713.
  13. Hardy J, Francis KP, DeBoer M, Chu P, Gibbs K, Contag CH. 2004. Extracellular replication of *Listeria monocytogenes* in the murine gall bladder. *Science* 303:851–853.
  14. Tanaka S, Kunath T, Hadjantonakis AK, Nagy A, Rossant J. 1998. Promotion of trophoblast stem cell proliferation by FGF4. *Science* 282:2072–2075.
  15. Erlebacher A, Price KA, Glimcher LH. 2004. Maintenance of mouse trophoblast stem cell proliferation by TGF-beta/activin. *Dev Biol* 275:158–169.
  16. Portnoy DA, Jacks PS, Hinrichs DJ. 1988. Role of hemolysin for the intracellular growth of *Listeria monocytogenes*. *J Exp Med* 167:1459–1471.
  17. Mi H, Muruganujan A, Ebert D, Huang X, Thomas PD. 2019. PANTHER version 14: more genomes, a new PANTHER GO-slim and improvements in enrichment analysis tools. *Nucleic Acids Res* 47:D419–D426.
  18. Szklarczyk D, Gable AL, Lyon D, Junge A, Wyder S, Huerta-Cepas J, Simonovic M, Doncheva NT, Morris JH, Bork P, Jensen LJ, Mering C von. 2019. STRING v11: protein-protein association networks with increased coverage, supporting functional discovery in genome-wide experimental datasets. *Nucleic Acids Res* 47:D607–D613.
  19. Afgan E, Baker D, Batut B, van den Beek M, Bouvier D, Cech M, Chilton J, Clements D, Coraor N, Grüning BA, Guerler A, Hillman-Jackson J, Hiltemann S, Jalili V, Rasche H, Soranzo N, Goecks J, Taylor J, Nekrutenko A, Blankenberg D. 2018. The Galaxy platform for accessible, reproducible and collaborative biomedical analyses: 2018 update. *Nucleic Acids Res* 46:W537–W544.
  20. Bolger AM, Lohse M, Usadel B. 2014. Trimmomatic: a flexible trimmer for Illumina sequence data. *Bioinformatics* 30:2114–2120.
  21. Kim D, Paggi JM, Park C, Bennett C, Salzberg SL. 2019. Graph-based genome alignment and genotyping with HISAT2 and HISAT-genotype. *Nat Biotechnol* 37:907–915.
  22. Liao Y, Smyth GK, Shi W. 2014. featureCounts: an efficient general purpose program for assigning sequence reads to genomic features. *Bioinformatics* 30:923–930.

23. Love MI, Huber W, Anders S. 2014. Moderated estimation of fold change and dispersion for RNA-seq data with DESeq2. *Genome Biol* 15:550.
24. Raudvere U, Kolberg L, Kuzmin I, Arak T, Adler P, Peterson H, Vilo J. 2019. g:Profiler: a web server for functional enrichment analysis and conversions of gene lists (2019 update). *Nucleic Acids Res* 47:W191–W198.
25. Blighe K, Rana S, Lewis M. 2018. EnhancedVolcano: publication-ready volcano plots with enhanced colouring and labeling. *EnhancedVolcano: Publication-ready volcano plots with enhanced colouring and labeling*.
26. Théry C, Witwer KW, Aikawa E, Alcaraz MJ, Anderson JD, Andriantsitohaina R, Antoniou A, Arab T, Archer F, Atkin-Smith GK, Ayre DC, Bach J-M, Bachurski D, Baharvand H, Balaj L, Baldacchino S, Bauer NN, Baxter AA, Bebawy M, Beckham C, et al. 2018. Minimal information for studies of extracellular vesicles 2018 (MISEV2018): a position statement of the International Society for Extracellular Vesicles and update of the MISEV2014 guidelines. *J Extracell Vesicles* 7:1535750.
27. Conner KN, Holman D, Lydic T, Hardy JW. 2022. Infection with *Listeria monocytogenes* alters the placental transcriptome and eicosanome. *BioRxiv*.
28. Prendergast EN, de Souza Fonseca MA, Dezem FS, Lester J, Karlan BY, Noushmehr H, Lin X, Lawrenson K. 2018. Optimizing exosomal RNA isolation for RNA-Seq analyses of archival sera specimens. *PLoS ONE* 13:e0196913.
29. Nguyen SL, Greenberg JW, Wang H, Collaer BW, Wang J, Petroff MG. 2019. Quantifying murine placental extracellular vesicles across gestation and in preterm birth data with tidyNano: A computational framework for analyzing and visualizing nanoparticle data in R. *PLoS ONE* 14:e0218270.
30. Kugeratski FG, Hodge K, Lilla S, McAndrews KM, Zhou X, Hwang RF, Zanivan S, Kalluri R. 2021. Quantitative proteomics identifies the core proteome of exosomes with syntenin-1 as the highest abundant protein and a putative universal biomarker. *Nat Cell Biol* 23:631–641.
31. Lydic TA, Townsend S, Adda CG, Collins C, Mathivanan S, Reid GE. 2015. Rapid and comprehensive “shotgun” lipidome profiling of colorectal cancer cell derived exosomes. *Methods* 87:83–95.
32. Trajkovic K, Hsu C, Chiantia S, Rajendran L, Wenzel D, Wieland F, Schwille P, Brügger B, Simons M. 2008. Ceramide triggers budding of exosome vesicles into multivesicular endosomes. *Science* 319:1244–1247.
33. Smith GA, Marquis H, Jones S, Johnston NC, Portnoy DA, Goldfine H. 1995. The two distinct phospholipases C of *Listeria monocytogenes* have overlapping roles in escape from a vacuole and cell-to-cell spread. *Infect Immun* 63:4231–4237.

34. Chiurchiù V, Leuti A, Maccarrone M. 2018. Bioactive lipids and chronic inflammation: managing the fire within. *Front Immunol* 9:38.
35. Xu R, Rai A, Chen M, Suwakulsiri W, Greening DW, Simpson RJ. 2018. Extracellular vesicles in cancer - implications for future improvements in cancer care. *Nat Rev Clin Oncol* 15:617–638.
36. White JR, Dauros-Singorenko P, Hong J, Vanholsbeeck F, Phillips A, Swift S. 2021. The complex, bidirectional role of extracellular vesicles in infection. *Biochem Soc Trans* <https://doi.org/10.1042/BST20200788>.
37. Yang Y, Boza-Serrano A, Dunning CJR, Clausen BH, Lambertsen KL, Deierborg T. 2018. Inflammation leads to distinct populations of extracellular vesicles from microglia. *J Neuroinflammation* 15:168.
38. Sork H, Corso G, Krjutskov K, Johansson HJ, Nordin JZ, Wiklander OPB, Lee YXF, Westholm JO, Lehtiö J, Wood MJA, Mäger I, El Andaloussi S. 2018. Heterogeneity and interplay of the extracellular vesicle small RNA transcriptome and proteome. *Sci Rep* 8:10813.
39. Uzbekova S, Almiñana C, Labas V, Teixeira-Gomes A-P, Combes-Soia L, Tsikis G, Carvalho AV, Uzbekov R, Singina G. 2020. Protein cargo of extracellular vesicles from bovine follicular fluid and analysis of their origin from different ovarian cells. *Front Vet Sci* 7:584948.
40. Abed M, Verschueren E, Budayeva H, Liu P, Kirkpatrick DS, Reja R, Kummerfeld SK, Webster JD, Gierke S, Reichelt M, Anderson KR, Newman RJ, Roose-Girma M, Modrusan Z, Pektas H, Maltepe E, Newton K, Dixit VM. 2019. The Gag protein PEG10 binds to RNA and regulates trophoblast stem cell lineage specification. *PLoS ONE* 14:e0214110.
41. Segel M, Lash B, Song J, Ladha A, Liu CC, Jin X, Mekhedov SL, Macrae RK, Koonin EV, Zhang F. 2021. Mammalian retrovirus-like protein PEG10 packages its own mRNA and can be pseudotyped for mRNA delivery. *Science* 373:882–889.
42. Abrami L, Brandi L, Moayeri M, Brown MJ, Krantz BA, Leppla SH, van der Goot FG. 2013. Hijacking multivesicular bodies enables long-term and exosome-mediated long-distance action of anthrax toxin. *Cell Rep* 5:986–996.
43. García-Martínez M, Vázquez-Flores L, Álvarez-Jiménez VD, Castañeda-Casimiro J, Ibáñez-Hernández M, Sánchez-Torres LE, Barrios-Payán J, Mata-Espinosa D, Estrada-Parra S, Chacón-Salinas R, Serafín-López J, Wong-Baeza I, Hernández-Pando R, Estrada-García I. 2019. Extracellular vesicles released by J774A.1 macrophages reduce the bacterial load in macrophages and in an experimental mouse model of tuberculosis. *Int J Nanomedicine* 14:6707–6719.

44. Nair RR, Mazza D, Brambilla F, Gorzanelli A, Agresti A, Bianchi ME. 2018. LPS-Challenged Macrophages Release Microvesicles Coated With Histones. *Front Immunol* 9:1463.
45. Kalbitz M, Grailer JJ, Fattahi F, Jajou L, Herron TJ, Campbell KF, Zetoune FS, Bosmann M, Sarma JV, Huber-Lang M, Gebhard F, Loaiza R, Valdivia HH, Jalife J, Russell MW, Ward PA. 2015. Role of extracellular histones in the cardiomyopathy of sepsis. *FASEB J* 29:2185–2193.
46. Ekaney ML, Otto GP, Sossdorf M, Sponholz C, Boehringer M, Loesche W, Rittirsch D, Wilharm A, Kurzai O, Bauer M, Claus RA. 2014. Impact of plasma histones in human sepsis and their contribution to cellular injury and inflammation. *Crit Care* 18:543.
47. Xu J, Zhang X, Pelayo R, Monestier M, Ammollo CT, Semeraro F, Taylor FB, Esmon NL, Lupu F, Esmon CT. 2009. Extracellular histones are major mediators of death in sepsis. *Nat Med* 15:1318–1321.
48. Geva E, Ginzinger DG, Zaloudek CJ, Moore DH, Byrne A, Jaffe RB. 2002. Human placental vascular development: vasculogenic and angiogenic (branching and nonbranching) transformation is regulated by vascular endothelial growth factor-A, angiopoietin-1, and angiopoietin-2. *J Clin Endocrinol Metab* 87:4213–4224.
49. Salomon C, Yee S, Scholz-Romero K, Kobayashi M, Vaswani K, Kvaskoff D, Illanes SE, Mitchell MD, Rice GE. 2014. Extravillous trophoblast cells-derived exosomes promote vascular smooth muscle cell migration. *Front Pharmacol* 5:175.
50. Salomon C, Kobayashi M, Ashman K, Sobrevia L, Mitchell MD, Rice GE. 2013. Hypoxia-induced changes in the bioactivity of cytotrophoblast-derived exosomes. *PLoS ONE* 8:e79636.
51. Chen K, Liang J, Qin T, Zhang Y, Chen X, Wang Z. 2022. The role of extracellular vesicles in embryo implantation. *Front Endocrinol (Lausanne)* 13:809596.
52. Mor G, Cardenas I, Abrahams V, Guller S. 2011. Inflammation and pregnancy: the role of the immune system at the implantation site. *Ann N Y Acad Sci* 1221:80–87.
53. Cross JC, Nakano H, Natale DRC, Simmons DG, Watson ED. 2006. Branching morphogenesis during development of placental villi. *Differentiation* 74:393–401.
54. Mihiu CM, Suşman S, Rus Ciucă D, Mihiu D, Costin N. 2009. Aspects of placental morphogenesis and angiogenesis. *Rom J Morphol Embryol* 50:549–557.
55. Mi S, Lee X, Li X, Veldman GM, Finnerty H, Racie L, LaVallie E, Tang XY, Edouard P, Howes S, Keith JC, McCoy JM. 2000. Syncytin is a captive retroviral envelope protein involved in human placental morphogenesis. *Nature* 403:785–789.

56. Dupressoir A, Marceau G, Vernochet C, Bénit L, Kanellopoulos C, Sapin V, Heidmann T. 2005. Syncytin-A and syncytin-B, two fusogenic placenta-specific murine envelope genes of retroviral origin conserved in Muridae. *Proc Natl Acad Sci USA* 102:725–730.
57. Johnson LJ, Azari S, Webb A, Zhang X, Gavrilin MA, Marshall JM, Rood K, Seveau S. 2021. Human Placental Trophoblasts Infected by *Listeria monocytogenes* Undergo a Pro-Inflammatory Switch Associated With Poor Pregnancy Outcomes. *Front Immunol* 12:709466.
58. Skog J, Würdinger T, van Rijn S, Meijer DH, Gainche L, Sena-Esteves M, Curry WT, Carter BS, Krichevsky AM, Breakefield XO. 2008. Glioblastoma microvesicles transport RNA and proteins that promote tumour growth and provide diagnostic biomarkers. *Nat Cell Biol* 10:1470–1476.
59. Valadi H, Ekström K, Bossios A, Sjöstrand M, Lee JJ, Lötvall JO. 2007. Exosome-mediated transfer of mRNAs and microRNAs is a novel mechanism of genetic exchange between cells. *Nat Cell Biol* 9:654–659.

## CHAPTER 4

### IMMUNE CELL RESPONSE TO EXTRACELLULAR VESICLES FROM INFECTED CELLS

## ABSTRACT

Extracellular vesicles (EVs) are involved in many diseases throughout our bodies. Previous studies have found EVs to activate immune cells during bacterial infections, a potential mechanism to coordinate a defense against the invaders. This chapter explores how EVs from infected trophoblasts may induce a response to placental colonization. We found that treatment of cells with trophoblast extracellular vesicles (tEVs) from infected trophoblast stem cells (TSCs) induces the production of TNF- $\alpha$ , a pro-inflammatory cytokine and a marker of macrophage activation. Most interestingly, this tEV treatment made certain cells more susceptible to subsequent infection, and this response required an active *Lm* infection of the TSCs. Macrophage activation had previously been observed when using EVs from infected macrophages, potentially suggesting a new mechanism of *Lm* infection and spread. However, increased susceptibility due to EV treatment has not been reported. These findings provide new insight about placental infection and immune response dynamics.

## INTRODUCTION

The immune system is a complex set of cells and responses that require fine-tuned coordination to defend against disease. During bacterial infections, these responses are required to stop the growth of the invaders and prevent damage to the host organs and systems. Extracellular vesicles (EVs) serve as a potential mechanism to organize such a response. Previous findings show that these vesicles can activate the production and release of pro-inflammatory cytokines, suggesting that they serve as a signaling mechanism (1–3). Additionally, some research has suggested that treatment with extracellular vesicles from infected cells (iEVs) may also protect against subsequent infection (4, 5). Using mouse models, similar results were seen *in vivo*, with the administration of iEVs stimulating the production of cytokines and cellular infiltration (5–8). Additionally, iEVs also induce the production of antibodies against bacterial proteins transported in the vesicles, suggesting that iEVs have the potential to become a candidate for vaccine development (9, 10). Outside of bacterial infections, EVs are also important during placental development and disease. EVs have been found to regulate the placental immune response, creating a permissive environment that allows the placenta and fetus to grow and develop (11, 12). Placental EVs can be turned into a pro-inflammatory signaling mechanism, though, and can induce disease (13–15).

In this chapter, I will explore how tEVs from *Listeria monocytogenes* (*Lm*)-infected TSCs affect the recipient cells. tEVs isolated from infected TSCs stimulated pro-inflammatory responses in recipient macrophage-like cells. Unexpectedly, we observed that certain macrophage cells became more susceptible to *Lm* infection after the tEV treatment, specifically tEVs from *Lm*-infected TSCs. This result was also seen when treated these cells with EVs from infected macrophages, suggesting this could be a conserved mechanism. Interestingly, this effect may also require *Lm*

cytosol invasion in the initially infected cells. We attempted to replicate our findings using an *in vivo* mouse model but were not able to see a significant difference in infection rates with any tEV treatment. Overall, we found that tEVs may induce a pro-inflammatory response in macrophages, and that this could be a way for *Lm* to spread intracellularly.

## MATERIALS AND METHODS

### *Bacterial cultures.*

*Listeria monocytogenes* 10403S bioluminescent strain 2C (Xen32) was used throughout the study (16). This strain has a *lux-kan* insertion in the *flaA* locus and has a four-fold increase in intravenous 50% lethal dose compared to wild type 10403S. It was grown in brain heart infusion medium (BHI) to mid-logarithmic phase for infection. The mutant strains were created in the Xen32 background with allelic exchange using pKSV7.

### *Cell culture.*

Trophoblasts stem cells (TSCs) were originally isolated from C57BL/6 mice and were graciously donated by Dr. Julie Baker (Stanford University, Palo Alto, CA) (17). They were grown in RPMI 1640 medium with GlutaMAX, 20% fetal bovine serum (FBS), and 1  $\mu$ M sodium pyruvate, as well as 35  $\mu$ g/mL fibroblast growth factor 4 (FGF-4), 10 ng/mL activin, and 1  $\mu$ g/mL heparin to maintain TSC replication (18). RAW 264.7 and J774 cells were obtained from ATCC and were grown in RPMI medium with GlutaMAX, 10% FBS, and 1  $\mu$ M sodium pyruvate. Bone marrow derived macrophages (BMDMs) were isolated from CD1 mice and were initially grown in RPMI medium with GlutaMAX, 10% FBS, 1  $\mu$ M sodium pyruvate, 10 ng/mL macrophage colony stimulating factor (M-CSF) (19).

### *Isolation of extracellular vesicles.*

$10^7$  TSCs, RAW 264.7 macrophage-like cells, J774 macrophage-like cells, or BMDMs in a 150  $\text{cm}^2$  flask were infected with *Lm* at a MOI of 10 (macrophages) or 100 (TSCs), or treated with an equivalent volume of BHI. After 1 hour, the cells are washed three times with PBS and medium depleted of EVs containing 5  $\mu$ g/mL gentamicin to ensure that there were no extracellular bacteria

(20). The media was depleted of EVs by a combination of filtration and ultracentrifugation. At 24 hours of infection, the conditioned medium from the infected and uninfected TSCs was collected and centrifuged at 4000 x g for 20 minutes in 50 mL conical tubes. The supernatants were transferred to fresh conical tubes and centrifuged again at 4000 x g for 30 minutes. The supernatants were then filtered with a 0.22  $\mu\text{m}$  filter using the Steriflip system. To collect large vesicles (L-tEVs), the filter was washed once with phosphate buffered saline (PBS), then 1 mL of PBS was repeatedly added to the top of the filter, which resuspended the tEVs from the filter. This preparation was then stored at  $-80^{\circ}\text{C}$ . To collect the small tEVs (S-tEVs), the flow through from the filter was ultracentrifuged at 100,000 g for 2 hours. The supernatant was carefully removed so that there was about 0.5 mL left at the bottom of the tube, then 25 mL of PBS was added, and the preparation was ultracentrifuged again at 100,000 g for 2 hours. Once again, the supernatant was carefully removed, and the pellet was resuspended in an additional 1 mL PBS. The preparation was stored at  $-80^{\circ}\text{C}$ .

*Listeria intracellular growth assay.*

Cells were plated into a 24 well plate at  $5 \times 10^4$  cells/well. After 24 h, the cells were treated with  $5 \times 10^6$  EVs from either uninfected or infected cells, or an equal amount of PBS. After another 24 h, the cells were washed three times with PBS. Medium with *Lm* was added at MOI of either 10 (macrophages) or 100 (TSCs) colony forming units (CFUs) of *Lm* per cell. After 1 h, the wells were washed 3 times with PBS and medium with 5  $\mu\text{g/mL}$  gentamicin was added. Bioluminescence images were taken at the given timepoints using an IVIS Lumina System (Perkin Elmer, Inc.), with 5 min of exposure and large binning, starting upon infection. The signal was quantified using Living Image software (Perkin Elmer).

### *TNF- $\alpha$ quantification.*

J774 and RAW 264.7 macrophages were plated into a 24-well plate at  $5 \times 10^4$  cells/well. After 24 h, the cells were treated with  $5 \times 10^6$  of tEVs from either uninfected or infected TSCs, or an equal volume of PBS. After 24 h, the conditioned medium was collected and TNF- $\alpha$  was quantified by enzyme-linked immunosorbent assay (ELISA) from R&D Systems according to the instructions of the manufacturer.

### *Mouse infections.*

All animal experiments were performed under IACUC-approved animal protocol 201800030 in accordance with BSL-2 guidelines established by Michigan State University Campus Animal Resources. Michigan State is an AAALAC International accredited institution. From 5 to 8-week-old BALB/c mice were obtained from Charles River Laboratories. They were housed in the Clinical Center Animal Wing at Michigan State University for two weeks to acclimate them. The mice were treated with either 200  $\mu$ L of PBS,  $10^8$  tEVs from uninfected TSCs, or  $10^8$  tEVs from *Lm*-infected TSC through tail vein injection. After 24 h, the mice were infected with either  $10^4$  or  $10^5$  *Lm* through tail vein infection. At 48 or 96 h post infection, the mice were imaged using the IVIS imaging system as described previously (16, 21) and humanely sacrificed using cervical dislocation in accordance with approved procedures while the animals were anesthetized. The spleens were harvested, mashed, serial diluted, and plated onto BHI plates with 50  $\mu$ g/mL kanamycin. Each spleen was diluted and plated in duplicate.

## RESULTS

### *tEV-mediated stimulation of macrophages.*

*Lm* infections lead to a pro-inflammatory response that is necessary to control the infection, with infected cells producing cytokines such as TNF- $\alpha$  (22). We hypothesized that tEVs can induce a similar pro-inflammatory response to *Lm* infection. To test this, we treated J774 and RAW 264.7 macrophage-like cells with  $5 \times 10^6$  tEVs derived from uninfected and infected TSCs, and after 24 h the TNF- $\alpha$  levels were measured using ELISA. We found that RAW 264.7 cells treated with L-tEVs or S-tEVs derived from *Lm*-infected cells resulted in the induction of TNF- $\alpha$ , while the treatment with PBS or tEVs from uninfected cells showed little TNF- $\alpha$  production (Fig. 4.1A). J774 cells, on the other hand, showed a significant increase of TNF- $\alpha$  only when treated with L-tEVs derived from infected cells, but not with S-tEVs from infected cells at the same concentration (Fig. 4.1B). Therefore, EVs isolated from *Lm*-infected TSCs can induce the production of a pro-inflammatory cytokine.

### *Listeria infection after tEV treatment.*

EVs have been proposed as vaccines because of their ability to stimulate macrophages and induce antigen-specific memory (7, 23, 24). Additionally, macrophage activation causes increased resistance to *Lm* infection (25). We hypothesized that macrophages activated by the tEVs would become more resistant to *Lm* infection. We again treated RAW 264.7 and J774 cells with  $5 \times 10^6$  S-tEVs, and after 24 h infected with bioluminescent *Lm*. In J774 cells, no difference was seen in *Lm* growth (Fig. 4.2A). This result was expected since these tEVs failed to induce TNF- $\alpha$  production in J774 cells. However, we found that treatment with S-tEVs from uninfected TSCs increased the susceptibility of RAW 264.7 cells to infection. Surprisingly, treatment with tEVs

from infected cells made the RAW 264.7 cells even more susceptible to infection (Fig. 4.2B). This result was unexpected, and as far as we are aware this is the first report of EVs of any kind inducing macrophages to become more susceptible to infection. Additional tEV treatment and infection with bone marrow derived macrophages (BMDMs) also showed an increase in susceptible with treatment of tEVs (Fig. 4.2C), particularly those from *Lm*-infected TSCs, showing that this effect is not just specific to RAW 264.7 cells. Additionally, tEV treatment also made the TSCs more susceptible to *Lm* infection, although not as starkly of a difference as with the macrophage-like cells (Fig. 4.3). Overall, we found that S-tEVs from infected TSCs makes certain cell types more susceptible to infection.

#### *Effect of Lm mutants on tEV capabilities.*

*Lm* needs to reach the cytosol of the host cell in order to replicate, and it uses the cytolysin listeriolysin O (LLO) to initiate the vacuolar escape into the cytosol (26). Previous work found that the invasion of the cytosol is necessary for iEVs from *Lm*-infected cells to elicit the production of IFN- $\beta$  in the recipient cells (3). To determine if cytosolic invasion is also required for the tEVs to have their effect. We isolated tEVs from TSCs infected with  $\Delta hly$  *Lm*, which lack LLO. When RAW 264.7 cells were treated with these S-tEVs and then infected with *Lm*, the level of *Lm* growth was similar to those treated with S-tEVs from uninfected cells (Fig. 4.4A). Similarly, when RAW 264.7 cells were treated with S-tEVs from TSCs that were treated with heat-killed (HK) *Lm*, subsequent *Lm* infection was at the level as the cells treated with PBS (Fig. 4.4B). These results were also seen in BMDMs, where S-tEVs from HK and  $\Delta hly$  *Lm* treated TSCs did not make the cells as susceptible to infection as S-tEVs from WT *Lm*-infected TSCs do (Fig. 4.4B). These results suggest that active infection is required for *Lm* to alter the EVs produce and to affect the recipient cells.

### *Macrophage EVs.*

So far, this chapter and the rest of the dissertation has focused on EVs produced by trophoblasts as a model of placental infection. Typically macrophages have been used to model *Lm* infections, since they are readily infected by *Lm* and are a major cell type of the immune system (20). We were curious as to whether the EV-dependent increase in susceptibility was trophoblast-specific, or also seen with EVs originating from other cells. We isolated S-EVs from infected RAW 264.7, J774, and BMDMs. We then treated these same macrophage-like cells with S-EVs from uninfected and infected cells (Figs. 5-7). For RAW 264.7 cells (Fig. 4.5) and BMDMs (Fig. 4.7), we again see an increase in subsequent *Lm* infection after EV treatment, especially with those from infected cells. For J774 cells, treatment with EVs from J774 and RAW 264.7 cells increased susceptibility (Fig. 4.6A+B). Interestingly, treatment with S-EVs from BMDMs did not change the level of infection (Fig. 4.6C), like what was seen with the tEVs. The results seen with EVs from macrophages suggest that this altered susceptibility to infection may be a conserved mechanism and that requires further study.

### *Treatment of mice with tEVs.*

Our *in vitro* results suggest that tEVs from *Lm*-infected TSCs make macrophages more susceptible to *Lm* infection. However, there was also an increase in tEV-induced TNF- $\alpha$  production associated with infection of the source TSC cells. We therefore sought to determine the effect of tEV pre-treatment on *in vivo* infection, and whether tEVs would exacerbate the infection as indicated by the macrophage result or lessen the infection due to the induction of cytokines. We treated nonpregnant BALB/c mice intravenously (IV) with  $10^8$  S-tEVs from uninfected or infected TSCs, or an equivalent amount of PBS. 24 h later,  $10^5$  bioluminescent *Lm*

were inoculated into the mice through IV injection (Fig. 4.8A). The initial plan was to image and sacrifice the mice at 72 hours post infection (HPI) but the mice were noticeably sick 48 HPI, so they were imaged using IVIS imaging at this time (Fig. 4.8B). The spleens from the animals were also collected and serial plated to determine CFUs. There was no statistically significant difference seen in the bioluminescence of the infection with any of the tEV conditions (Fig. 4.8C), and although there was a slight decrease in spleen CFU recovered with mice treated with tEVs, this was also not statistically significant (Fig. 4.8D). We repeated this experiment, except this time we used a lower dose of *Lm* and let the infection go to 72 HPI (Fig. 4.9A). Again, there were reduced bioluminescence seen in mice treated with tEVs and we recovered lower CFUs in the mice treated with infection tEVs, but these differences were also insignificant (Fig. 4.9C+D). Taken together, tEV pretreatment does not appear to significantly affect the susceptibility of nonpregnant mice to *Lm* infection.

## DISCUSSION

EVs are the subject of exciting new research that offers the potential for novel approaches for diagnosis and treatment of many diseases. A primary function of EVs appears to be the stimulation of cell signaling pathways in recipient cells, including immune cells, activating them in some instances and dampening responses in others. This delicate balance can be altered during disease and infection. For example, certain cancers secrete EVs that suppress immune cell activity, allowing the malignancy to proliferate (27). Conversely, cells infected with intracellular pathogens secrete pro-inflammatory EVs that help to control infection, although EVs from infected cells may sometimes have the opposite effect (28).

*Lm* is an intracellular pathogen that normally grows rapidly in macrophages *in vitro* unless the macrophage has been activated towards a pro-inflammatory phenotype. For example, RAW 264.7

macrophage-like cells treated with IFN- $\gamma$  are resistant to infection and kill intracellular *Lm* (25). Unexpectedly, we found that treatment with tEVs isolated from *Lm*-infected TSCs did not lead to increased *Lm* death; instead, this treatment made the cells more permissive for growth of the bacteria. This result occurred despite the induction of TNF- $\alpha$ , which normally indicates stimulation of macrophages resulting in greater resistance to infection. As far as the authors are aware, this is the first account of an EV treatment that causes cells to become more susceptible to *Lm* infection. Interestingly, this phenotype was not observed J774 cells. Both RAW 264.7 and J774 macrophage-like cell lines originate from BALB/c mice and have long been used in infection studies, although RAW 264.7 cells are from a male and J774 cells are from a female. J774 cells are more permissive for growth of *Lm*, and we expected activation by tEVs to reduce bacterial replication in these cells. The observation that these cells were equally permissive for *Lm* growth in all conditions was unexpected. The mechanisms of increased susceptibility in RAW 264.7 cells (and other cell types) but not J774 cells remains of interest for future work. In addition, how the tEVs from infected TSCs stimulate recipient cells in the absence of bacterial products is under investigation and will require directed manipulation of the altered contents.

EVs represent a potential strategy by *Lm* to spread throughout the host by rendering recipient cells more susceptible to the bacteria. *Lm* invades humans through epithelial cells that line the intestines, and from there the pathogen relies on cell-to-cell spread to access the rest of the body. Adding to these intriguing results is the fact that the increase in susceptibility was not seen when using  $\Delta hly$  *Lm* or HK *Lm* on the initial infection, suggesting that it requires cytosol invasion. A previous report indicated that inhibiting EV formation attenuated *Lm* growth in the spleens of mice, further suggesting that *Lm* could be hijacking host EV function for its own benefit (3). That report found that EVs from *Lm*-infected cells carried *Listeria* DNA and activated the cGAS-STING

pathway. This result is notable because this pathway leads to the release of type I interferons, which enhance *Lm* growth *in vivo* (29–31). Further studies will be needed to identify these pathways and define the role tEVs play during placental infection.

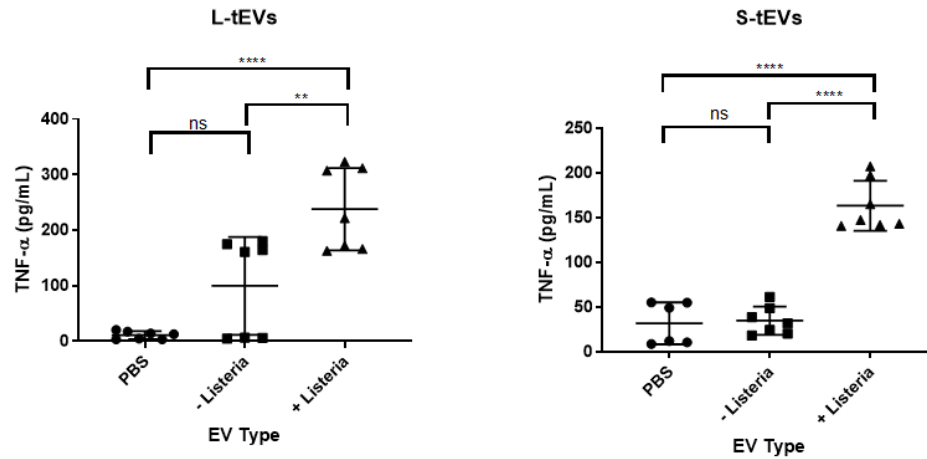
In mice, tEVs from infected TSCs detectably reduced infection, but the result was not statistically significant to  $p = 0.05$ . The reduction was modest, which could have been due to many factors. The number of tEVs administered ( $10^8$  tEVs), single vs. multiple tEV injections, whether or not the mice are pregnant, the timing and infectious dose of *Lm*, and the strain of mouse used may all be important, and we did not fully explore these parameters.

Overall, we show that infection of TSCs with *Lm* alters tEV production and function in unexpected ways. tEVs from *Lm*-infected TSCs elicit TNF- $\alpha$  production in RAW 264.7 macrophage-like cells. We also found that infection tEVs make certain cell types less resistant to subsequent infection, which was unexpected. The mechanism of this interaction is of great interest and is the subject of current investigation.

## APPENDIX

**Figure 4.1.** tEVs from *Lm*-infected TSCs induce the production of TNF- $\alpha$ .  $5 \times 10^5$  RAW 264.7 (A) and J774 (B) macrophage-like cells were treated with  $5 \times 10^6$  tEVs from uninfected and *Lm*-infected TSCs and the production of TNF- $\alpha$  was measured using enzyme-linked immunosorbent assay (ELISA). Comparisons for the TNF- $\alpha$  analysis was the Student's T-test; \*\*  $P < .01$ , \*\*\*\*  $P < .0001$ .

A



B

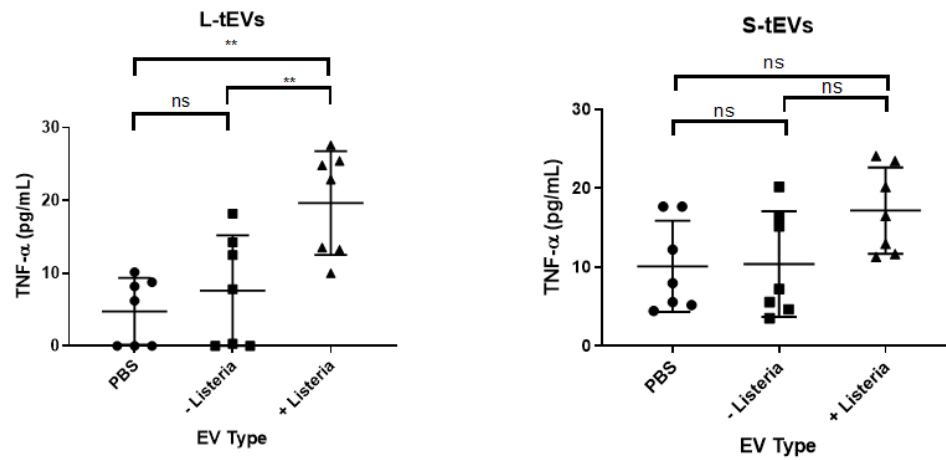


**Figure 4.2. tEVs from *Lm*-infected TSCs alter macrophage susceptibility to infection.**  $5 \times 10^5$  J774 cells (A), RAW 264.7 cells (B), and BMDMs (C) were treated with  $5 \times 10^6$  S-tEVs. After 24 h, the cells were infected at MOI=10 with mid-log bioluminescent *Lm*. The cells were imaged using the PerkinElmer in vivo imaging system (IVIS). Each group consisted of six replicates. At each timepoint, the EV groups were compared using Tukey's post hoc multiple comparison test. The stars indicate the any statistical difference between the + Listeria and PBS groups; \*  $P < .05$ , \*\*  $P < .01$ , \*\*\*\*  $P < .0001$ .

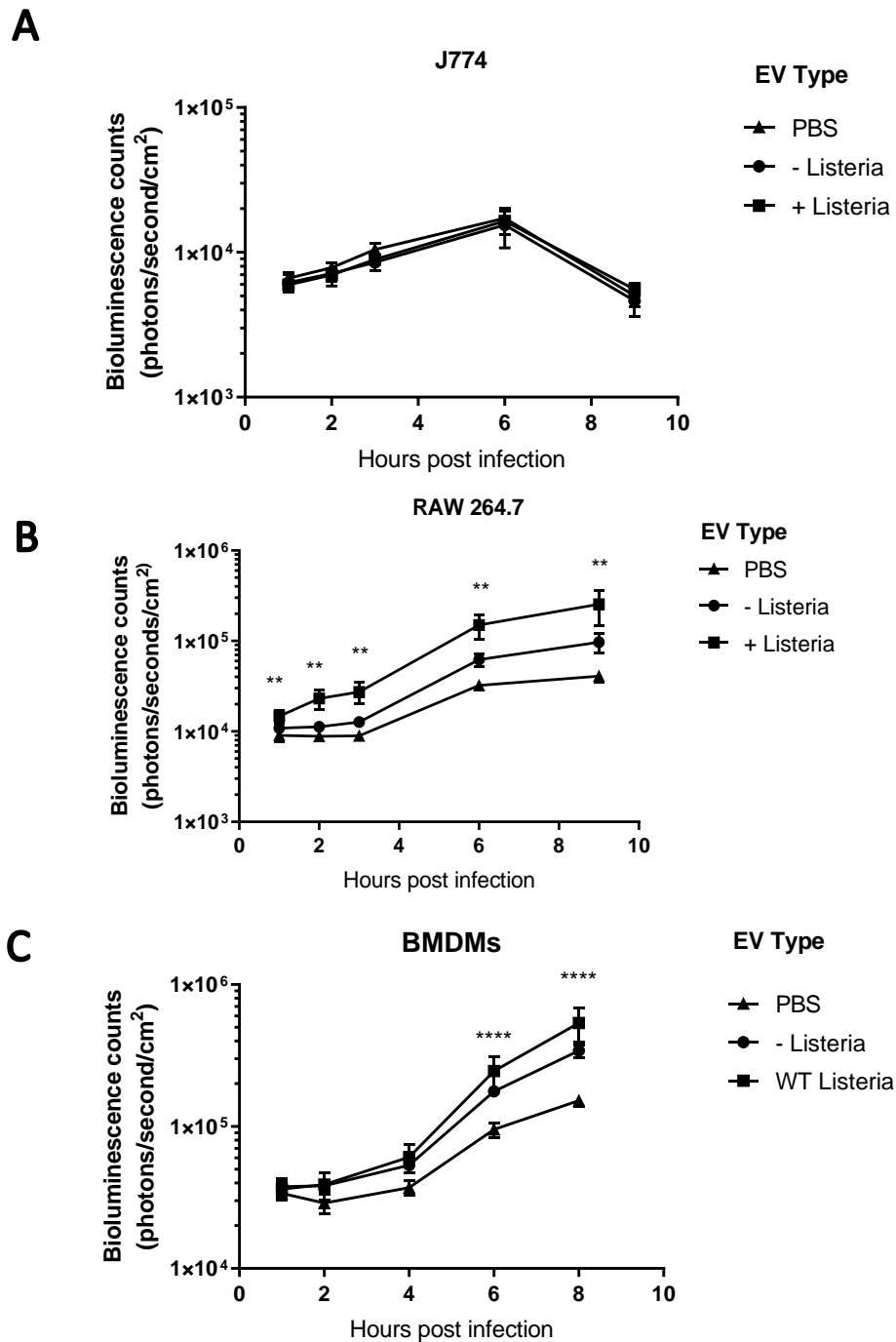


**Figure 4.3. tEVs slightly affect TSC susceptibility to *Lm* infection.** TSCs were treated with  $5 \times 10^6$  S-tEVs. After 24 h, the cells were infected at MOI=100 with mid-log bioluminescent *Lm*. The cells were imaged using the PerkinElmer IVIS system. Each group consisted of six replicates. At each timepoint, the EV groups were compared using Tukey's post hoc multiple comparison test. The stars indicate the any statistical difference between the + Listeria and PBS groups; \*  $P < .05$ , \*\*\*\*  $P < .0001$ .

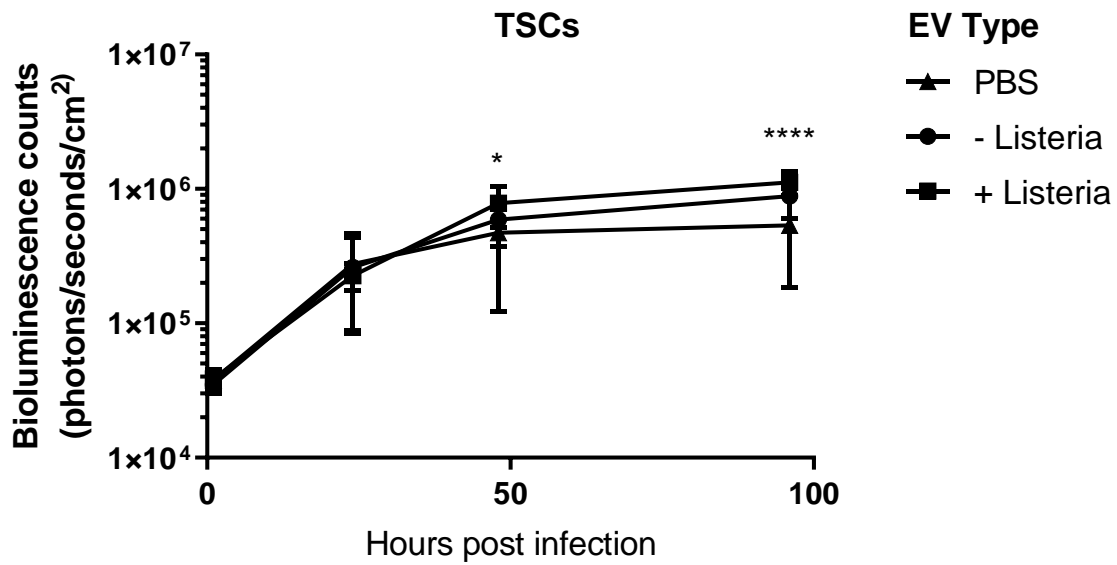


**Figure 4.4. *Lm* mutants of initial infection alter tEV effect on recipient cells.**  $5 \times 10^5$  RAW 264.7 cells (A+B) and BMDMs (C) were treated with  $5 \times 10^6$  S-tEVs from TSCs that were infected with either WT *Lm*,  $\Delta hly$  *Lm*, or heat-killed (HK) *Lm*. After 24 h, the cells were infected at MOI=10 with mid-log bioluminescent WT *Lm*. The cells were imaged using the PerkinElmer IVIS system. Each group consisted of six replicates. At each timepoint, the EV groups were compared using Tukey's post hoc multiple comparison test. The stars indicate the any statistical difference between the + Listeria and either  $\Delta hly$  Listeria (A+C) or HK Listeria (B) group; \*\* P<.01, \*\*\* P<.001, \*\*\*\* P<.0001.

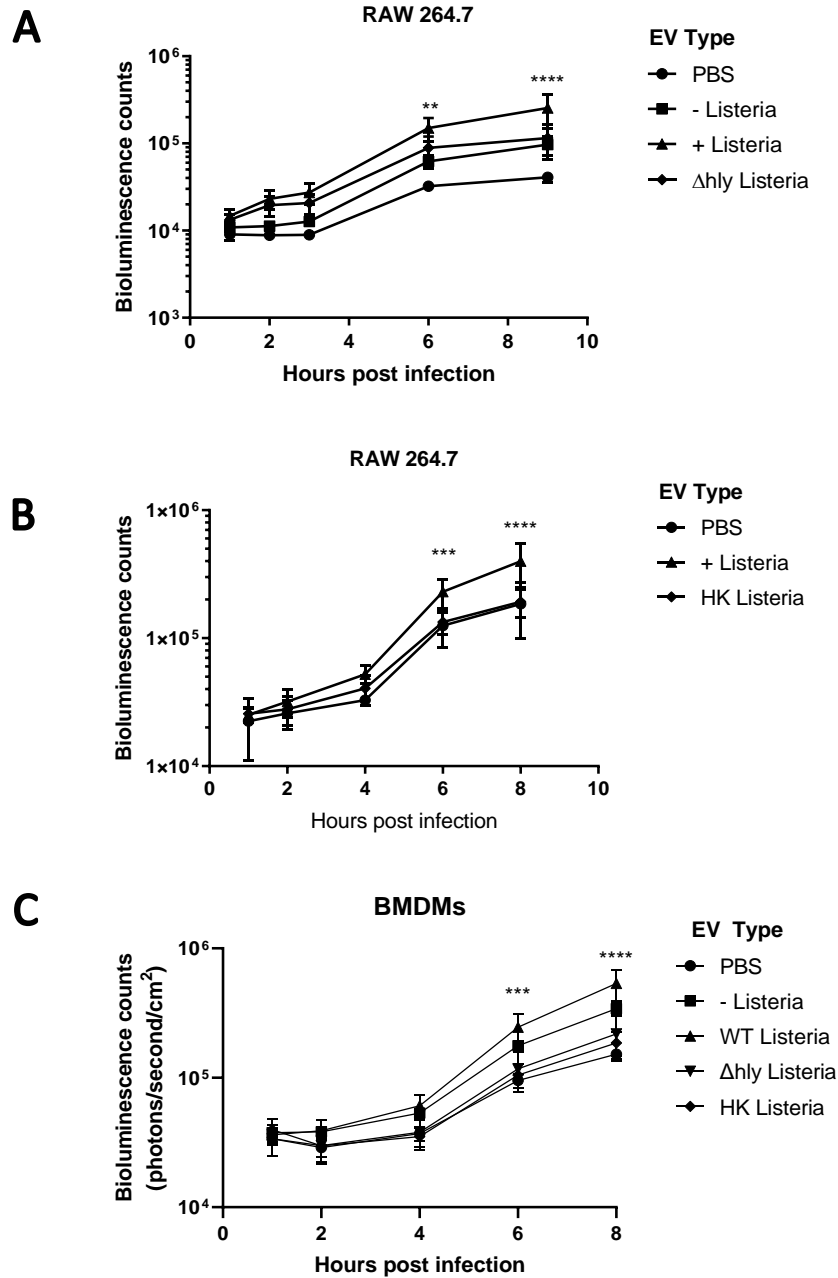


**Figure 4.5. Macrophage S-EVs alter RAW 264.7 cells susceptibility to *Lm*.**  $5 \times 10^5$  RAW 264.7 cells were treated with  $5 \times 10^6$  S-EVs from either RAW 264.7 (A), J774 (B), or BMDMs (C). After 24 h, the cells were infected at MOI=10 with mid-log bioluminescent *Lm*. The cells were imaged using the PerkinElmer IVIS system. Each group consisted of four replicates. At each timepoint, the EV groups were compared using Tukey's post hoc multiple comparison test. The stars indicate the any statistical difference between the + Listeria and PBS groups; \*\* P<.01, \*\*\* P<.001, \*\*\*\* P<.0001.

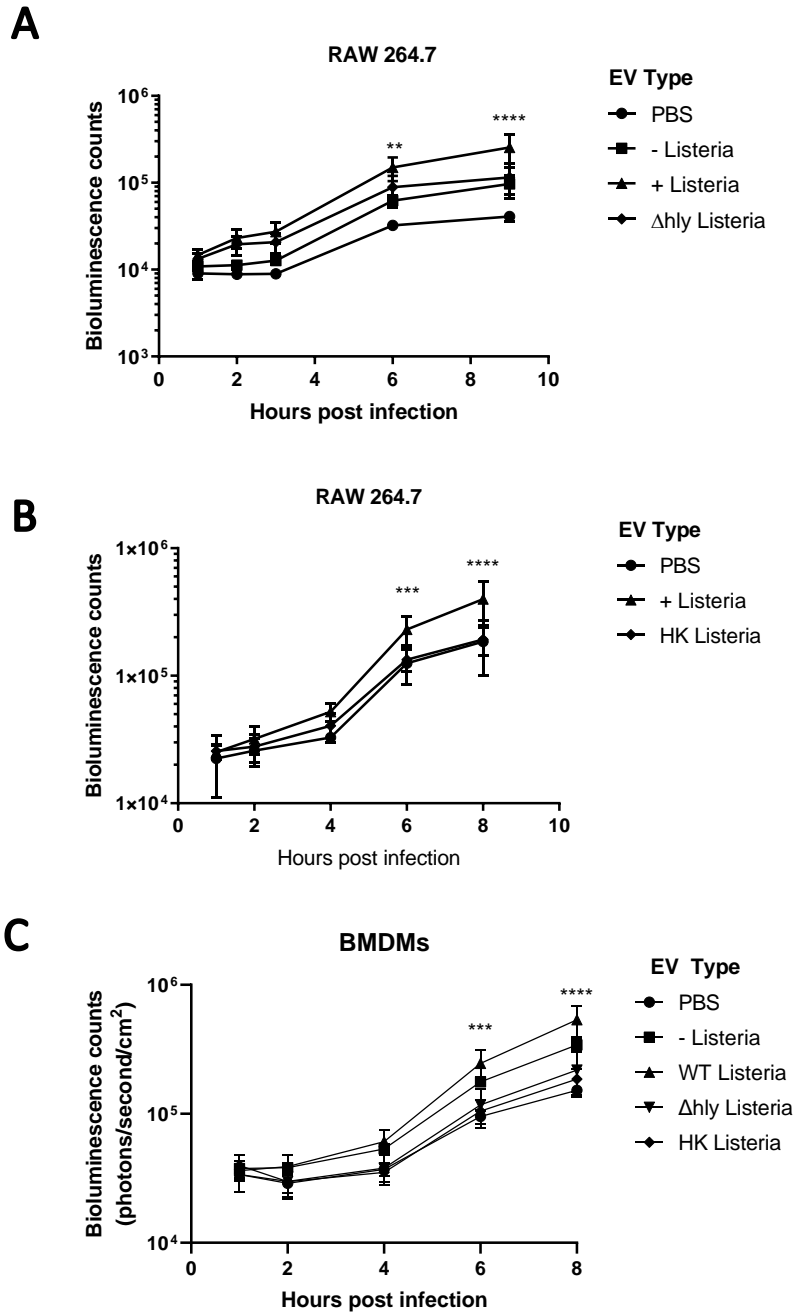


**Figure 4.6. Macrophage S-EVs alter J774 cells susceptibility to *Lm*.**  $5 \times 10^5$  J774 cells were treated with  $5 \times 10^6$  S-EVs from either RAW 264.7 (A), J774 (B), or BMDMs (C). After 24 h, the cells were infected at MOI=10 with mid-log bioluminescent *Lm*. The cells were imaged using the PerkinElmer IVIS system. Each group consisted of four replicates. At each timepoint, the EV groups were compared using Tukey's post hoc multiple comparison test. The stars indicate the any statistical difference between the + Listeria and PBS groups; \*\* P<.01, \*\*\* P<.001, \*\*\*\* P<.0001.

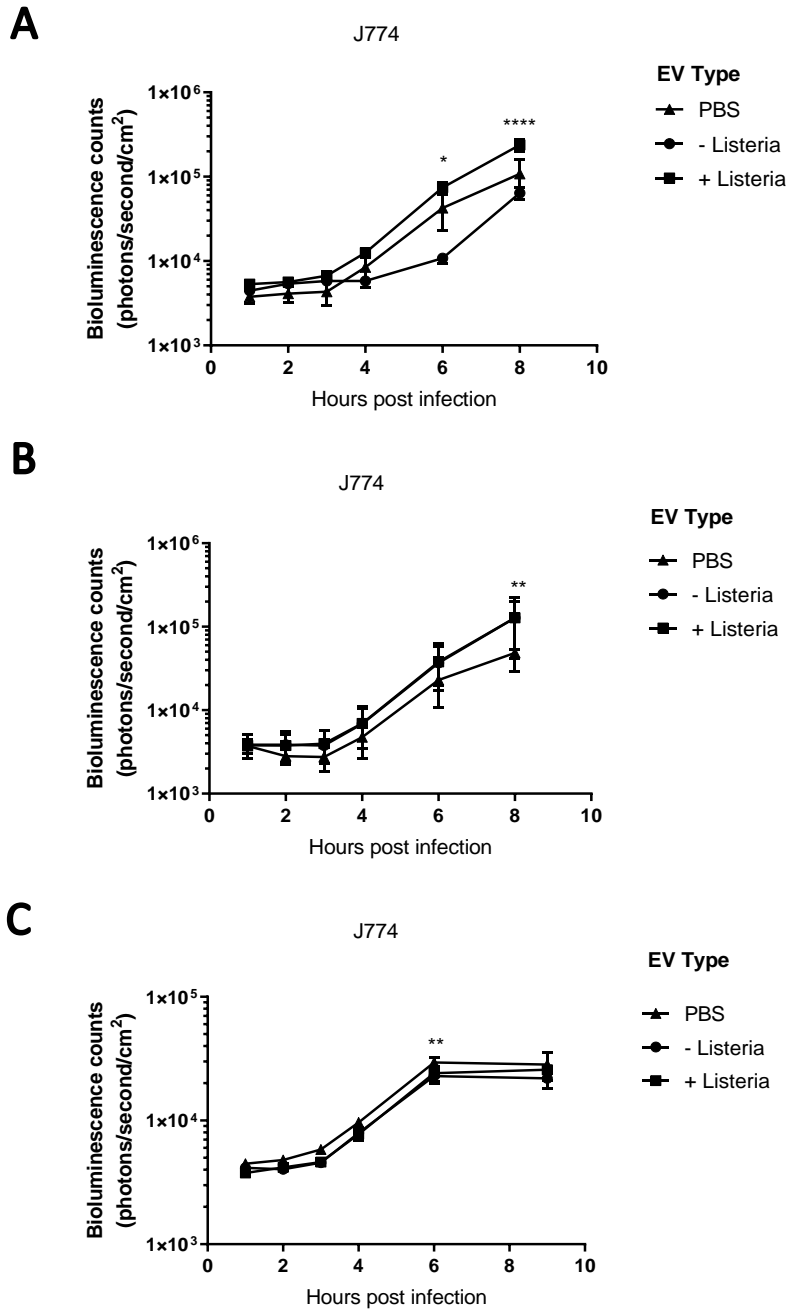


**Figure 4.7. BMDM S-EVs alter BMDMs susceptibility to *Lm*.**  $5 \times 10^5$  BMDMs were treated with  $5 \times 10^6$  S-EVs from BMDMs. After 24 h, the cells were infected at MOI=10 with mid-log bioluminescent *Lm*. The cells were imaged using the PerkinElmer IVIS system. Each group consisted of four replicates. At each timepoint, the EV groups were compared using Tukey's post hoc multiple comparison test. The stars indicate the any statistical difference between the + *Listeria* and PBS groups; \*\*\*\* P<.0001.

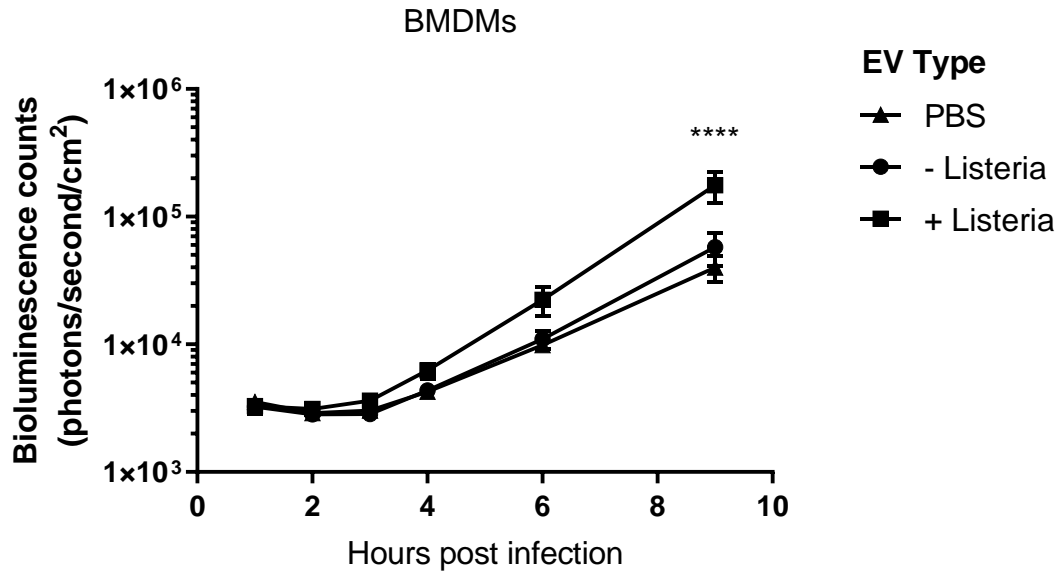
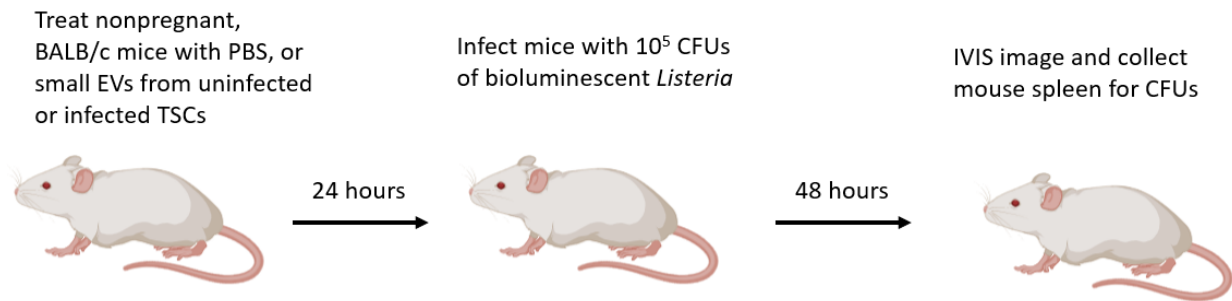


**Figure 4.8. tEVs do not change mouse resistance to *Lm*.** (A) Diagram of treatment of BALB/c mice with tEVs from TSCs before infection with bioluminescent *Lm*. Images made with BioRender. (B) IVIS images of mice 48 hours after infection. (C) Quantification of bioluminescence radiance signifying bacterial growth in the mice. (D) Bacterial growth measured by plate counting serial dilutions of spleens. Non-parametric one-way ANOVA (Kruskal-Wallis test) was used for comparison of the groups.

A



B

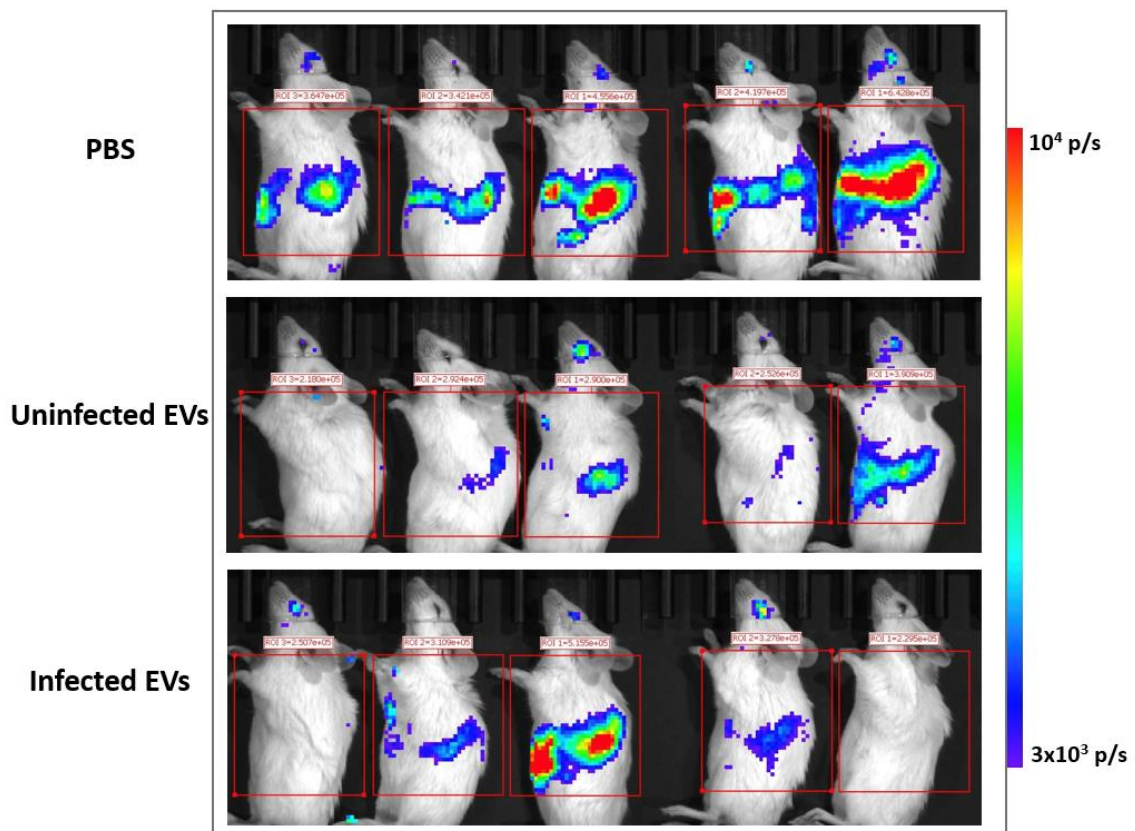
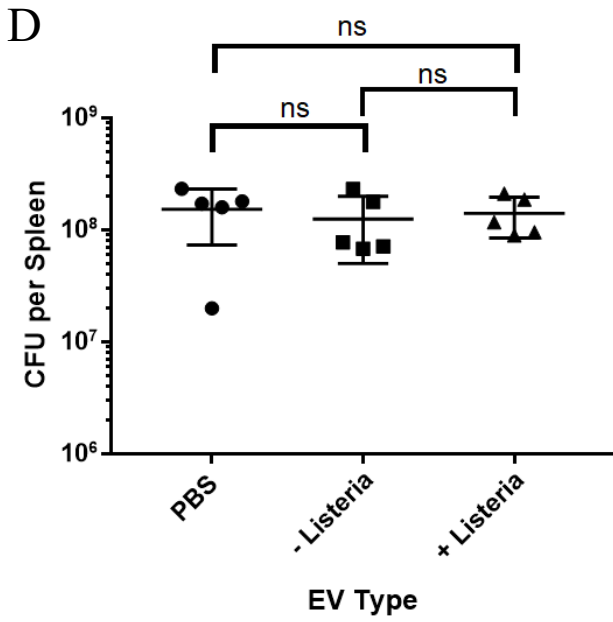
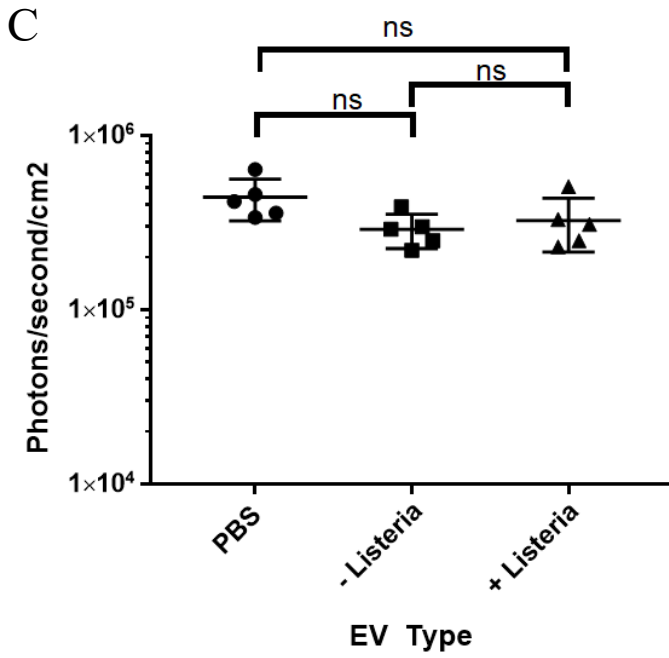
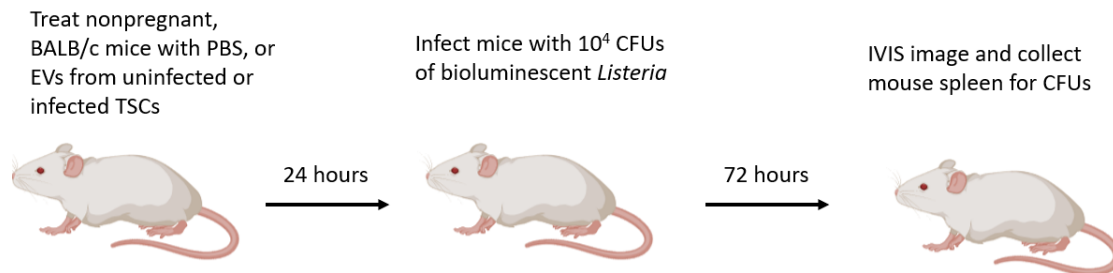


Figure 4.8 (cont'd)



**Figure 4.9. tEVs do not change mouse resistance to *Lm* in different experimental setup.** (A) Diagram of treatment of BALB/c mice with tEVs from TSCs before infection with bioluminescent *Lm*. Images made with BioRender. (B) IVIS images of mice 72 hours after infection. (C) Quantification of bioluminescence radiance signifying bacterial growth in the mice. (D) Bacterial growth measured by plate counting serial dilutions of spleens. Non-parametric one-way ANOVA (Kruskal-Wallis test) was used for comparison of the groups.

A



B

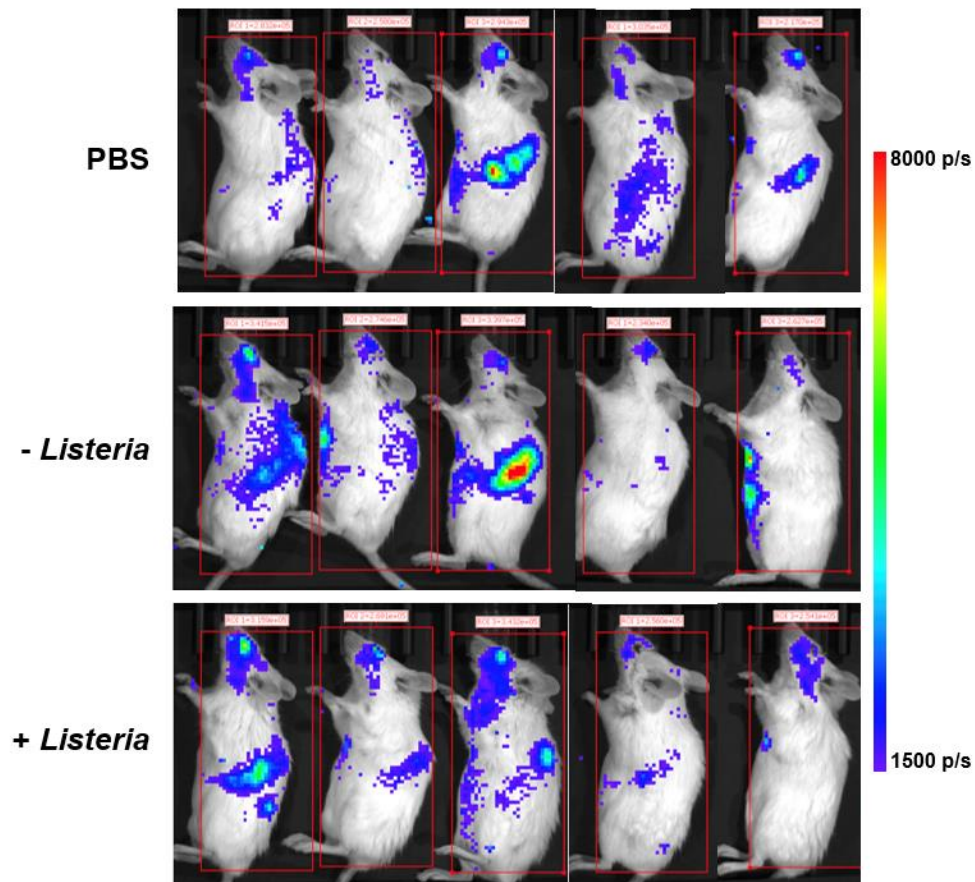
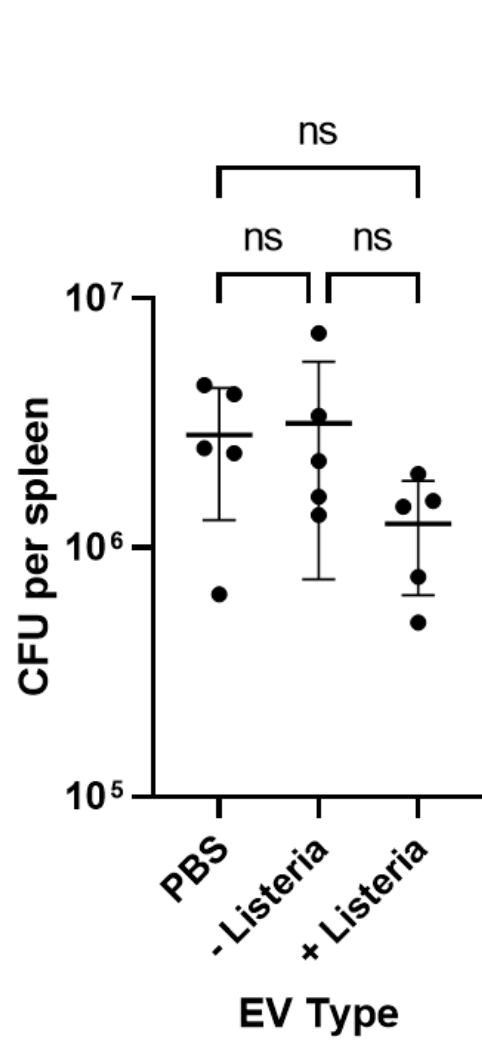
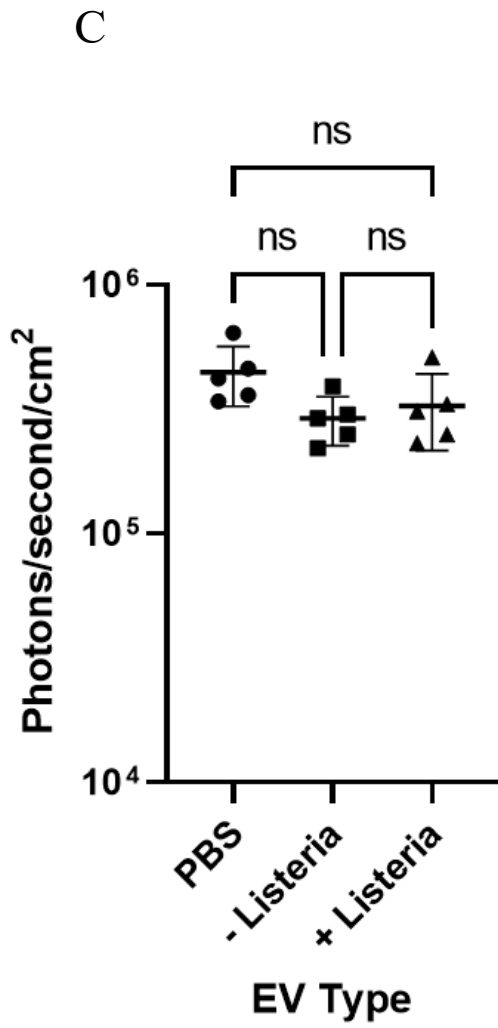


Figure 4.9 (cont'd)



## REFERENCES

## REFERENCES

1. Bhatnagar S, Schorey JS. 2007. Exosomes released from infected macrophages contain *Mycobacterium avium* glycopeptidolipids and are proinflammatory. *J Biol Chem* 282:25779–25789.
2. Hui WW, Hercik K, Belsare S, Alugubelly N, Clapp B, Rinaldi C, Edelmann MJ. 2018. *Salmonella enterica* Serovar Typhimurium Alters the Extracellular Proteome of Macrophages and Leads to the Production of Proinflammatory Exosomes. *Infect Immun* 86.
3. Nandakumar R, Tschismarov R, Meissner F, Prabakaran T, Krissanaprasit A, Farahani E, Zhang B-C, Assil S, Martin A, Bertrams W, Holm CK, Ablasser A, Klause T, Thomsen MK, Schmeck B, Howard KA, Henry T, Gothelf KV, Decker T, Paludan SR. 2019. Intracellular bacteria engage a STING-TBK1-MVB12b pathway to enable paracrine cGAS-STING signalling. *Nat Microbiol* 4:701–713.
4. Alvarez-Jiménez VD, Leyva-Paredes K, García-Martínez M, Vázquez-Flores L, García-Paredes VG, Campillo-Navarro M, Romo-Cruz I, Rosales-García VH, Castañeda-Casimiro J, González-Pozos S, Hernández JM, Wong-Baeza C, García-Pérez BE, Ortiz-Navarrete V, Estrada-Parra S, Serafín-López J, Wong-Baeza I, Chacón-Salinas R, Estrada-García I. 2018. Extracellular Vesicles Released from *Mycobacterium tuberculosis*-Infected Neutrophils Promote Macrophage Autophagy and Decrease Intracellular *Mycobacterial* Survival. *Front Immunol* 9:272.
5. Cheng Y, Schorey JS. 2019. Extracellular vesicles deliver *Mycobacterium* RNA to promote host immunity and bacterial killing. *EMBO Rep* 20.
6. Giri PK, Schorey JS. 2008. Exosomes derived from *M. Bovis* BCG infected macrophages activate antigen-specific CD4+ and CD8+ T cells in vitro and in vivo. *PLoS ONE* 3:e2461.
7. Cheng Y, Schorey JS. 2013. Exosomes carrying mycobacterial antigens can protect mice against *Mycobacterium tuberculosis* infection. *Eur J Immunol* 43:3279–3290.
8. Giri PK, Kruh NA, Dobos KM, Schorey JS. 2010. Proteomic analysis identifies highly antigenic proteins in exosomes from *M. tuberculosis*-infected and culture filtrate protein-treated macrophages. *Proteomics* 10:3190–3202.
9. Colino J, Snapper CM. 2006. Exosomes from bone marrow dendritic cells pulsed with diphtheria toxoid preferentially induce type 1 antigen-specific IgG responses in naive recipients in the absence of free antigen. *J Immunol* 177:3757–3762.

10. Hui WW, Emerson LE, Clapp B, Sheppe AE, Sharma J, del Castillo J, Ou M, Maegawa GHB, Hoffman C, Larkin, III J, Pascual DW, Edelmann MJ. 2021. Antigen encapsulating host extracellular vesicles derived from Salmonella-infected cells stimulate pathogen-specific Th1-type responses in vivo . *PLoS Pathog* 17:1–27.
11. Sabapatha A, Gercel-Taylor C, Taylor DD. 2006. Specific isolation of placenta-derived exosomes from the circulation of pregnant women and their immunoregulatory consequences. *Am J Reprod Immunol* 56:345–355.
12. Stenqvist A-C, Nagaeva O, Baranov V, Mincheva-Nilsson L. 2013. Exosomes secreted by human placenta carry functional Fas ligand and TRAIL molecules and convey apoptosis in activated immune cells, suggesting exosome-mediated immune privilege of the fetus. *J Immunol* 191:5515–5523.
13. Han C, Han L, Huang P, Chen Y, Wang Y, Xue F. 2019. Syncytiotrophoblast-Derived Extracellular Vesicles in Pathophysiology of Preeclampsia. *Front Physiol* 10:1236.
14. Han C, Wang C, Chen Y, Wang J, Xu X, Hilton T, Cai W, Zhao Z, Wu Y, Li K, Houck K, Liu L, Sood AK, Wu X, Xue F, Li M, Dong J-F, Zhang J. 2019. Placenta-derived extracellular vesicles induce preeclampsia in mouse models. *Haematologica* <https://doi.org/10.3324/haematol.2019.226209>.
15. Gill M, Motta-Mejia C, Kandzija N, Cooke W, Zhang W, Cerdeira AS, Bastie C, Redman C, Vatish M. 2019. Placental Syncytiotrophoblast-Derived Extracellular Vesicles Carry Active NEP (Neprilysin) and Are Increased in Preeclampsia. *Hypertension* 73:1112–1119.
16. Hardy J, Francis KP, DeBoer M, Chu P, Gibbs K, Contag CH. 2004. Extracellular replication of *Listeria monocytogenes* in the murine gall bladder. *Science* 303:851–853.
17. Tanaka S, Kunath T, Hadjantonakis AK, Nagy A, Rossant J. 1998. Promotion of trophoblast stem cell proliferation by FGF4. *Science* 282:2072–2075.
18. Erlebacher A, Price KA, Glimcher LH. 2004. Maintenance of mouse trophoblast stem cell proliferation by TGF-beta/activin. *Dev Biol* 275:158–169.
19. Trouplin V, Boucherit N, Gorvel L, Conti F, Mottola G, Ghigo E. 2013. Bone marrow-derived macrophage production. *J Vis Exp* e50966.
20. Portnoy DA, Jacks PS, Hinrichs DJ. 1988. Role of hemolysin for the intracellular growth of *Listeria monocytogenes*. *J Exp Med* 167:1459–1471.
21. Hardy J, Kirkendoll B, Zhao H, Pisani L, Luong R, Switzer A, McConnell MV, Contag CH. 2012. Infection of pregnant mice with *Listeria monocytogenes* induces fetal bradycardia. *Pediatr Res* 71:539–545.

22. Pamer EG. 2004. Immune responses to *Listeria monocytogenes*. *Nat Rev Immunol* 4:812–823.
23. Mohammadzadeh R, Ghazvini K, Farsiani H, Soleimanpour S. 2020. *Mycobacterium tuberculosis* extracellular vesicles: exploitation for vaccine technology and diagnostic methods. *Crit Rev Microbiol* 1–21.
24. Liu Y, Hammer LA, Liu W, Hobbs MM, Zielke RA, Sikora AE, Jerse AE, Egilmez NK, Russell MW. 2017. Experimental vaccine induces Th1-driven immune responses and resistance to *Neisseria gonorrhoeae* infection in a murine model. *Mucosal Immunol* 10:1594–1608.
25. Portnoy DA, Schreiber RD, Connelly P, Tilney LG. 1989. Gamma interferon limits access of *Listeria monocytogenes* to the macrophage cytoplasm. *J Exp Med* 170:2141–2146.
26. Tilney LG, Portnoy DA. 1989. Actin filaments and the growth, movement, and spread of the intracellular bacterial parasite, *Listeria monocytogenes*. *J Cell Biol* 109:1597–1608.
27. Xu R, Rai A, Chen M, Suwakulsiri W, Greening DW, Simpson RJ. 2018. Extracellular vesicles in cancer - implications for future improvements in cancer care. *Nat Rev Clin Oncol* 15:617–638.
28. White JR, Dauros-Singorenko P, Hong J, Vanholsbeeck F, Phillips A, Swift S. 2021. The complex, bidirectional role of extracellular vesicles in infection. *Biochem Soc Trans* <https://doi.org/10.1042/BST20200788>.
29. Shaabani N, Vartabedian VF, Nguyen N, Honke N, Huang Z, Teijaro JR. 2021. IFN- $\beta$ , but not IFN- $\alpha$ , is Responsible for the Pro-Bacterial Effect of Type I Interferon. *Cell Physiol Biochem* 55:256–264.
30. O’Connell RM, Saha SK, Vaidya SA, Bruhn KW, Miranda GA, Zarnegar B, Perry AK, Nguyen BO, Lane TF, Taniguchi T, Miller JF, Cheng G. 2004. Type I interferon production enhances susceptibility to *Listeria monocytogenes* infection. *J Exp Med* 200:437–445.
31. Auerbuch V, Brockstedt DG, Meyer-Morse N, O’Riordan M, Portnoy DA. 2004. Mice lacking the type I interferon receptor are resistant to *Listeria monocytogenes*. *J Exp Med* 200:527–533.

## CHAPTER 5

### CONCLUSIONS AND FUTURE DIRECTIONS

This dissertation aims to determine how *Listeria monocytogenes* (*Lm*) placental infection alters the production of extracellular vesicles, and what effect that could have on the immune response to the pathogens. To answer this question, we established *in vitro* models to study *Lm* infection, particularly a trophoblast stem cell (TSC) model to study placental colonization (Chapter 2). From this TSC system, we isolated trophoblast EVs (tEVs) and determined how infection changes the host cargo loaded into the vesicles (Chapter 3). Lastly, we treated macrophages with the EVs to elucidate how the infection EVs may activate and affect the immune response (Chapter 4). This dissertation has shown that *Lm* infection of TSCs alters the mRNAs and proteins found in the tEVs, and that these tEVs induce the production of TNF- $\alpha$  in macrophages. This activation also led to the cells becoming more susceptible to subsequent infection, a result also seen with macrophage EV treatment. This chapter will delve into additional analysis of these results and potential future directions for the project.

### *Chapter 2: Modeling Listeria monocytogenes infections.*

The first step in understanding host-pathogen interactions is establishing systems to study these infections in the laboratory. The placenta is particularly challenging to model, as trophoblasts can be difficult to cultivate and maintain in cell culture. One solution to this problem is the use of trophoblast stem cells. TSCs are isolated from the placentas of mice and humans and are maintained with the use of growth factors, which allow for the replication of these cells for an indefinite period (1, 2). TSCs act as the cell of origin for the various types of trophoblasts found throughout the placenta. We infected the TSCs with *Lm* to determine their susceptibility to infection. Using fluorescence microscopy and infection with bioluminescent *Lm*, we found that TSCs can indeed support the invasion and growth of *Lm*. That said, this required a relatively high amount of *Lm* and longer time course compared to infections of other cell types, specifically

macrophages. This supports results from guinea pig infections, where the placenta invaded with *Lm* at a low rate (3). To further understand the mechanism of TSC infection, I used a variety of *Lm* mutants that represent different stages of the *Lm* intracellular lifecycle. Interestingly, we did not see a decrease in growth when infecting with an *Lm* strain that lacks internalin A and B, which are used to mediate bacterial uptake in other cell types (4). We did see decrease in growth with strains that lack either listeriolysin O (LLO) ( $\Delta hly$ ) or ActA ( $\Delta actA$ ). The decrease in growth with the  $\Delta hly$  *Lm* is to be expected, as LLO facilitates vacuolar escape, a required step for *Lm* to grow in cells (5). Decreased growth with the  $\Delta actA$  mutant is more surprising, as ActA is not required for cytosolic replication, but instead for cell-to-cell spread (6). Overall, we see *Lm* establishing its intracellular lifecycle in TSCs, paving the way for their use as an infection model.

An important aspect to the use of TSCs as a model for the placenta is their ability to be differentiated into syncytiotrophoblasts (SynTs) or trophoblast giant cells (TGCs), trophoblast types that are also found in the mouse placenta (7). Previous work with TSCs found that they can be differentiated into SynTs or TGCs with the removal of growth factors and the addition of chemical activators (8–10). Here, we show that differentiated trophoblasts were very resistant to *Lm* infection. Previous findings found that a formed syncytia helps prevent *Lm* from establishing infection, providing a potential mechanism for the resistance (11, 12). Additionally, since differentiation is the antithesis of cellular replication, it is possible that there are just lower amounts of cells to act as hosts for *Lm*. Regardless, the ability of TSCs to differentiate into physiologically relevant trophoblast types leads to the potential follow-up experiment of generating tEVs from the infected cells. This may be more relevant than looking at tEVs from the infected TSCs since SynTs are the cells that come into contact with the maternal blood (11).

In addition to the TSCs, we also show that HTR-8/SVneo trophoblast cells can be infected with *Lm*, although this also required a high MOI. HTR-8/SVneo cells were originally isolated from humans and can serve as a model of extravillous trophoblasts (similar to murine TGCs), a cell type that TSCs cannot be differentiated into (13). Like the differentiated TSCs, an area to explore in follow-up to this thesis would be generate tEVs from these cells and compare how they differ from the infection tEVs from TSCs. In a similar vein, there are primary trophoblast systems that may serve as more accurate models than our TSCs. The issue with these primary trophoblasts, which can be isolated from either humans or mice, is that they are laborious to isolate, expensive, and have limited use since they are non-replicative. That said, since we have established a protocol for infecting trophoblasts to generate and isolate tEVs, it would be appropriate to reconduct our experiments in a model that may require more resources but could serve as a more physiological relevant model for placental infection. Additionally, trophoblast-like cells have been differentiated from human induced pluripotent stem cells, providing an additional model to study placental interactions (14).

The last portion of Chapter 2 focused on infecting neural progenitor cells, which are continuously replicating cell lines that could serve in studies of *Lm* invasion of the brain and central nervous system (CNS). I showed that these cells allow for the intracellular growth of *Lm*, even at low MOIs. This model has the potential to study which bacterial factors could be essential for infection, such as InlF, which was identified in a previous study as a key virulence factor for *Lm* colonization of the brain and CNS (15). Similarly, these cells could be used to understand host response to *Lm* crossing the blood-brain barrier, an area of great interest.

*Chapter 3: Listeria monocytogenes infection alters extracellular vesicles produced by trophoblast stem cells.*

Chapter 3 focuses on characterizing tEVs produced by TSCs, and how *Lm* infection alters their production and composition. This was first accomplished by establishing a protocol to isolate tEVs from TSCs, one which was inspired by protocols used in other EV models (16). We use a combination of filtration and ultracentrifugation to isolate EVs of different sizes. It is still debated which isolation method is best for EVs, considering factors including EV preservation, time and cost requirements, and potential for contamination. While ultracentrifugation is currently seen as the most reliable and consistent method for EV isolation, it is important to note that the isolation method chosen may influence our results.

To determine how *Lm* infection changes tEVs, we first performed mass spectrometry on small tEVs (S-tEVs) from uninfected and *Lm*-infected TSCs. We saw a much higher rate of unique proteins identified in the tEVs from infected cells, as well as these tEVs having higher abundance of many proteins compared to the tEVs from uninfected cells. Interestingly, gene ontology (GO) analysis showed that the main pathways involved with the proteins overrepresented in the infection tEVs were RNA binding and processing. This likely due to the large number of ribosomal proteins seen in the infection tEVs. A similar result was seen in microglial cells, where lipopolysaccharide (LPS) treatment led to ribosomal proteins being transported in tEVs (17). In fact, there were several proteins overlapping between our findings and theirs. They speculated that this increase of ribosomal proteins in EVs was due to an increase in cellular activity because of infection, and that the increase in cellular ribosomes would correlate with higher amounts of ribosomes found in EVs. RNA sequencing on trophoblasts infected with *Lm* did show an upregulation in RNA processing and translation genes, although it was not to the same degree that we see increased in the tEVs (18). A better comparison would be to perform proteomic analysis on the cellular proteins during infection, which would serve to confirm whether the increase in EV proteins is just due to a higher

abundance in the cell or if there is selective loading of the vesicles. Immunofluorescence or western blots with antibodies specific to ribosomes could also be used to determine if there is an increase in ribosomes in infected cells.

The presence of the RNA binding proteins in the tEVs from infected cells made us wonder if infection also alters the RNAs in the tEVs. We performed RNA sequencing (RNAseq) on the S-tEVs from uninfected and *Lm*-infected TSCs. We found many overrepresented mRNAs in both types of tEVs, signaling that *Lm* infection does affect the RNAs loaded into tEVs. The mRNAs identified in the tEVs from infected cells represented genes involved in vasculature and placental development. As mRNAs can be translated to proteins in recipient cells, there is potential that the mRNAs in the infection tEVs could be activating these pathways (19). There is some evidence that EVs help establish the placenta in the decidua and allows it to develop, a process that requires inflammation (20). It is possible that *Lm* infection affects the tEVs produced so they act in a similar manner, although this will require much further study.

Our proteomics results found virtually no *Lm* proteins in the tEVs. This was unexpected given previous results that showed bacterial proteins in EVs from infected cells. That said, there may be other bacterial components loaded into the tEVs that we did not search for. The RNA sequencing we performed was geared to probe for eukaryotic mRNA, so it would have missed any *Lm* RNA present. Another aspect that we have not investigated yet is the presence of DNA. Previous work with *Lm* infections found that host EVs contain *Lm* DNA, which is then recognized by recipient cells (21). An exciting next step would be to investigate whether *Lm* infection changes the DNA composition in tEVs, and especially if *Lm* DNA is present. Another component that may be affected by *Lm* infection is the presence of microRNA (miRNA). miRNA has been of interest for EV studies since it was discovered that miRNA is commonly found in EVs and EVs from diseased

cells have unique miRNA profiles (22). *Lm* infection induces the production of certain miRNAs, and tEVs have previously been shown to carry distinct miRNA species (23, 24).

Our studies investigating the contents of the tEVs focused exclusively on S-tEVs and not on large tEVs (L-tEVs). The reason for this was because we recover more S-tEVs and we wanted to ensure that we had enough material to properly perform the investigations, all of which require a minimal amount of the material being investigated. Additionally, similar studies also focused on S-EVs since they are interested in exosomes, and this EV type is predicted to be included with that EV isolation protocol. Probing L-tEVs for their protein, nucleic acid, and lipid content after infection would be an interesting study to either verify what we found in the S-tEVs, or if that is a unique result for those EVs.

#### *Chapter 4: Immune cell response to extracellular vesicles from infected cells.*

EVs have been found to play an important role in cellular communication and immune coordination, particularly during bacterial infections (25, 26). This inspired us to investigate what effects the tEVs from infected TSCs would have on immune cells. We discovered that treatment of macrophage-like cells with infection tEVs induces the production of TNF- $\alpha$ , a pro-inflammatory cytokine. This result suggests that the tEVs from infected TSCs can activate an immune response to *Lm* infection, although we only did measure the response of a single cytokine. Follow-up work can determine if the tEVs also stimulate the production of other cytokines, for example IFN- $\beta$ , IL-1 $\beta$ , and RANTES, which are all produced in cells infected with *Lm* (27–29). This would give a more complete picture as to the pro-inflammatory effects of the tEVs.

With this potential activation of macrophage-like cells, we predicted that the tEV treatment would make the cells resistant to subsequent *Lm* infection. Our results were the exact opposite of this

prediction, as cells treated with S-tEVs, especially S-tEVs from *Lm*-infected TSCs, became more permissive to *Lm* growth. The cause of this permissiveness is still unknown. One potential mechanism is that any activation of the cells by the tEVs made them more phagocytic, swallowing *Lm* at a higher rate and allowing a greater number of bacteria to enter the cytosol of the host cell and replicate. Potential evidence for this hypothesis is the increase of *Lm* growth at 2 hours post infection with the cells treated with tEVs, an early timepoint in the *Lm* infections. There are commercially available assays to measure phagocytosis, which could help use answer this question. Another possible way to test this hypothesis would be to image the infections using confocal microscopy at early timepoints to determine if there are indeed higher numbers of bacteria early on, before they would have a chance to replicate. Using confocal microscopy could also determine if there is another mechanism at play that could affect other stages of the *Lm* lifecycle, such as increased vacuolar escape. Additionally, tEVs may induce the expression of genes that alter the cells susceptibility to *Lm* infection. This can be determined by performing RNAseq on cells treated with tEVs. RNAseq would also give additional insight into the pro-inflammatory response infection tEVs elicit.

Interestingly, we also saw the increase in susceptibility to *Lm* infection after treatment with S-EVs from macrophages. Using RAW 264.7, J774, and bone marrow derived macrophages (BMDMs) EVs, we again saw greater *Lm* growth in most of the cells that were treated with EVs from infected cells. This suggests that EV modification of recipient cells could be conserved across cell types. Future work can explore if the differences seen in the infection tEVs, such as the increase in RNA-binding proteins and mRNAs from vasculogenesis genes, also seen with the EVs from macrophages. Additionally, while macrophages have been the primary immune cell type of this study, it is not the only immune cell found in the placental environment. In fact, the primary

immune cell are uterine natural killer (uNK) cells, specialized cells that aid in crafting the proper environment for placentas to develop (30). Detailing the response of these and other placental cells will give additional insight into how tEVs may affect the immune response.

*Final Takeaways.*

This dissertation explores the ability of EVs from infected trophoblast cells to elicit an immune response. We found that *Lm* infection alters the tEVs produced, that the tEVs can be immunostimulatory, and that the tEVs made recipient macrophages more susceptible to infection. These results aid our understanding of not only *Lm* infections, but placental infection as a whole. Infections are a major source of disease in pregnant people, resulting in horrific outcomes. Additionally, inadvertent placental inflammation can also lead to impaired development of the fetus. This research may help lead to better understanding of the placental immune system, and how we could recognize and prevent disease. EVs have already been of interest to develop into diagnostic methods, and our results could be a potential starting point for the creation of diagnostic tools for placental disease. Further understanding how the immune response is activated to the placenta could also lead to novel therapeutic applications that could potentially help the prognosis for those dealing with these types of diseases. I hope that one day this research will help spawn new advancements that help pregnant parents and families facing terrible situations.

## REFERENCES

## REFERENCES

1. Tanaka S, Kunath T, Hadjantonakis AK, Nagy A, Rossant J. 1998. Promotion of trophoblast stem cell proliferation by FGF4. *Science* 282:2072–2075.
2. Okae H, Toh H, Sato T, Hiura H, Takahashi S, Shirane K, Kabayama Y, Suyama M, Sasaki H, Arima T. 2018. Derivation of human trophoblast stem cells. *Cell Stem Cell* 22:50-63.e6.
3. Bakardjiev AI, Theriot JA, Portnoy DA. 2006. *Listeria monocytogenes* traffics from maternal organs to the placenta and back. *PLoS Pathog* 2:e66.
4. Ireton K, Mortuza R, Gyanwali GC, Gianfelice A, Hussain M. 2021. Role of internalin proteins in pathogenesis of *Listeria monocytogenes*. *Mol Microbiol* <https://doi.org/10.1111/mmi.14836>.
5. Portnoy DA, Jacks PS, Hinrichs DJ. 1988. Role of hemolysin for the intracellular growth of *Listeria monocytogenes*. *J Exp Med* 167:1459–1471.
6. Tilney LG, Portnoy DA. 1989. Actin filaments and the growth, movement, and spread of the intracellular bacterial parasite, *Listeria monocytogenes*. *J Cell Biol* 109:1597–1608.
7. Simmons DG, Fortier AL, Cross JC. 2007. Diverse subtypes and developmental origins of trophoblast giant cells in the mouse placenta. *Dev Biol* 304:567–578.
8. Zhu D, Gong X, Miao L, Fang J, Zhang J. 2017. Efficient Induction of Syncytiotrophoblast Layer II Cells from Trophoblast Stem Cells by Canonical Wnt Signaling Activation. *Stem Cell Reports* 9:2034–2049.
9. Choi HJ, Sanders TA, Tormos KV, Ameri K, Tsai JD, Park AM, Gonzalez J, Rajah AM, Liu X, Quinonez DM, Rinaudo PF, Maltepe E. 2013. ECM-dependent HIF induction directs trophoblast stem cell fate via LIMK1-mediated cytoskeletal rearrangement. *PLoS ONE* 8:e56949.
10. Yan J, Tanaka S, Oda M, Makino T, Ohgane J, Shiota K. 2001. Retinoic acid promotes differentiation of trophoblast stem cells to a giant cell fate. *Dev Biol* 235:422–432.
11. Robbins JR, Skrzypczynska KM, Zeldovich VB, Kapidzic M, Bakardjiev AI. 2010. Placental syncytiotrophoblast constitutes a major barrier to vertical transmission of *Listeria monocytogenes*. *PLoS Pathog* 6:e1000732.
12. Zeldovich VB, Clausen CH, Bradford E, Fletcher DA, Maltepe E, Robbins JR, Bakardjiev AI. 2013. Placental syncytium forms a biophysical barrier against pathogen invasion. *PLoS Pathog* 9:e1003821.

13. Weber M, Knoefler I, Schleussner E, Markert UR, Fitzgerald JS. 2013. HTR8/SVneo cells display trophoblast progenitor cell-like characteristics indicative of self-renewal, repopulation activity, and expression of “stemness-” associated transcription factors. *Biomed Res Int* 2013:243649.
14. Li Z, Kurosawa O, Iwata H. 2019. Establishment of human trophoblast stem cells from human induced pluripotent stem cell-derived cystic cells under micromesh culture. *Stem Cell Res Ther* 10:245.
15. Ghosh P, Halvorsen EM, Ammendolia DA, Mor-Vaknin N, O’Riordan MXD, Brumell JH, Markovitz DM, Higgins DE. 2018. Invasion of the Brain by *Listeria monocytogenes* Is Mediated by InlF and Host Cell Vimentin. *MBio* 9.
16. Théry C, Witwer KW, Aikawa E, Alcaraz MJ, Anderson JD, Andriantsitohaina R, Antoniou A, Arab T, Archer F, Atkin-Smith GK, Ayre DC, Bach J-M, Bachurski D, Baharvand H, Balaj L, Baldacchino S, Bauer NN, Baxter AA, Bebawy M, Beckham C, et al. 2018. Minimal information for studies of extracellular vesicles 2018 (MISEV2018): a position statement of the International Society for Extracellular Vesicles and update of the MISEV2014 guidelines. *J Extracell Vesicles* 7:1535750.
17. Yang Y, Boza-Serrano A, Dunning CJR, Clausen BH, Lambertsen KL, Deierborg T. 2018. Inflammation leads to distinct populations of extracellular vesicles from microglia. *J Neuroinflammation* 15:168.
18. Johnson LJ, Azari S, Webb A, Zhang X, Gavrilin MA, Marshall JM, Rood K, Seveau S. 2021. Human Placental Trophoblasts Infected by *Listeria monocytogenes* Undergo a Pro-Inflammatory Switch Associated With Poor Pregnancy Outcomes. *Front Immunol* 12:709466.
19. Valadi H, Ekström K, Bossios A, Sjöstrand M, Lee JJ, Lötvall JO. 2007. Exosome-mediated transfer of mRNAs and microRNAs is a novel mechanism of genetic exchange between cells. *Nat Cell Biol* 9:654–659.
20. Es-Haghi M, Godakumara K, Häling A, Lättekivi F, Lavrits A, Viil J, Andronowska A, Nafee T, James V, Jaakma Ü, Salumets A, Fazeli A. 2019. Specific trophoblast transcripts transferred by extracellular vesicles affect gene expression in endometrial epithelial cells and may have a role in embryo-maternal crosstalk. *Cell Commun Signal* 17:146.
21. Nandakumar R, Tschismarov R, Meissner F, Prabakaran T, Krissanaprasit A, Farahani E, Zhang B-C, Assil S, Martin A, Bertrams W, Holm CK, Ablasser A, Klause T, Thomsen MK, Schmeck B, Howard KA, Henry T, Gothelf KV, Decker T, Paludan SR. 2019. Intracellular bacteria engage a STING-TBK1-MVB12b pathway to enable paracrine cGAS-STING signalling. *Nat Microbiol* 4:701–713.

22. Skog J, Würdinger T, van Rijn S, Meijer DH, Gainche L, Sena-Esteves M, Curry WT, Carter BS, Krichevsky AM, Breakefield XO. 2008. Glioblastoma microvesicles transport RNA and proteins that promote tumour growth and provide diagnostic biomarkers. *Nat Cell Biol* 10:1470–1476.
23. Schnitger AKD, Machova A, Mueller RU, Androulidaki A, Schermer B, Pasparakis M, Krönke M, Papadopoulou N. 2011. *Listeria monocytogenes* infection in macrophages induces vacuolar-dependent host miRNA response. *PLoS ONE* 6:e27435.
24. Cronqvist T, Tannetta D, Mörgelin M, Belting M, Sargent I, Familiarì M, Hansson SR. 2017. Syncytiotrophoblast derived extracellular vesicles transfer functional placental miRNAs to primary human endothelial cells. *Sci Rep* 7:4558.
25. Raposo G, Stoorvogel W. 2013. Extracellular vesicles: exosomes, microvesicles, and friends. *J Cell Biol* 200:373–383.
26. White JR, Dauros-Singorenko P, Hong J, Vanholsbeeck F, Phillips A, Swift S. 2021. The complex, bidirectional role of extracellular vesicles in infection. *Biochem Soc Trans* <https://doi.org/10.1042/BST20200788>.
27. Sauer J-D, Sotelo-Troha K, von Moltke J, Monroe KM, Rae CS, Brubaker SW, Hyodo M, Hayakawa Y, Woodward JJ, Portnoy DA, Vance RE. 2011. The N-ethyl-N-nitrosourea-induced Goldenticket mouse mutant reveals an essential function of Sting in the in vivo interferon response to *Listeria monocytogenes* and cyclic dinucleotides. *Infect Immun* 79:688–694.
28. Sauer J-D, Witte CE, Zemansky J, Hanson B, Lauer P, Portnoy DA. 2010. *Listeria monocytogenes* triggers AIM2-mediated pyroptosis upon infrequent bacteriolysis in the macrophage cytosol. *Cell Host Microbe* 7:412–419.
29. McCaffrey RL, Fawcett P, O’Riordan M, Lee K-D, Havell EA, Brown PO, Portnoy DA. 2004. A specific gene expression program triggered by Gram-positive bacteria in the cytosol. *Proc Natl Acad Sci USA* 101:11386–11391.
30. Moffett A, Colucci F. 2014. Uterine NK cells: active regulators at the maternal-fetal interface. *J Clin Invest* 124:1872–1879.